FEASIBILITY OF A CASCADE TYPE

HYDROELECTRIC GENERATOR SYSTEM

.by

ALAN G. BUCHKOWSKI; B.ENG.

A Thesis

Submitted to the School of Graduate Studies

in Partial Fulfilment of the Requirements

for the Degree

Master of Engineering

McMaster University

April 1981

MASTER OF ENGINEERING (1981)   McMASTER UNIVERSITY
(Mechanical Engineering)   Hamilton, Ontario

TITLE: Feasibility of a Cascade Type
       Hydroelectric Generator System

AUTHOR: Alan G. Buchkowski, B.Eng. (McMaster
               University)

SUPERVISORS: Professor J. N. Siddall, Dr. B. Latto

NUMBER OF PAGES: (ix), 153

To My Parents

ABSTRACT

The feasibility of an alternative concept of a small scale hydroelectricity generation system which is suited to high volume, low head flows was investigated. The device consists of a cascade of hydrofoils which are mounted in an arrangement which resembles a conveyor belt. The investigation included the use of a computer model which simulated the water flow through the cascade. A sensitivity analysis was done using the model to establish the effects of varying the design variables which defined the system. On the basis of the analysis, a prototype was designed with the consideration of the material, configuration, safety and environmental requirements. A cost estimate and economic analysis were made of the prototype and subsequently the concept was evaluated.

(iii)

ACKNOWLEDGEMENTS

The author wishes to express his sincere gratitude to his supervisor Professor J. N. Siddall for his constant guidance and encouragement.

The author sincerely appreciates the valuable information and guidance provided by his co-supervisor Dr. B. Latto.

The author would like to thank the Natural Sciences and Engineering Research Council for financial support.

The comradship of Mr. E. Chu, Mr. W. D'Netto and Mr. A. Abd Rabbo throughout this project is appreciated.

The author would like to thank Ms. L. Whitehead for her enthusiastic encouragement and Ms. B. Bedell and Miss L. Oneschuk for their expert typing of the manuscript.

TABLE OF CONTENTS

LIST OF FIGURES

LIST OF TABLES

CHAPTER 1

INTRODUCTION

Energy has become a major topic of concern among political, economic and engineering circles in the world. The increase in demand, the realization of the finiteness of fossil fuels and environmental pollution problems have initiated searches for clean and efficient energy sources. Many proposals which have been made are questionable in their engineering and economic feasibilities. It is the obligation of the engineering communities to assess new developments and make recommendations as to their implementation.

One subject area that has attracted much attention as a result of the search for clean and safe energy is that of small scale hydroelectric power [5, 30].* Although the technology has existed for some time, modern small scale hydroelectricity generator systems have not evolved because of cheaper electricity generation from fossil fuels and nuclear reactors. Recently however, several versions of small scale devices have been proposed. These systems may be viable in the near future if not presently, when the rising fossil fuel costs and the safety aspects of nuclear reactors are considered.

---

* Numbers in brackets refer to similarly numbered references at the end of the paper.

One such device is that of the "water ladder". (The term "water ladder" is used because the system's blades have the same configuration as rungs of a ladder and are immersed in water). Basically it is a hydroelectric device which utilizes a cascade of hydrofoils to produce electricity. The concept is to withdraw energy from low head, high volume water flows such as those encountered in many of our rivers. The device is pictured in Figure (1-1). The water passes over the blades, induces lift and causes the foils to translate. Although the motion is slow, high torques are produced which, with appropriate gearing, allow the attachment of a generator.

The water ladder system offers the potential of drawing energy from sources which could not be tapped by existing hydroelectric equipment. There is also the prospect of the system's implementation in the Third World, by playing a role in an Appropriate Technology exchange. It is suspected that the system would be economic since only a small reservoir if any would be required, and as a result of the simplicity of the design. There appeared to be no adverse environmental effects inherent in the concept of the system.

The intention of this thesis is to present the results of an investigation of the water ladder system. The approach taken was to first of all formulate a computer model to calculate the fluid flow characteristics of the system. The results of the model plus the general configuration requirements were used to design a full scale prototype. Therefore it was possible to estimate the cost of the prototype. An

WATER LEVEL

RIVER FLOW
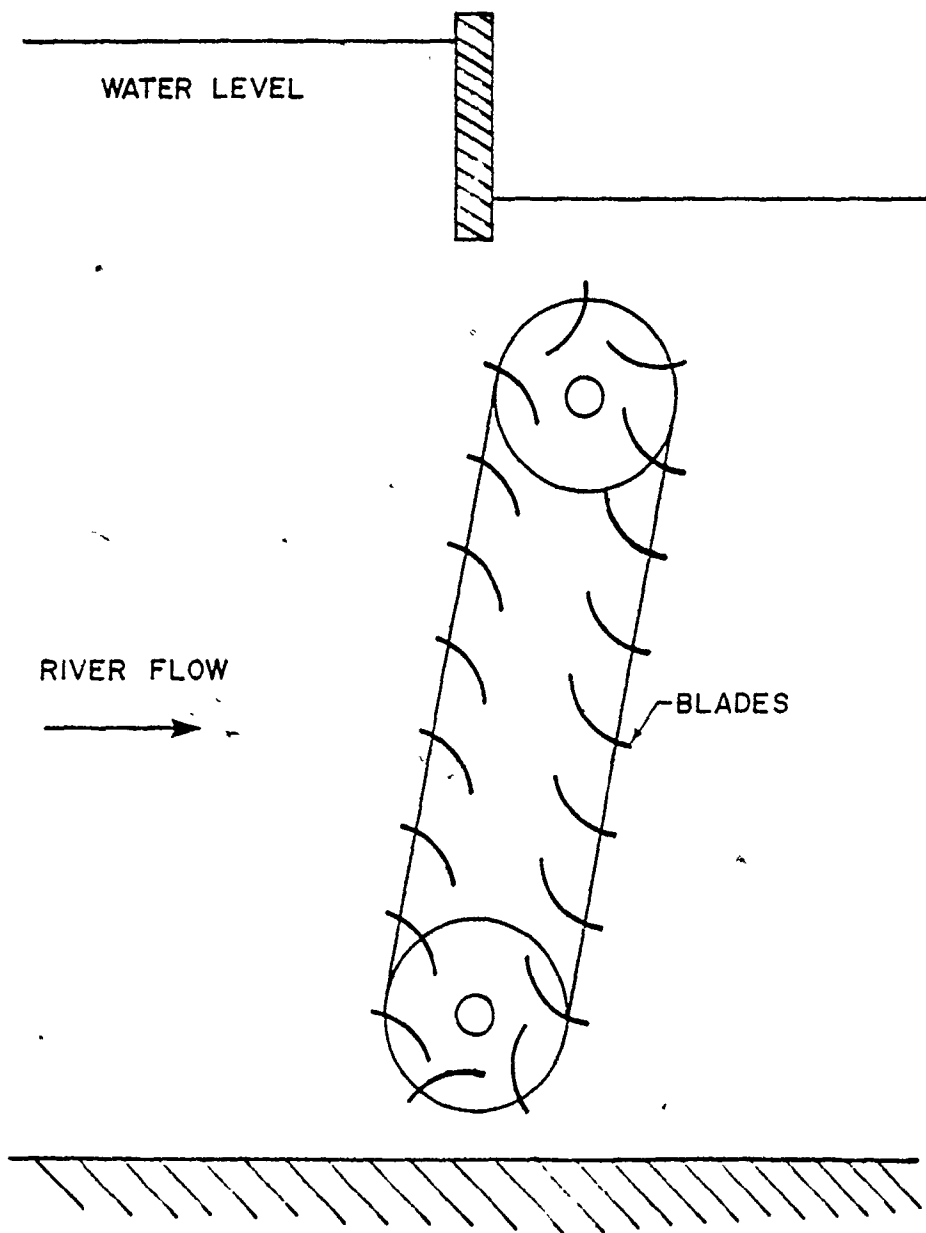
BLADES

FIGURE 1-1

CONFIGURATION OF THE WATER LADDER

analysis was done to determine the econqmic feasibility of the project.

CHAPTER 2

MODEL FORMULATION

The computer model that was produced is a simulation of fluid flow over a single blade. The model deals with basic flow directions and energy transfer, and incorporates several assumptions to simplify the calculations involved. These assumptions were as follows:

(1)   Losses over the blade are a function of the total head.

(2)   The exit velocity of the fluid is uniform over the entire exit plane.

(3)   The flow is incompressible.

(4)   Incident and deviation angles have small effects.

(5)   No separation or cavitation occurs.

(6)   Blades are thin with respect to blade spacing.

(7)   There is no boundary layer influence.

The validity of these assumptions will be discussed after considering the results of the simulation.

In formulating the model a number of variables were defined. These variables are listed below and are shown in Figure (2-1).

2.1   Model Notation

V_1 = absolute fluid inlet velocity $(v)^*$

---

* (v) denotes a vector quantity.

5
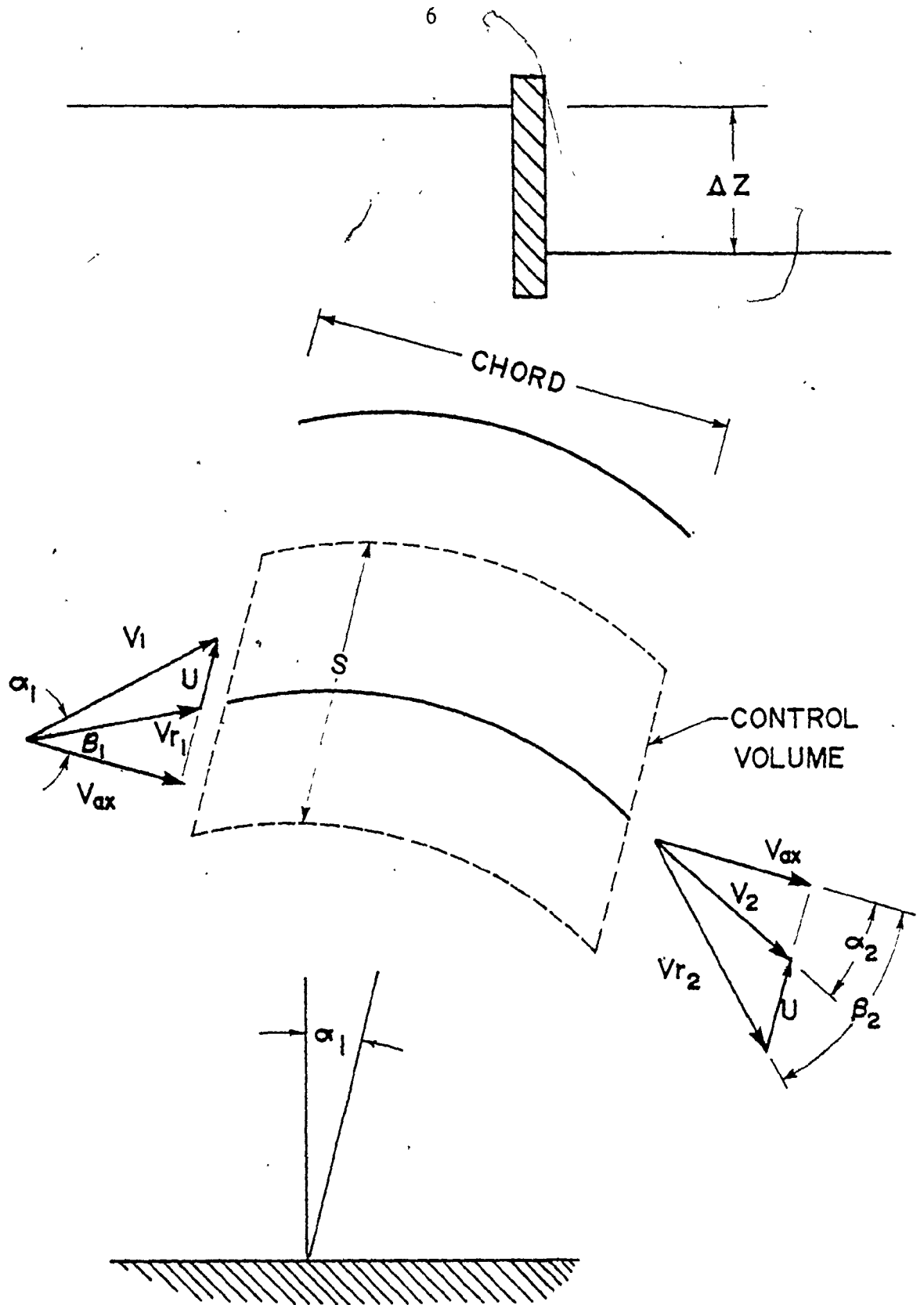
FIGURE 2-1

MODEL DEFINITION

Vr_1 = relative fluid inlet velocity (v)

V_2 = absolute fluid exit velocity (v)

Vr_2 = relative fluid exit velocity (v)

u = blade velocity (v)

V_{RIV} = upstream river velocity (v)

V_{ax} = axial velocity in the cascade (v)

A_{RIV} = cross-sectional area of river upstream in one dimension

A_1 = cross-sectional area of river at the cascade inlet

D = depth of the river

W = width of the river

α_1 = absolute inlet velocity direction V_1

α_2 = direction of V_2

β_1 = direction of Vr_1

β_2 = direction of Vr_2

$\theta = \beta_2 - \beta_1$ = turning angle

s = the space between blades

c = the chord of the blades

s/c_{ax} = solidity = s/axial chord

F_y = the upward force on the blade in the direction of u

F_x = the axial force on the blades in the direction of V_{ax}

η = the efficiency of the blade system

p = the power output of the system

P_T = the power output per unit vertical depth-horizontal span

C_m = the energy loss coefficient defined in the model

Δz = the head differential over a blade

Note that a head differential, Δz may be created by a retaining structure which forms part of the water ladder system. Δz is also affected by the shape of the blades since their shape determines the water flow rate through the cascade and hence the retention of fluid upstream of the cascade.

2.2   Model Derivation

Several of the variables were selected as design variables from which the other parameters were calculated. These design variables were V_{RIV}, Depth, u, Δz, α_1, C_m and c. These specified variables were used in the two-dimensional model to estimate the power output, efficiency and force on a blade.

The following is a derivation of the computer model. Throughout this derivation the laws of continuity, momentum and energy conservation were maintained.

From Figure (2-1),

$$A_{RIV} = \text{Depth}$$

$$A_1 = A_{RIV} - \Delta z \qquad\qquad (2.1)$$

As a result of continuity,

$$V_1 = A_{RIV} \cdot (V_{RIV}/A_1) \qquad\qquad (2.2)$$

The axial velocity was calculated as

$$V_{ax} = V_1 \cdot (\cos \alpha_1) \qquad\qquad (2.3)$$

Referring to the vector diagram in Figure (2-1), the

relative inlet velocity is derived from

$$u = V_1 \sin \alpha_1 - Vr_1 \sin \beta_1$$

and
$$Vr_1 \cos \beta_1 = V_1 \cos \alpha_1$$

Thus

$$u = V_1 \sin \alpha_1 - V_1 \cos \alpha_1 \cdot \tan \beta_1$$

$$\frac{u}{V_1 \cos \alpha_1} = \tan \alpha_1 - \tan \beta_1$$

$$\frac{u}{V_{ax}} = \tan \alpha_1 - \tan \beta_1 \qquad (2.4)$$

$$\beta_1 = \arctan(\tan \alpha_1 - \frac{u}{V_{ax}}) \qquad (2.5)$$

and

$$Vr_1 = V_{ax}/\cos \beta_1 \qquad (2.6)$$

The exit variables were calculated by applying the energy equation across a blade, written as,

$$_1 q_2 + z_1 g + \frac{V_1^2}{2} + h_1 = z_2 g + \frac{V_2^2}{2} + {_1 w_2} + h_2 \qquad (2.7)$$

where q = heat input

z_1 = head

h = enthalpy

w = work output

In terms of a relative axis,

$$_1q_2 + z_1g + \frac{Vr_1^2}{2g} + h_1 = z_2g + \frac{Vr_2^2}{2} + {}_1w_2 + h_2$$

where $w = q = 0$

$\Delta z = z_1 - z_2$

since $u = 0$

In a moving control volume $w = 0$ and flow is adiabatic. The equation becomes

$$\Delta z + \frac{Vr_1^2}{2g} = \frac{Vr_2^2}{2g} + \frac{(h_2 - h_1)}{g} \qquad (2.8)$$

The expression $(h_2 - h_1)$ is the change in specific enthalpy across the blade, which partially results from the loss of energy which occurs due to friction, etc. The change in enthaply may be expressed as

$$\Delta h = C_p \Delta T, \quad \text{since } C_p = \text{constant}$$

Losses which occur produce a temperature rise in the fluid. The rise in temperature was considered to be quite small, hence the change in enthalpy is small. If there is virtually no temperature change, the energy equation can be rewritten as

$$\Delta z + \frac{Vr_1^2}{2g} = \frac{Vr_2^2}{2g} + \text{losses} \qquad (2.9)$$

where 'losses' represents the energy lost as friction.

In ideal flow the losses are zero.

Much research has been done in the area of predicting losses for airfoils and hydrofoils. Examples are given in

references [25, 32, 45]. To date the prediction of losses is based on empirical formulae and experimental results [25].

It was decided to define a loss coefficient for this model analysis. Losses may be expressed as a percentage of the total static and dynamic heads available upstream or the downstream dynamic head.

Explicitly,

$$\text{Losses} = C_m \ (\frac{Vr_2^2}{2g})$$

Thus

$$\Delta z + \frac{Vr_1^2}{2g} = \frac{Vr_2^2}{2g} (1 + C_m) \qquad (2.10)$$

$$Vr_2 = [\frac{2g \ \Delta z + Vr_1^2}{1 + C_m}]^{1/2}$$

or

$$C_m = \frac{\Delta z \ 2g + Vr_1^2}{Vr_2^2} - (\frac{Vr_2}{Vr_2})^2$$

which is the total change in energy compared to the exit energy.

In turbomachinery analysis, a loss coefficient $c = Vr_2/Vr_1$ is often used. For comparative purposes,

$$Vr_2 = c \ Vr_1$$

$$= (a+b) \ Vr_1$$

where   b = the vector magnitude contributed by a pressure change

   a = the vector magnitude representing actual losses.

In ideal flow,

$$\frac{Vr_1{}^2}{2g} + \Delta z = \frac{Vr_2{}^2}{2g} = \frac{b^2 Vr_1{}^2}{2g}$$

Substituting into Equation (2.10),

$$(1 + C_m) \frac{Vr_1{}^2}{2g} = \Delta z + \frac{Vr_1{}^2}{2g} = b^2 \frac{Vr_1{}^2}{2g}$$

$$C_m = b^2 \frac{Vr_1{}^2}{Vr_2{}^2} - 1$$

$$= b^2 \frac{1}{(a+b)^2} - 1 \quad ,$$

$$= b^2 \frac{1}{c^2} - 1$$

The significance of the relation between c and C_m as given above is not explicit. The relation is dependent upon the pressure change produced by Δz as reflected in b. Hence no conclusion can be made regarding c and C_m.

Further equations were formulated to define the exit parameters. For continuity,

$$Vr_1 \cos \beta_1 = Vr_2 \cos \beta_2 = V_{ax} \qquad (2.11)$$

Assuming that the cross-sectional area of the fluid passage remains unchanged

$$\beta_2 = - \arccos \left(\frac{V_{ax}}{Vr_2}\right) \qquad (2.12)$$

Referring to Figure (2-1), expressions for the absolute exit angle α_2 and the fluid velocity V_2 were obtained as

follows;

$$u = V_2 \sin \alpha_2 - Vr_2 \sin \beta_2$$

$$= Vr_2 \cos \beta_2 \tan \alpha_2 - Vr_2 \sin \beta_2$$

$$\frac{u}{V_{ax}} = \tan \alpha_2 - \tan \beta_2$$

$$\alpha_2 = \arctan \left(\frac{u}{V_{ax}} + \tan \beta_2\right) \tag{2.13}$$

and

$$V_2 = \frac{V_{ax}}{\cos \alpha_2} \tag{2.14}$$

The force on the blade may be obtained from momentum considerations.

$$F_y = \rho Vr_{1x} \cdot s \cdot (Vr_{1y} - Vr_{2y})$$

$$= \rho V_{ax} \cdot s \cdot (Vr_1 \sin \beta_1 - Vr_2 \sin \beta_2)$$

$$= \rho V_{ax}^2 \cdot s \cdot (\tan \beta_1 - \tan \beta_2) \tag{2.15}$$

In the computer program s was set equal to one metre and therefore the calculated force on the blade is expressed in terms of unit spacing.

The power output may be written as the product of the blade velocity and the force on the blade,

$$p = F_y \cdot u \tag{2.16}$$

The total power per metre span per metre depth of river (as opposed to per metre along the height of the cascade), may·

be expressed as,

$$P_T = p/\cos \alpha_1 \qquad (2.17)$$

The total power output of a particular system with a cross-sectional area of Width * Depth is then

$$\text{total power} = T_p \cdot W \cdot D \qquad (2.18)$$

Efficiency of the system is defined as

$$\eta = \frac{\text{power taken out of the system}}{\text{ideal power removed}}$$

Applying Equation (2.7)

$$POWID = \rho \cdot s \cdot V_1 \, [(V_1^2 - V_2^2)/2 + \Delta z \cdot g] \qquad (2.19)$$

where   POWID is the ideal power output of the cascade. Hence

$$\eta = \frac{POWER}{POWID} \qquad (2.20)$$

It is informative to define the efficiency relative to the inlet energy level only, i.e.

$$\eta = \frac{\text{power taken out of the system}}{\text{power available to the system on entry}}$$

Thus

$$POWID = \rho \cdot s \cdot V_1 \, [\frac{V_1^2}{2} + \Delta z \cdot g] \qquad (2.21)$$

This efficiency indicates what portion of the available power is being removed.

Both of the efficiency definitions were employed in the computer model.

The spacing of the cascade blades greatly affects the efficiency of the system. If the spacing is small, "the fluid tends to receive maximum guidance although frictional losses are large. With large spacing, frictional losses are reduced but because of poor guidance the losses from separation are high" ([9], pg. 85). In turbomachinery analysis, a rule of thumb that is often employed is that proposed by Zwieful [47], who found optimal spacing exists when

$$2 \left(\frac{s}{c}\right) \cos^2 \alpha_2 (\tan \alpha_1 + \tan \alpha_2) = .8 \qquad (2.22)$$

where   s = blade spacing

   c = axial chord

Figure (2-1) identifies these parameters.

Equation (2.22) was used to calculate the s/c ratio and the spacing s. Hence s is dependent upon the blade chord selected.

The preceding fluid flow theory is simplistic and as previously stated does include several confining assumptions. However for the purposes of this study the model as formulated is considered reasonable.

The computer program that was created is given in Appendix (A). A plotting routine was also included in the program in order to display trends in the variables. This computer package was used in a sensitivity analysis as discussed in the following section.

CHAPTER 3

SENSITIVITY ANALYSIS

The computer model permits a macroscopic study of the fluid flow properties of the cascade. The design variables which were defined in Chapter (2) were assigned an acceptable range of magnitude. By modifying the magnitude of these variables within this range, an indication of their sensitivity was obtained. The effect on the output parameters, namely the power output and the force on the blade, was used to evaluate the importance of each design variable.

Of the seven design variables which were specified in the previous chapter, two were assigned constant values. The blade chord does not enter into the calculations in the computer model as a result of the assumptions made. Hence the chord was assigned a value of .6 m, the reasons for which will be discussed in Chapter (4). The river depth was found to be linearly proportional to the power output, therefore the depth would not provide any additional insight into the performance characteristics. The depth, D, was assigned a value of 4.2 m. This appeared to be an appropriate depth in which the system could operate.

The remaining five design variables, Δz, C_m, u, α_1, and V_{RIV}, were varied as given in Table (3-1). The following is a discussion on the results of the computer simulations.

Table 3-1

Extent of the Sensitivity Analysis

Program	Variables				
	C_m (m)	Δz (m)	u (m/s)	α_1 (radians)	V_i (m/s)
DEOC	0.0-.38	0.0-.76	.25	.2	1.0
DEUU	.02	0.0-.95	0.0-.95	.2	1.0
DEAL	.02	0.0-.95	.25	0.0-.38	1.0
DRIV	.02	0.0-.95	.5	.2	.55-1.5

3.1   Loss Coefficient C_m

Figures (3-1) through (3-5) show the effect of vary-
ing the loss coefficient C_m on several of the characteristic
parameters. An increase in C_m does not greatly affect the
relationship between the head difference Δz and β_2, the
relative fluid exit angle, as shown in Figure (3-1). An
increase in the value of C_m, which can be interpreted as an
increase in the energy lost to friction, resulted in a decrease
in the force on the blade and in the power output, as shown
in Figures (3-2) and (3-3) respectively. This trend was as
expected. Figure (3-4) shows the effect C_m had on the
efficiency of the system. Finally, C_m plays a minimal role
in the relation between the fluid turning angle θ, and the
power output. (See Figure (3-5)) i.e., energy lost over the
cascade is small when compared with the energy transferred as
power output.

As a result of these trends, it was concluded that the
final design calculations would be quite insensitive to
inaccuracies in the value of C_m, hence specific accurate data
for the loss coefficient was considered unnecessary in a
preliminary study.

3.2   Head Differential, Δz

The head difference over the cascade, Δz, appeared
to be the most sensitive design variable among those studied.
The sensitivity of Δz on other flow characteristics is shown
in Figures (3-1) through (3-5). Figure (3-1) illustrates
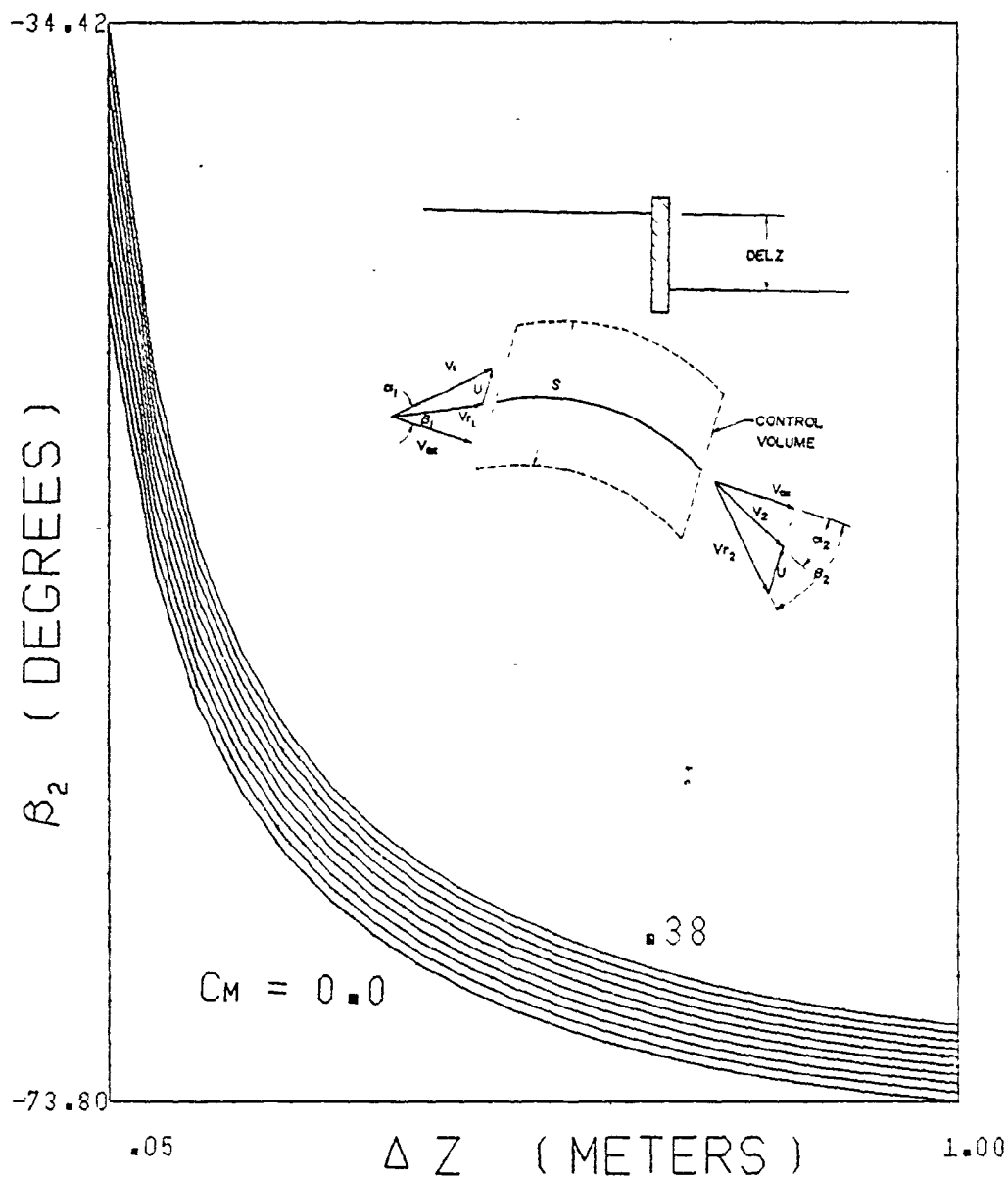
Figure 3-1   The Relative Exit Angle versus the Head Differential.
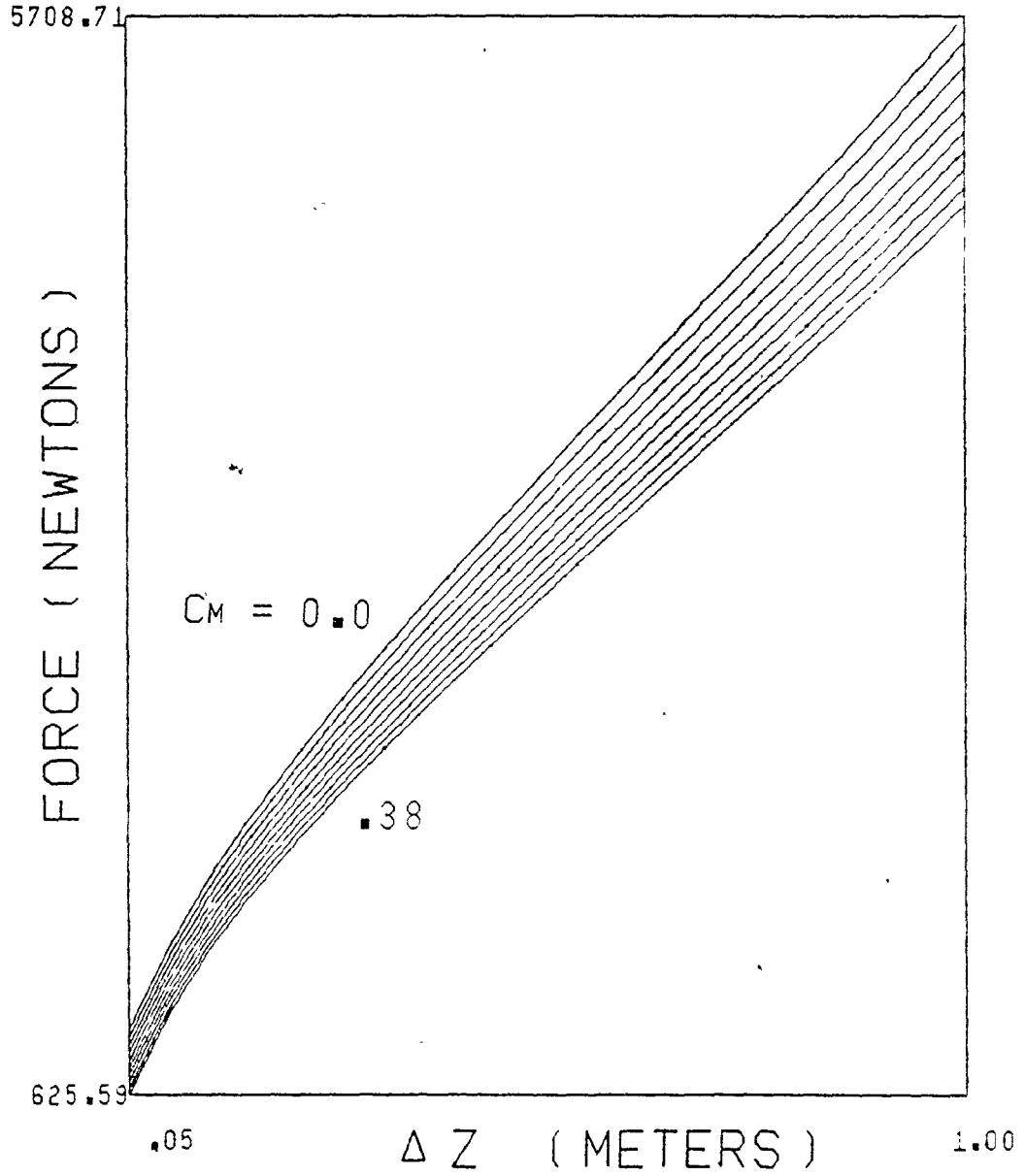
Figure 3-2   The Force on a Blade versus the Head Differential.

PROGRAM DEOC   U = .25 M/S
                ALPHA1 = .2 R
                VRIV = 1 M/S
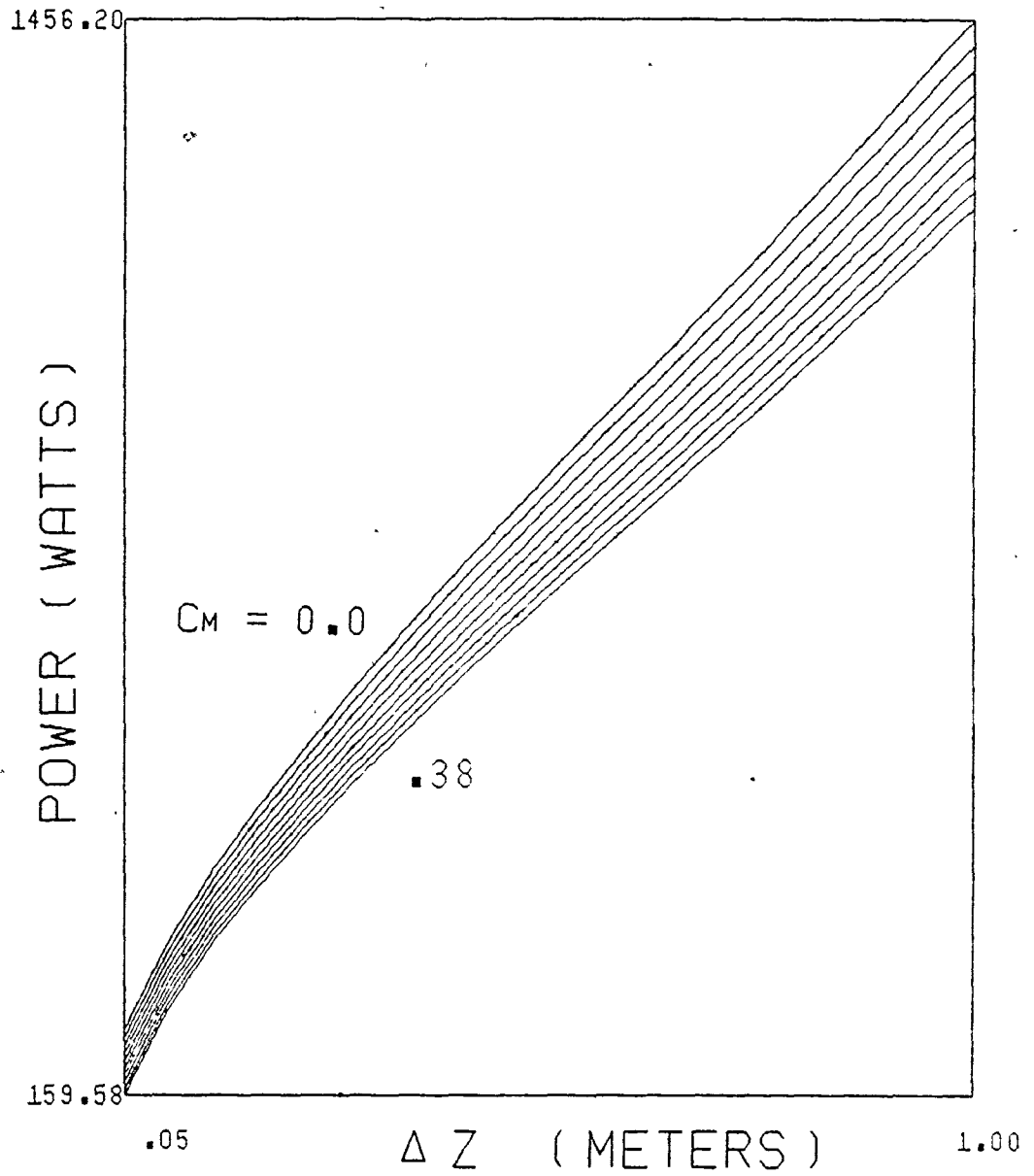
Figure 3-3   The Power Output versus the Head Differential.

PROGRAM DEOC   U = .25 M/S
                ALPHA1 = .2 R
                VRIV = 1 M/S
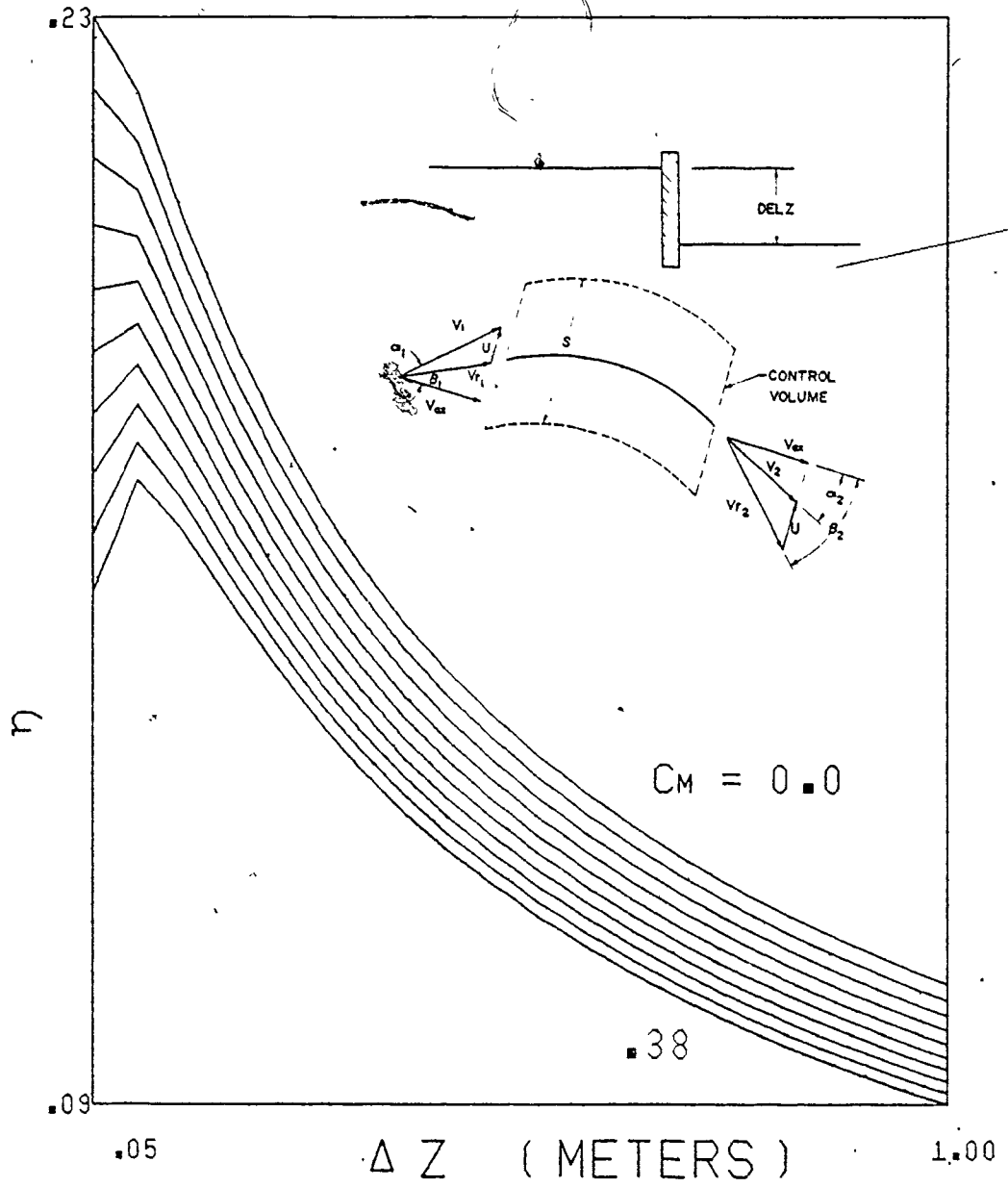
Figure 3-4   Efficiency versus the Head Differential.

PROGRAM DEOC   U = .25 M/S
                 ALPHA1 = .2 R
                 VRIV = 1 M/S
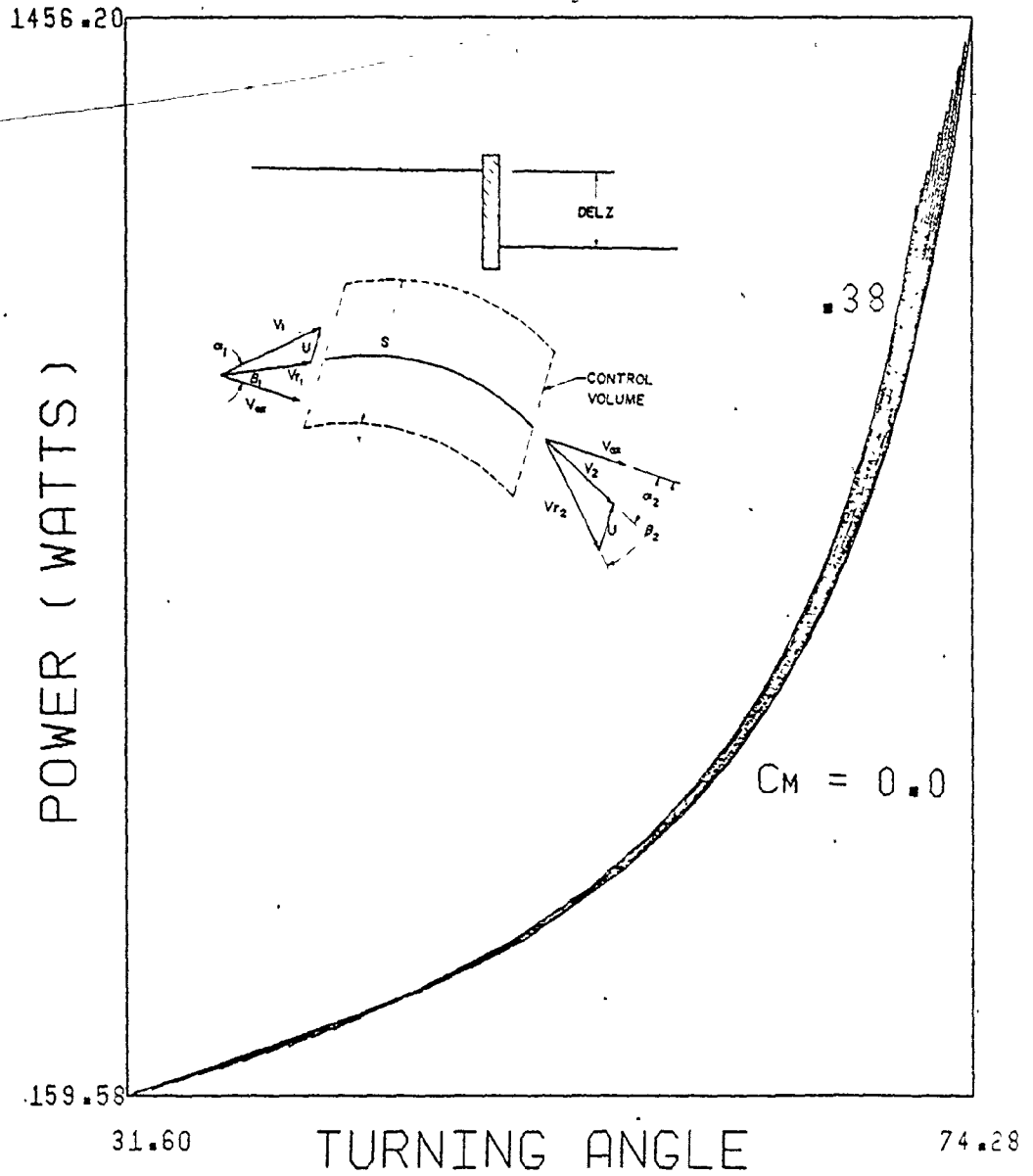
Figure 3-5   The Power Output versus the Fluid Turning Angle.

the large effect Δz has on the relative exit angle, β_2. A large Δz corresponded to a large β_2. This relationship plays a limiting role in maximum value of efficiency in the water ladder system. Figures (3-2) and (3-3) show that the force on the blade and the power output increased with increasing Δz. Figure (3-5) illustrates that an increasing power output corresponds to an increasing turning angle θ, which is associated with an increasing Δz. Finally Figure (3-4) shows that the system is most efficient under low heads. Here efficiency is defined as the ratio between the power removed to the total available power (Equation (2.21)). The higher head differential corresponds to a larger inlet velocity V_1 as a result of the greater difference between the cross-sectional areas A_{RIV} and A_1. This larger V_1 reduces the effect of Δz, i.e. A_{RIV} the ratio between the dynamic head and the static head is increased. The dynamic head is maintained downstream as a result of continuity considerations. Hence, the energy withdrawn as power is derived from Δz. The head difference Δz, being a smaller component of the total available head, appears to lower the efficiency regardless of the fact that a greater power output results.

As a result of the trends in Δz it is apparently desirable to specify a large head differential in the possible final design, acknowledging however that this results in a large fluid turning angle, which can be limited by the fluid flow characteristics such as separation and cavitation.

3.3   The Blade Velocity, u

Figures (3-6) through (3-10) illustrate the effect varying the blade velocity, u, on several flow and energy variables. For example in Figure (3-7) the relative exit angle, β_2 is not greatly affected by u. However Figures (3-8) and (3-9) show that for an increasing blade velocity, the force on the blade decreases, whereas the power output increases. It was evident that a definite relationship exists between these two parameters and the blade velocity. This aspect will be discussed in Chapter (4).

Figure (3-10) shows that the efficiency increases with increasing blade velocity. The vertical intercept is 0.0. Therefore for $\Delta z \doteq 0.0$ a negative efficiency results implying that a power input is required to move the cascade. The fact that the $\Delta z = .05$ curve crosses other curves indicates that there is a relationship between the magnitude of Δz and the efficiency. That is for a given value of Δz, there may exist a maximum value for the efficiency. This relationship was not investigated any further, however, could be pursued in subsequent work to determine optimum design specifications.

Considering the results obtained in the sensitivity analysis on the blade speed, it was evident that a high speed was very desirable. This fact was as expected since it was consistent with trends for turbomachinery where a high specific speed is also advantageous.
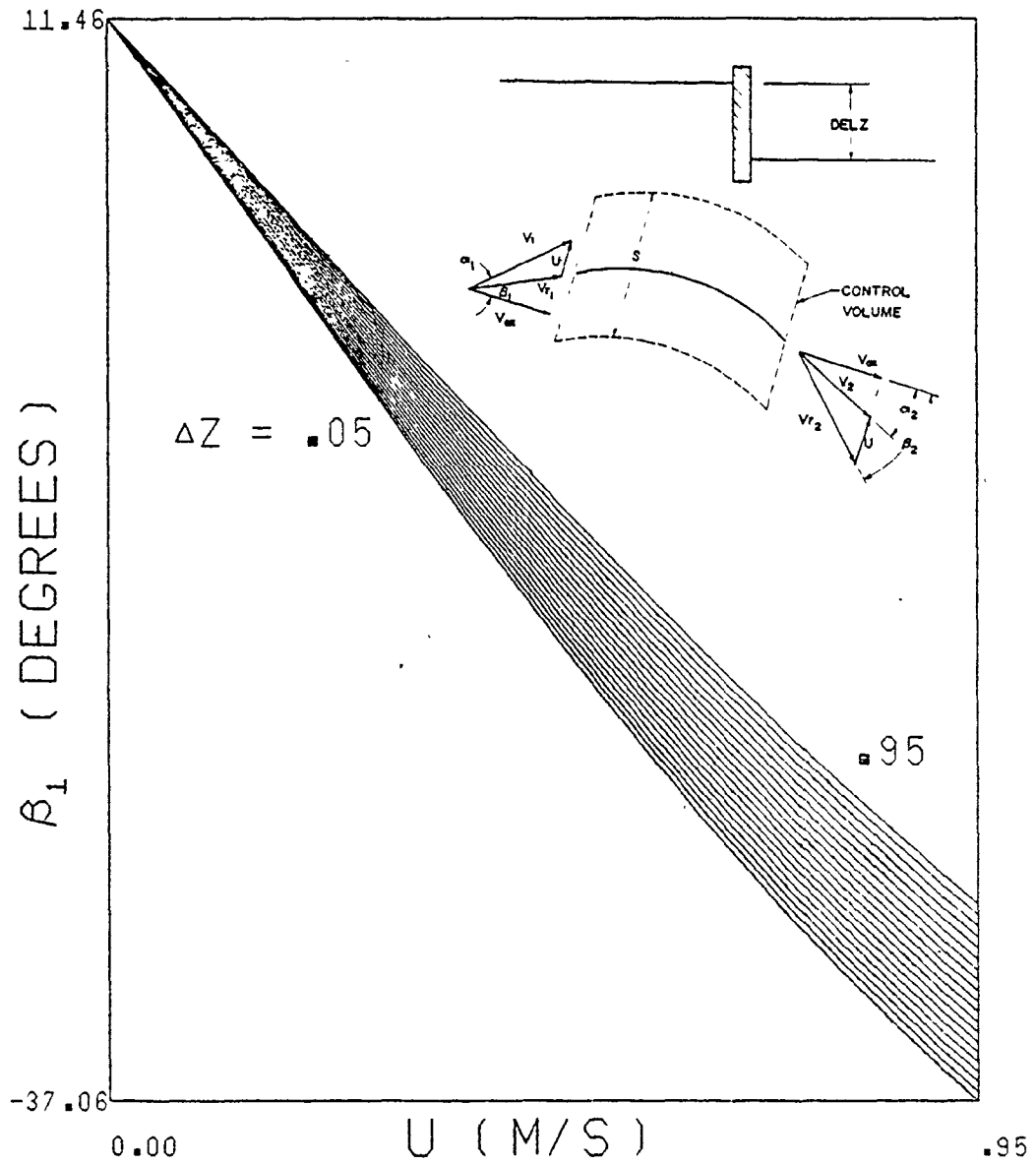
Figure 3-6   The Relative Inlet Angle versus the Blade Velocity.

PROGRAM DEUU   ALPHA1 = .2 R
COLOS = .02
VRIV = 1 M/S

ΔZ = .05

β_2 (DEGREES)

-44.37

-73.82

0.00   U (M/S) ΔZ = .95   .95
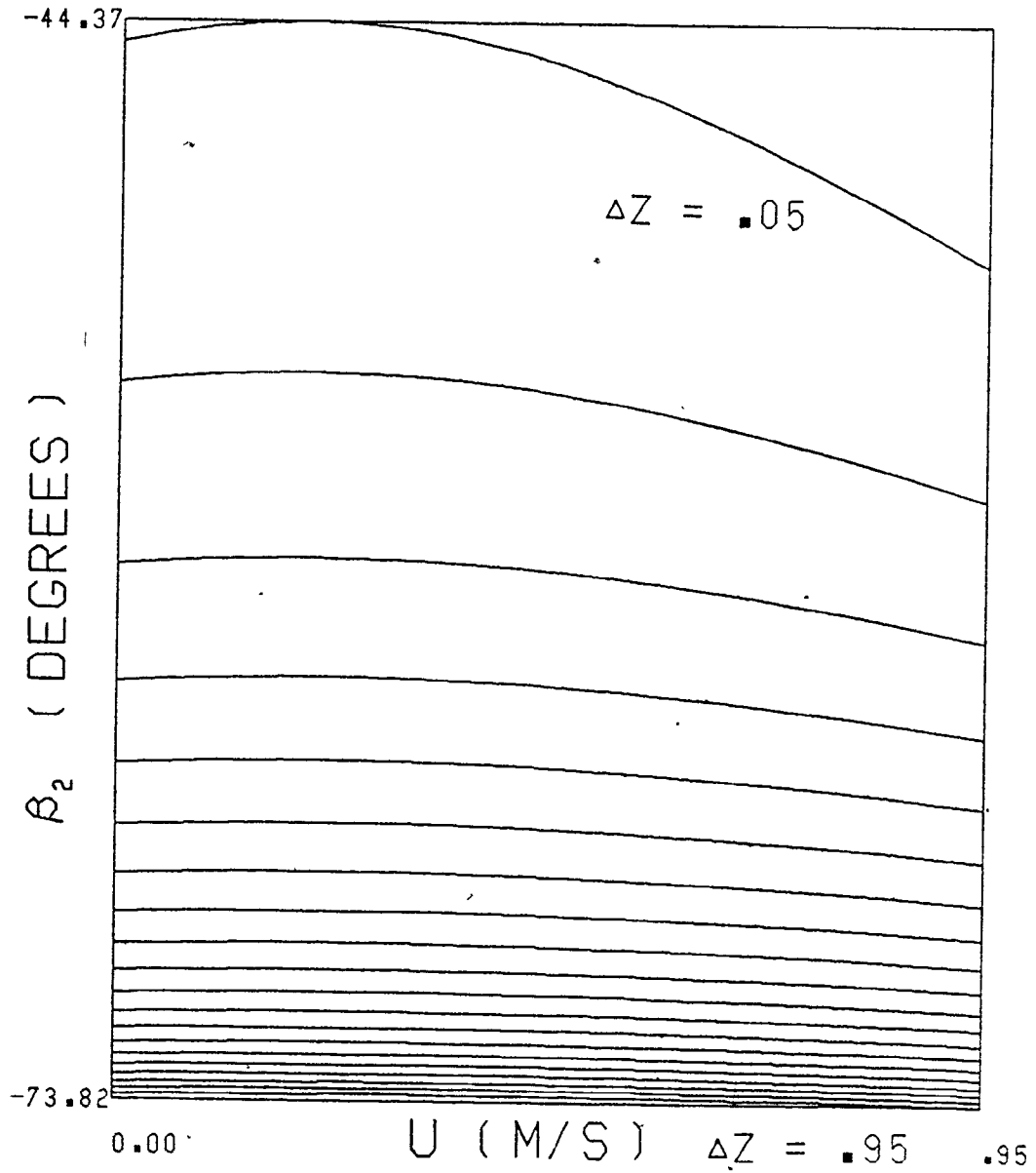
Figure 3-7   The Relative Exit Angle versus the Blade Velocity.

PROGRAM DEUU   ALPHA1 = .2 R
                COLOS = .02
                VRIV = 1 M/S
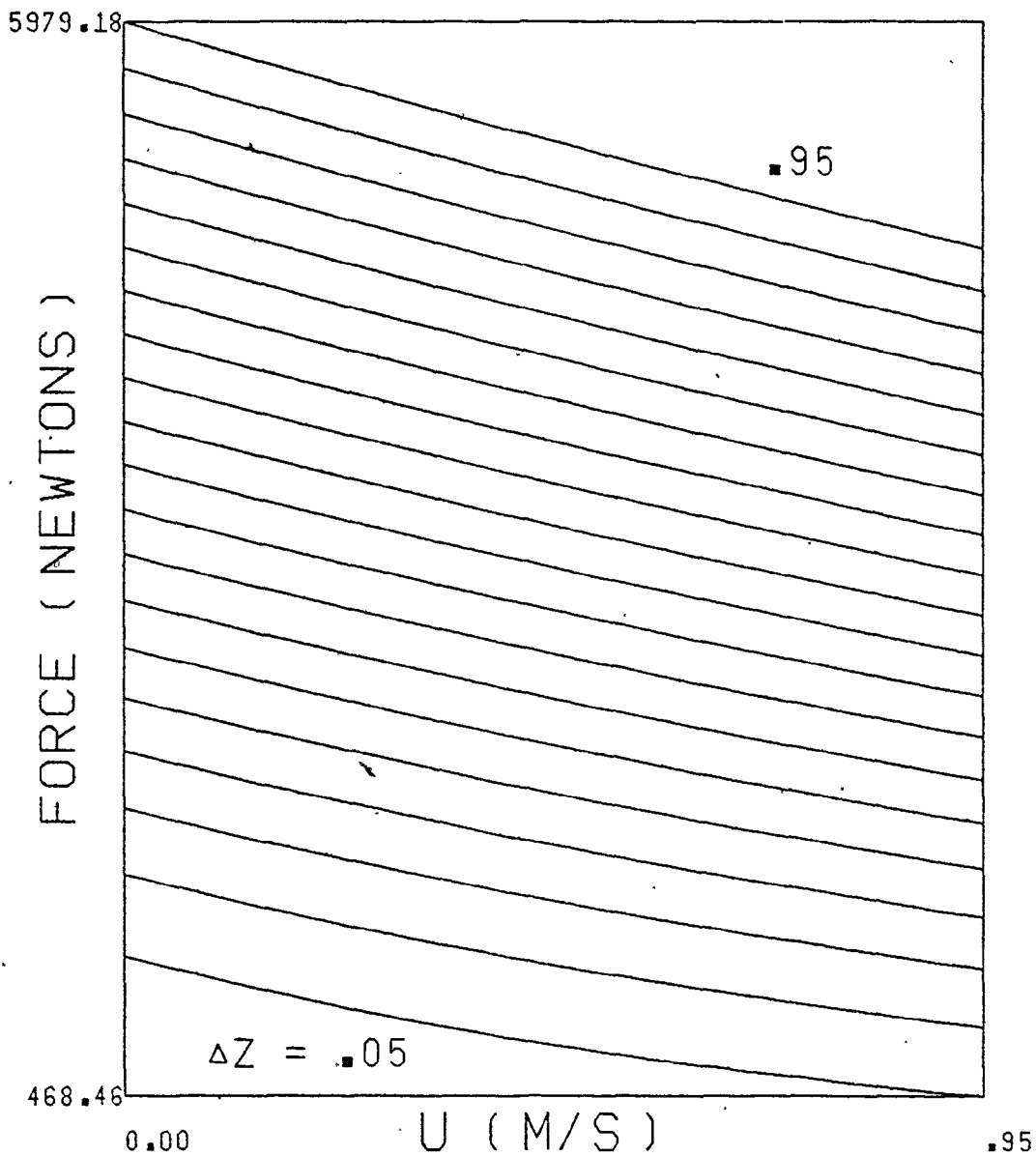
Figure 3-8   The Force on a Blade versus the Blade Velocity.

PROGRAM DEUU ALPHA1 = .2 R
COLOS = .02
VRIV. = 1 M/S
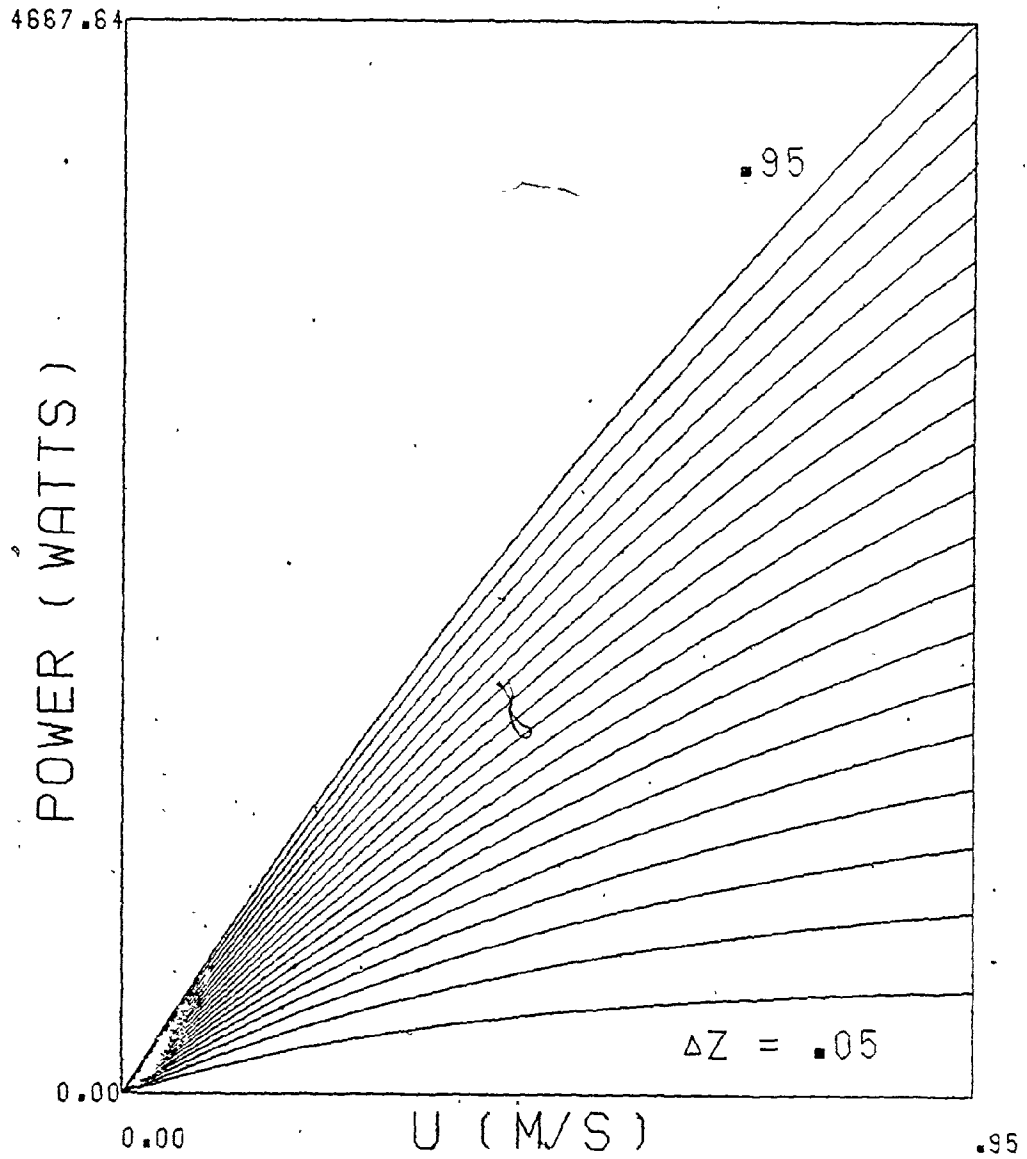
Figure 3-9 The Power Output versus the Blade Velocity.

PROGRAM DEUU   ALPHA1 = .2 R
                COLOS = .02
                VRIV = 1 M/S
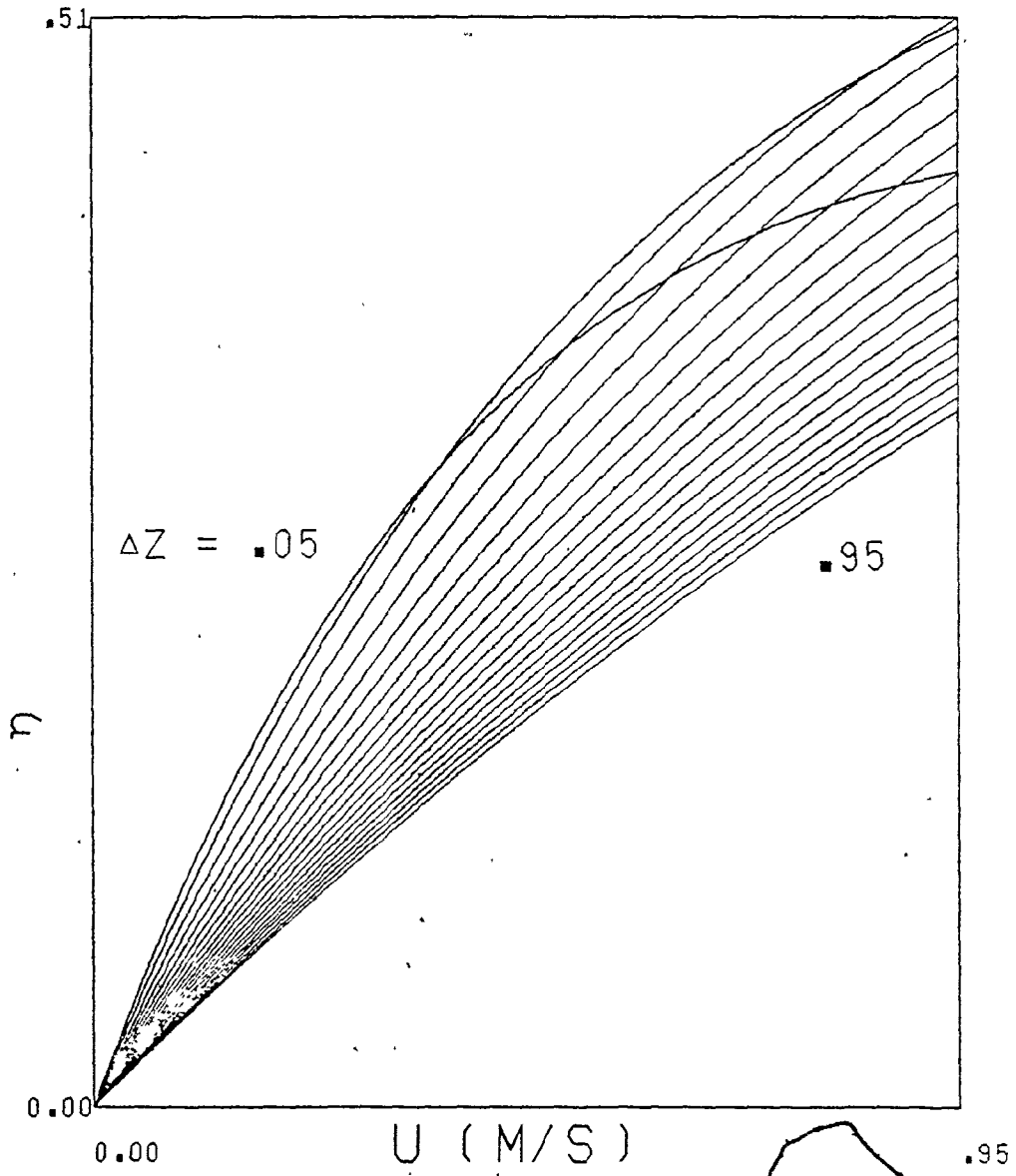
Figure 3-10   Efficiency versus the Blade Velocity

3.4 Stagger Angle, α_1

The relationships between the stagger angle, α_1 and several system characteristics are shown in Figures (3-11) through (3-15). Increasing α_1 results in an increase in the force on the blade. This is as expected since as α_1 increases β_1 and θ increase, and the turning angle determines the change in fluid direction, hence the force on the blade. A slight rise in the efficiency and power output may be realized by an increase in α_1, as shown in Figures (3-12) and (3-14) respectively. This slight change in the efficiency and power output was attributed to two conflicting trends. That is, as the stagger angle increases, the turning angle increases, hence the power output correspondingly increases. However, since the vertical component of the inlet area decreases, the volume of fluid which each blade is subjected to decreases. This leads to a decrease in the power output. The plot shows an increasing output for an increasing stagger angle, hence it appears that the former trend dominates and thus α_1 should be assigned a value greater than zero. It is difficult to ascertain from the plots what magnitude of α_1 is optimum. Further discussion on the matter appears in Chapter (4).

3.5 The River Velocity, V_{RIV}

The river velocity is essentially an uncontrollable input into the system because it is subject to weather conditions in the watershed upstream of the water ladder site.

PROGRAM DEAL   U = .25 M/S
                 COLOS = .02
                 VRIV = 1 M/S
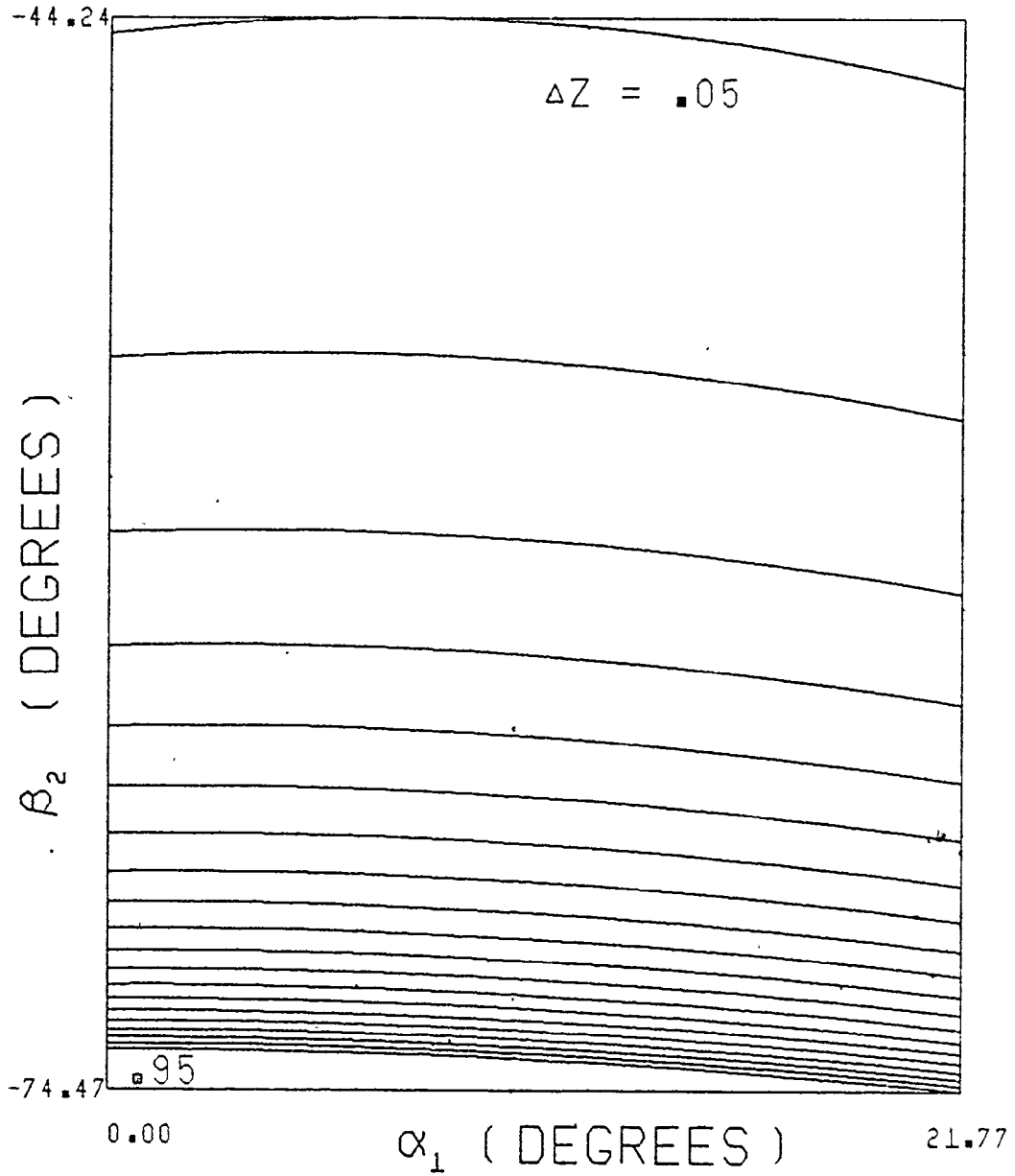
Figure 3-11   The Relative Exit Angle versus the Stagger Angle.

PROGRAM DEAL   U = .25 M/S
                 COLOS = .02
                 VRIV = 1 M/S
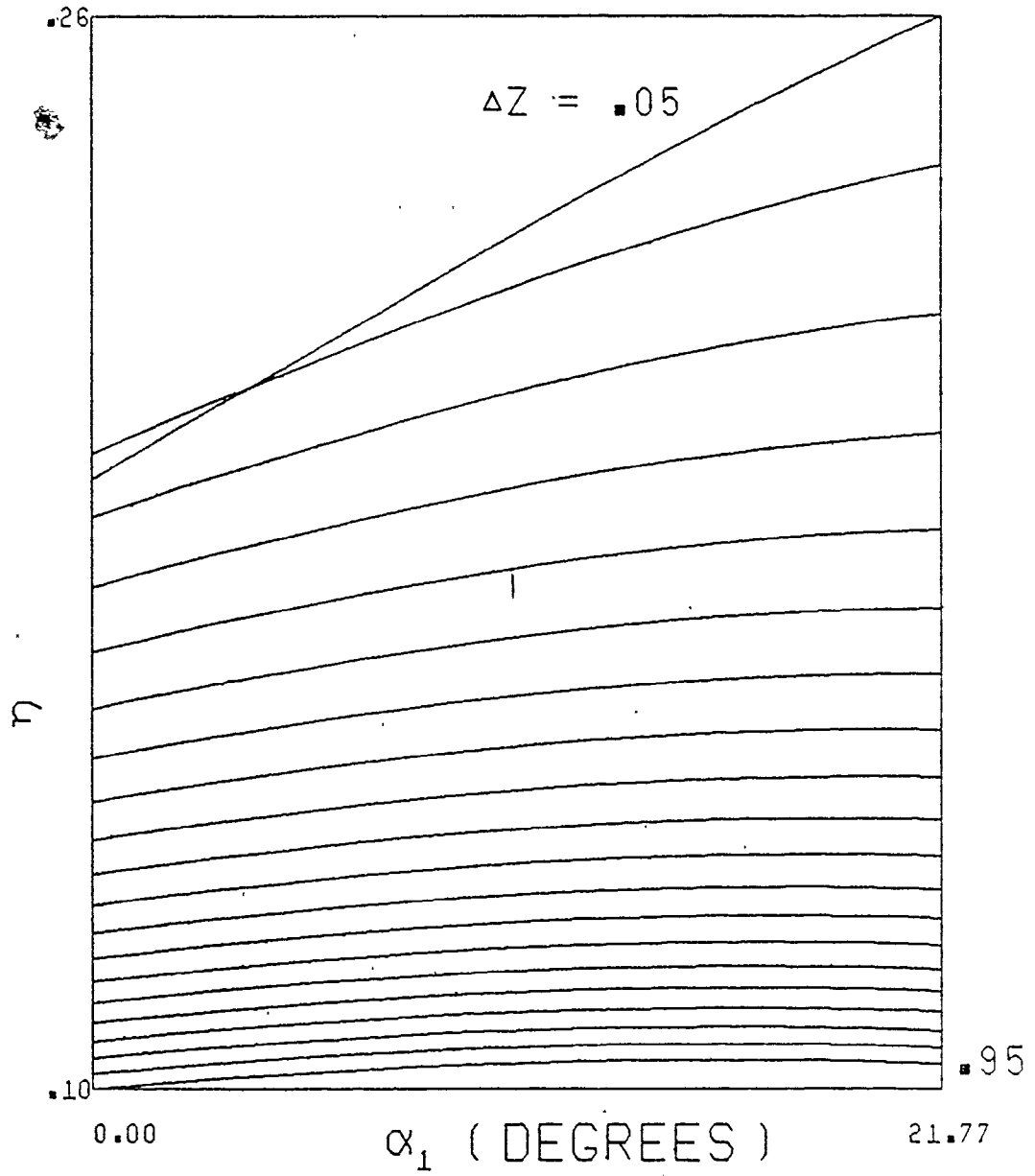
Figure 3-12 Efficiency versus the Stagger Angle.

PROGRAM DEAL   U = .25 M/S
                 COLOS = .02
                 VRIV = 1 M/S
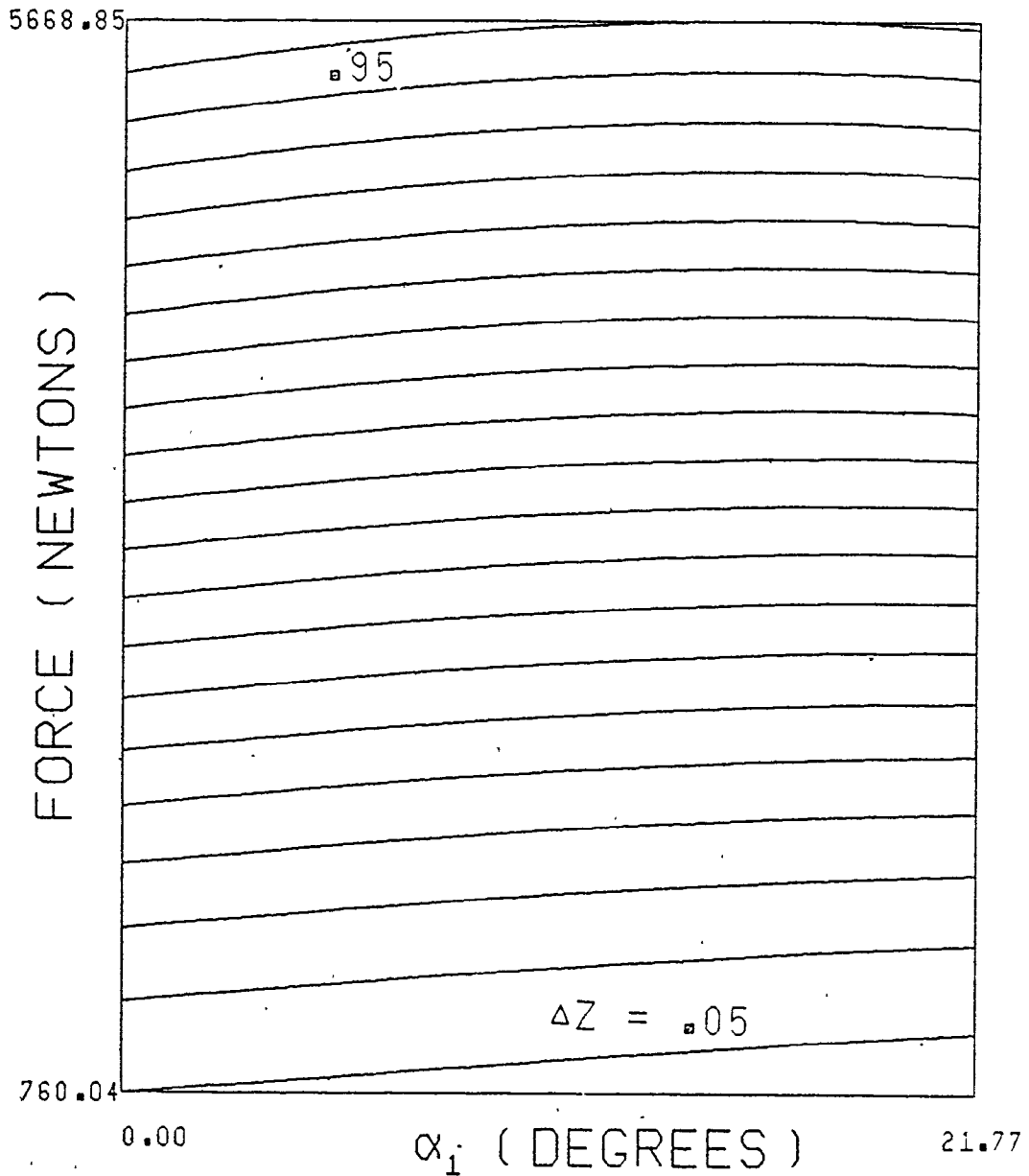
Figure 3-13   The Force on a Blade versus the Stagger Angle.
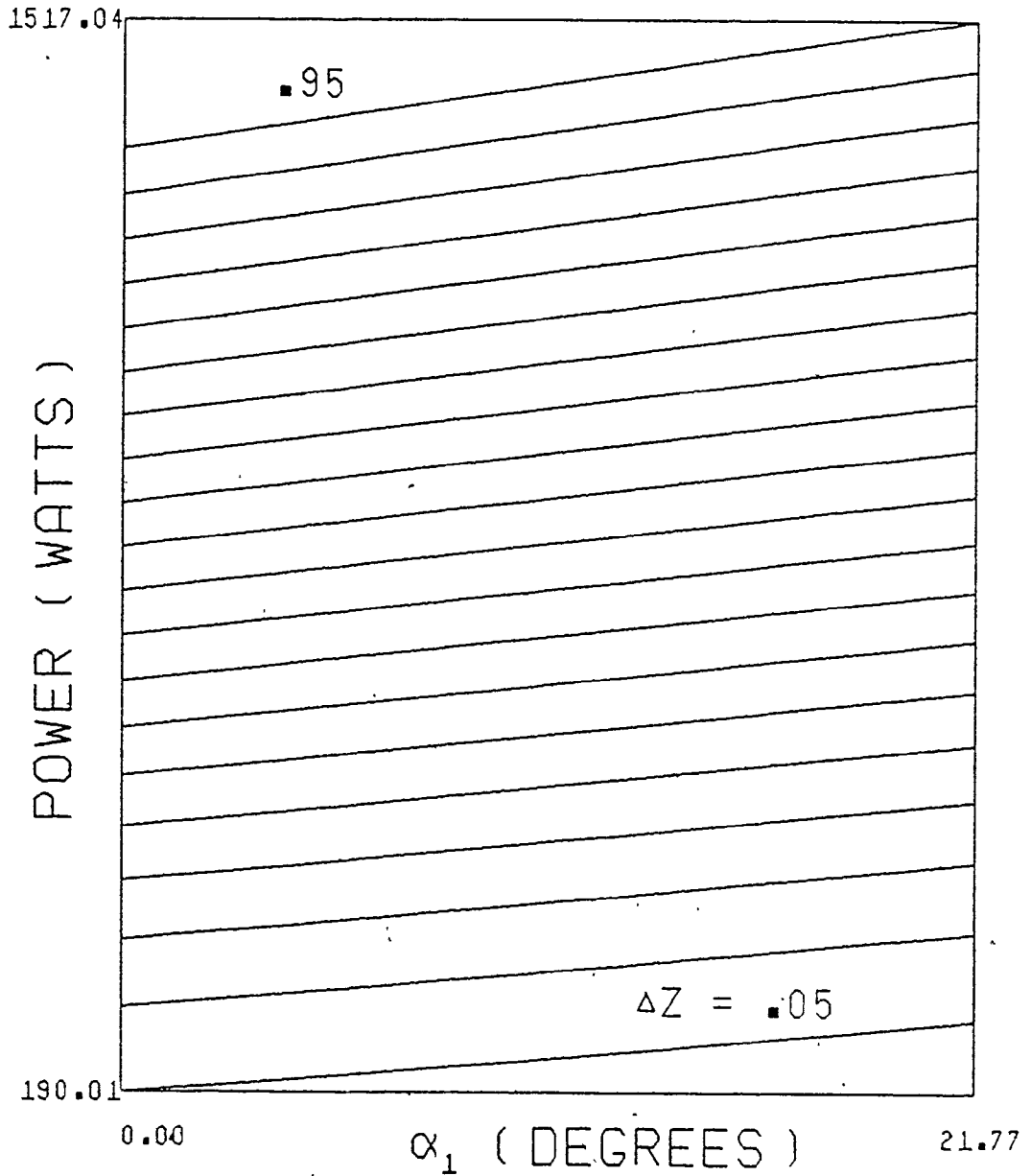
Figure 3-14   The Power Output versus the Stagger Angle.
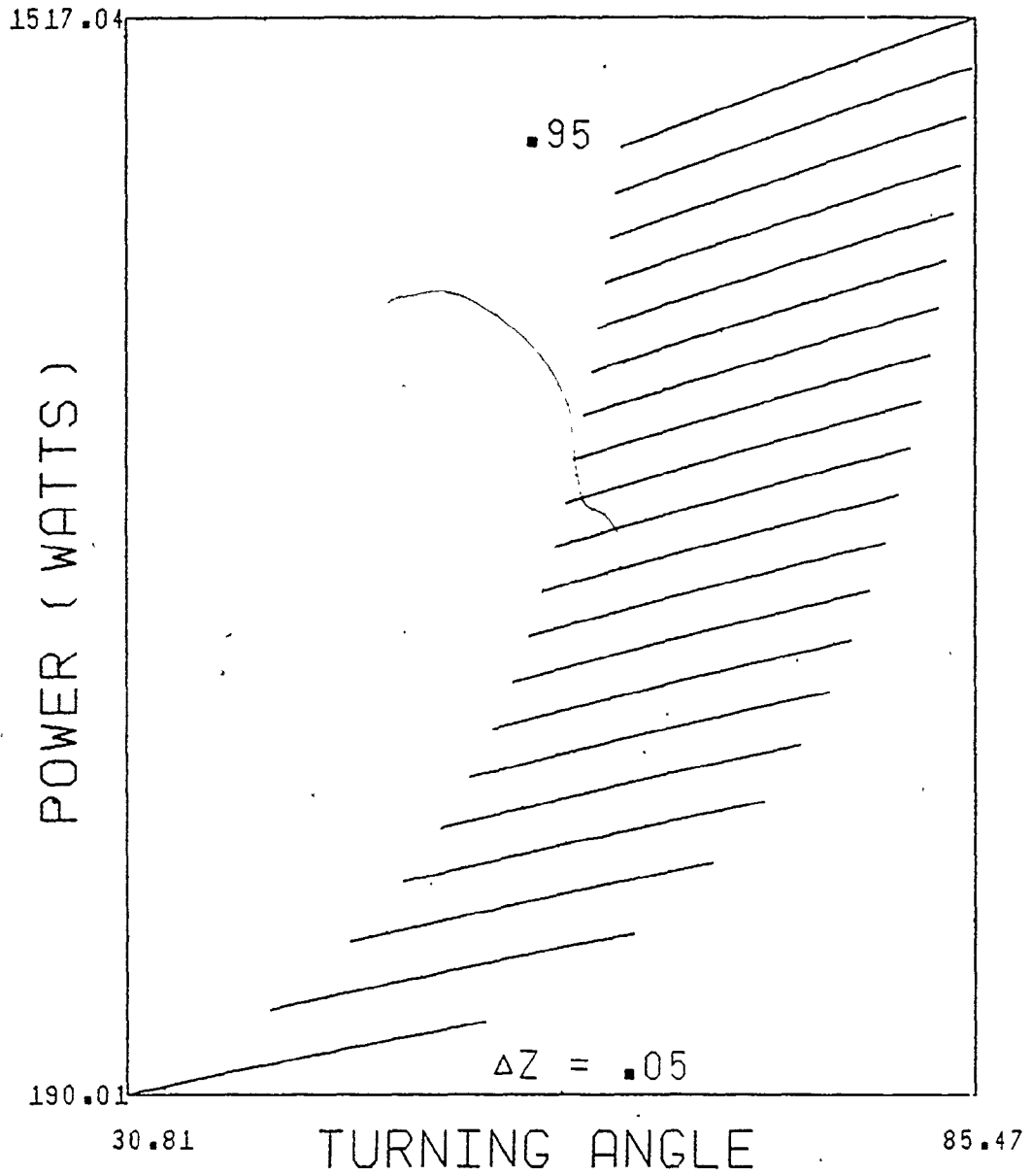
Figure 3-15   The Power Output versus the Fluid Turning Angle.

It was considered most important to investigate the
effect of the river velocity on the system since, if its
effect was large, an unmanageable range of power outputs or
flow velocities may result. This range depends upon the
cross-sectional area of the river in question since larger
rivers are less sensitive to upstream watershed conditions.

The river velocity V_{RIV} was plotted with the head
differential, Δz in Figures (3-16) through (3-22). If flood-
ing conditions were to occur, water would be retained upstream
because of the flow restriction caused by the system. The
resulting plots indicate the magnitude of the effect of
water retention.

Figure (3-16) and (3-17) are plots of β_1 versus V_{RIV}
and β_2 versus V_{RIV} respectively. Increasing V_{RIV} requires
both a smaller β_1 and β_2. However the effect is not as
pronounced on β_2 as it is on β_1. It was evident that large
river velocities may be compensated for by altering the blade
velocity of the cascade. Attention to this fact should be
given in the design of a prototype.

A plot of Vr_2 versus V_{RIV} is given in Figure (3-18).
Increasing V_{RIV} caused an increase in Vr_2, however the effect
appears to be insignificant.

Figures (3-19), (3-20) and (3-21) are plots of V_{RIV}
versus F_y, η and Power, respectively. As expected an increase
in V_{RIV} causes an increase in the force on the blade and the
power output from the system. The efficiency of the system
decreased with increasing V_{RIV} especially for lower values of Δz,
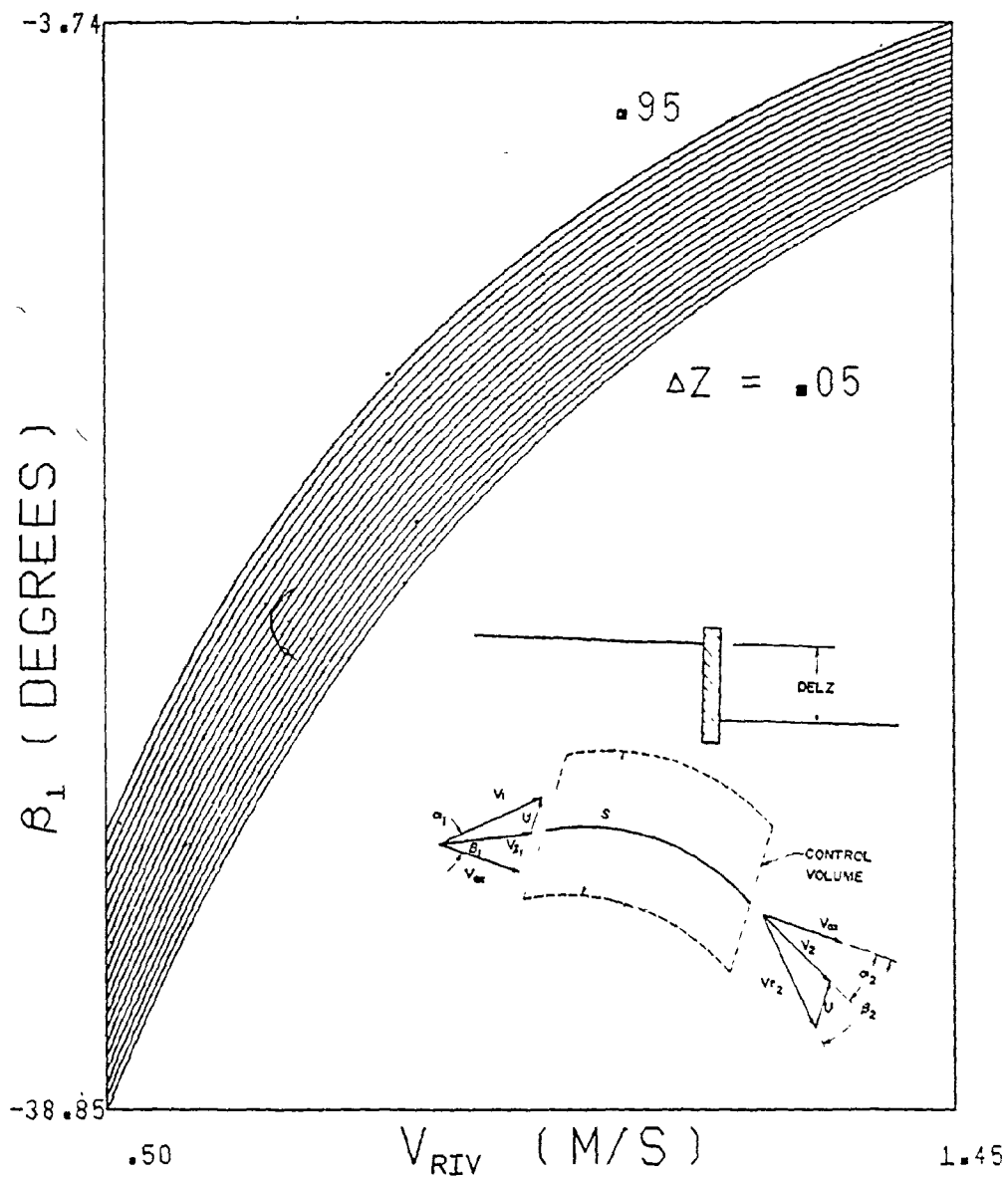
Figure 3-16   The Relative Inlet Angle versus the Upstream River Velocity.

PROGRAM DRIV   U = .5 M/S
                COLOS = .02
                ALPHA1 = .2 R
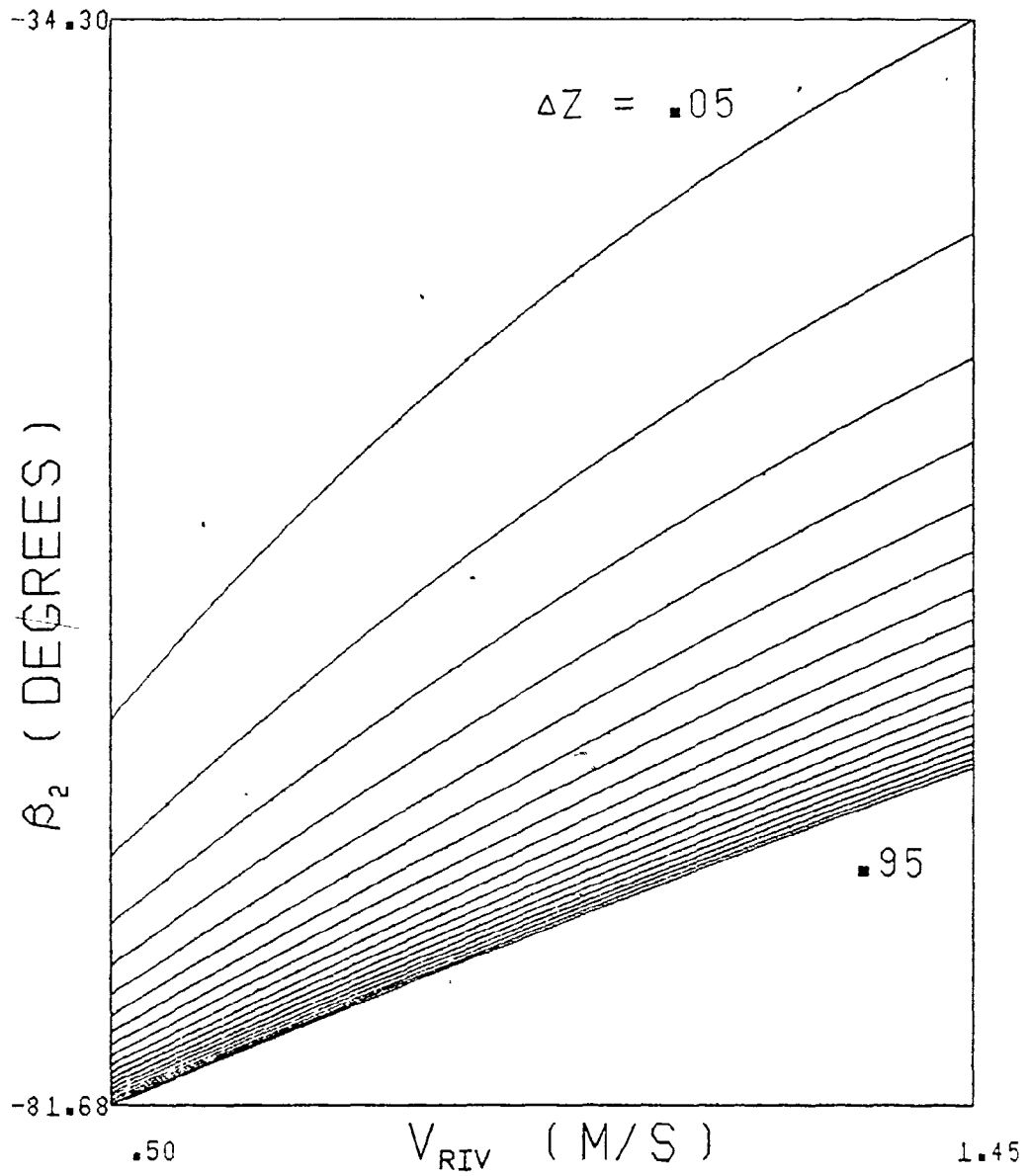
Figure 3-17   The Relative Exit Angle versus the Upstream River Velocity.

PROGRAM DRIV   U = .5 M/S
                 COLOS = .02
                 ALPHA1 = .2 R
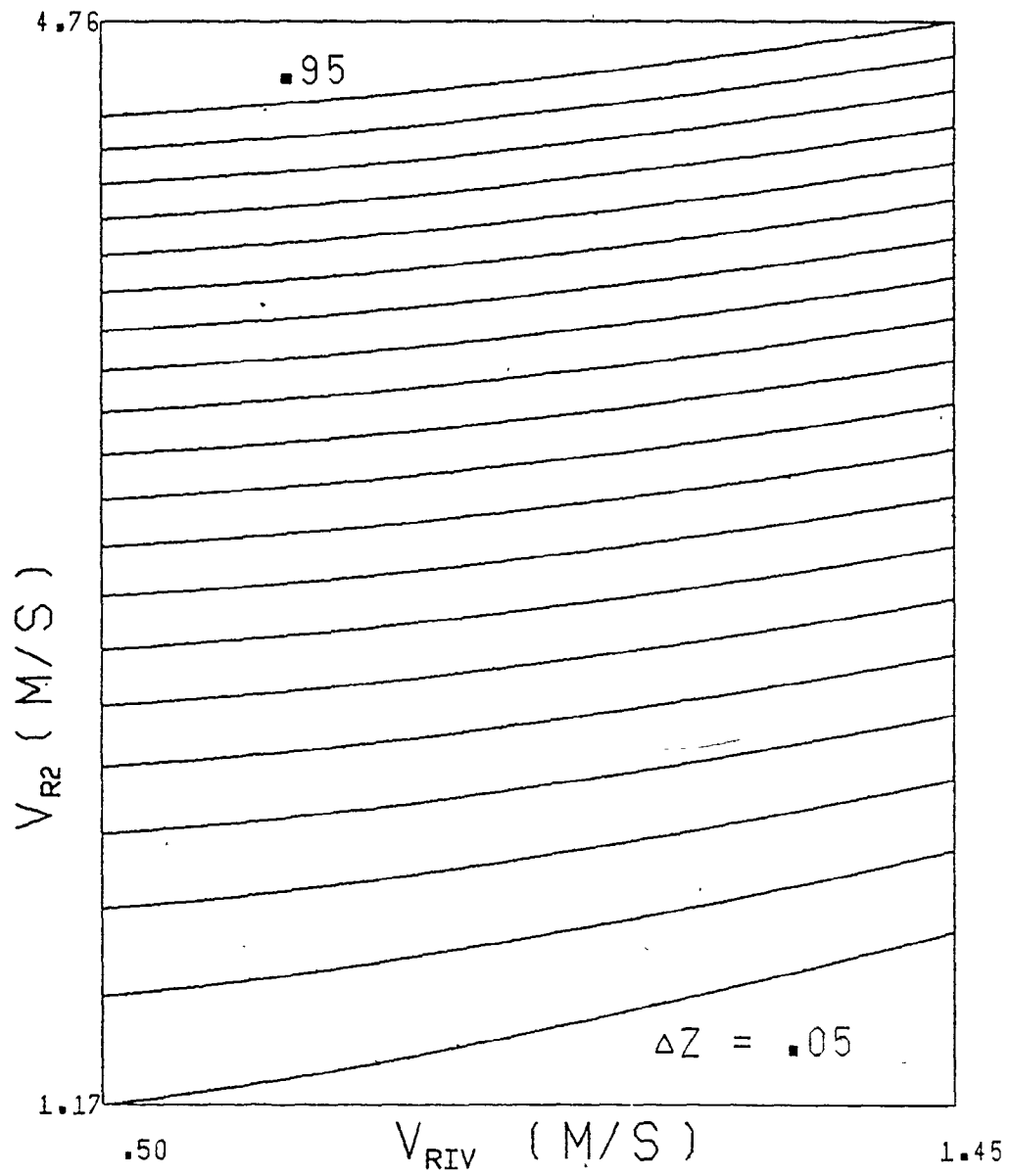
Figure 3-18   The Relative Exit Velocity versus the Upstream River Velocity.

PROGRAM DRIV   U = .5 M/S
                 COLOS = .02
                 ALPHA1 = .2 R
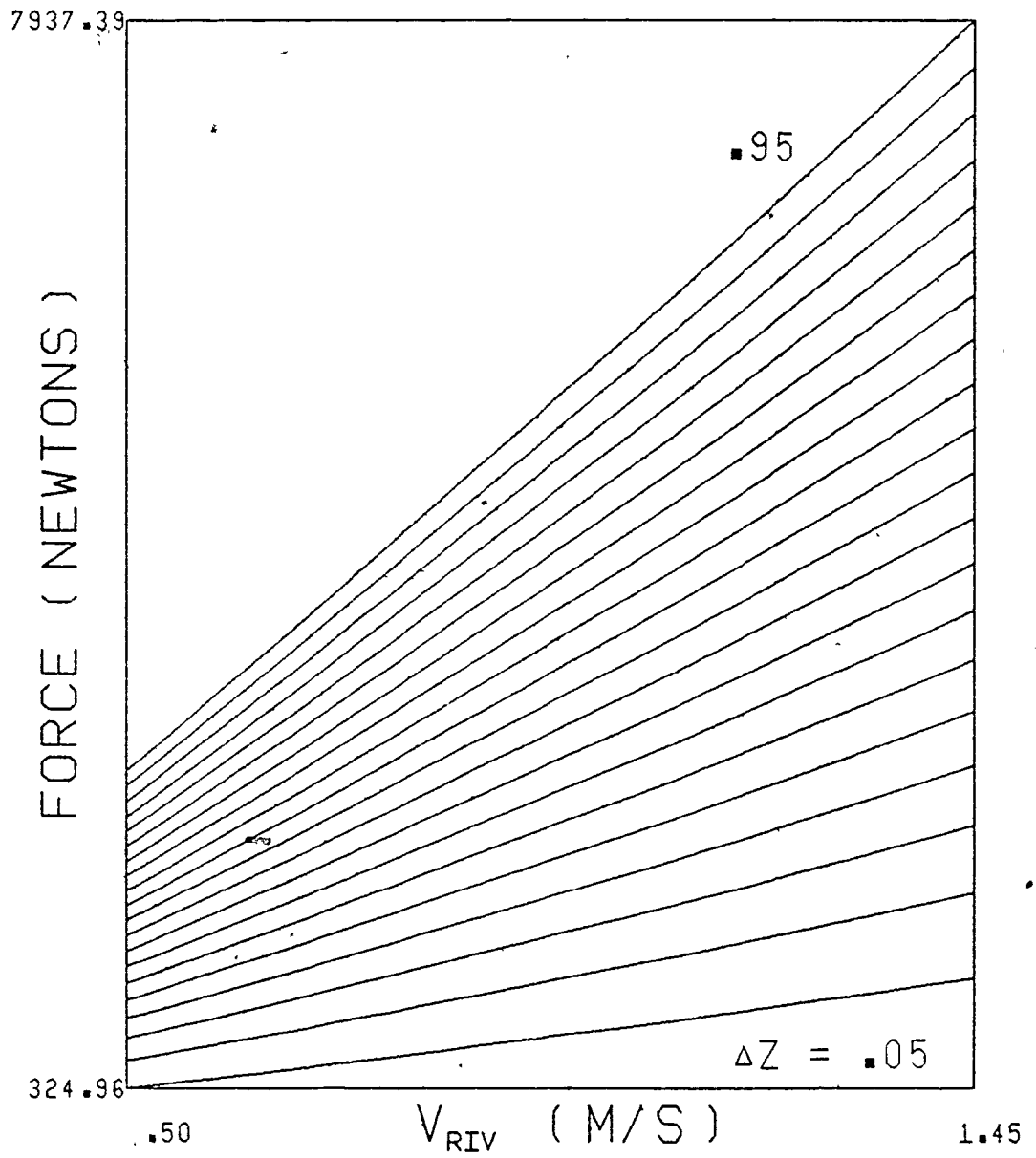
Figure 3-19   The Force on a Blade versus the Upstream River Velocity.

PROGRAM DRIV   U = .5 M/S
                 COLOS = .02
                 ALPHA1 = .2 R
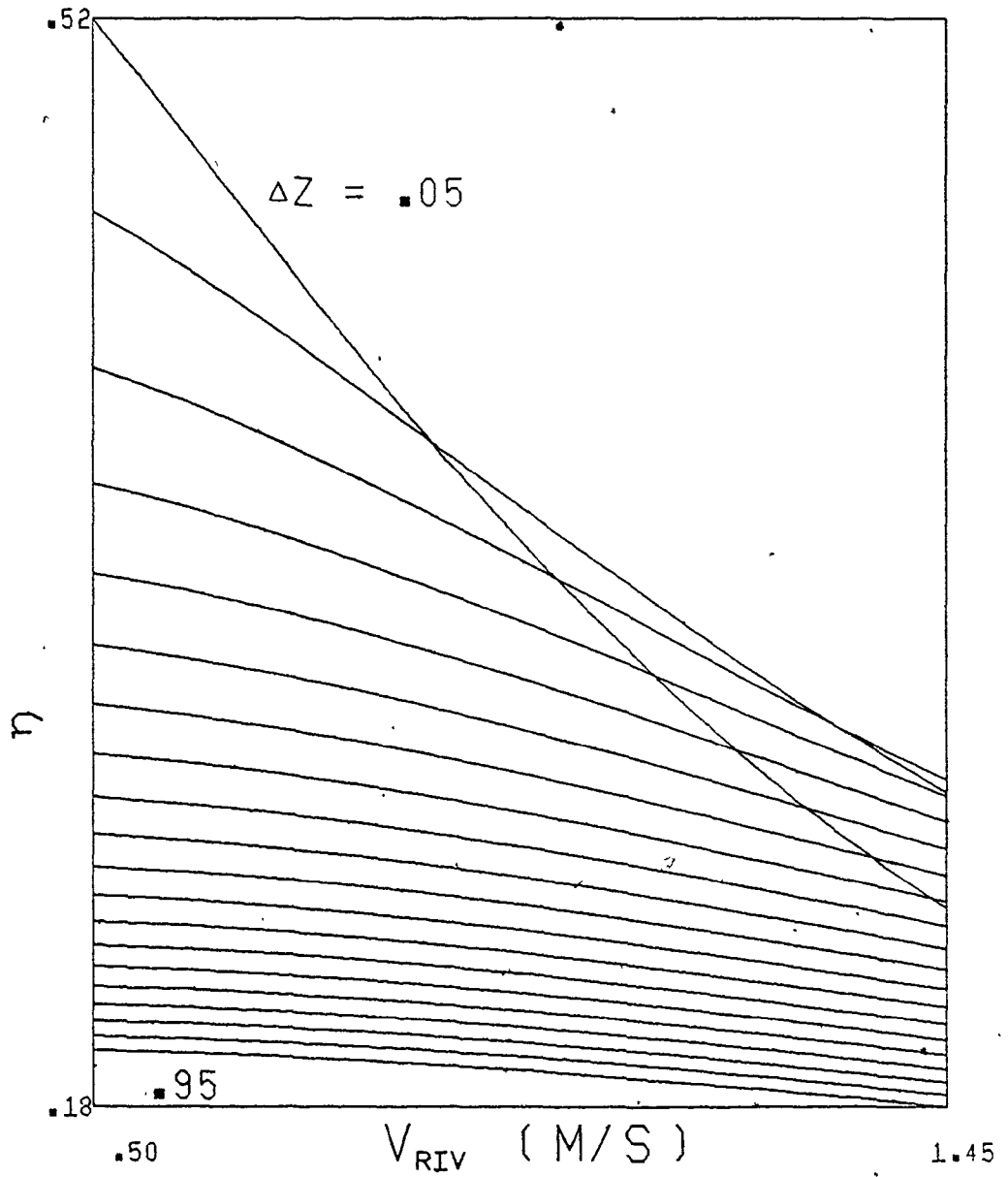
Figure 3-20   Efficiency versus the Upstream River Velocity.

PROGRAM DRIV   U = .5 M/S
                 COLOS = .02
                 ALPHA1 = .2 R
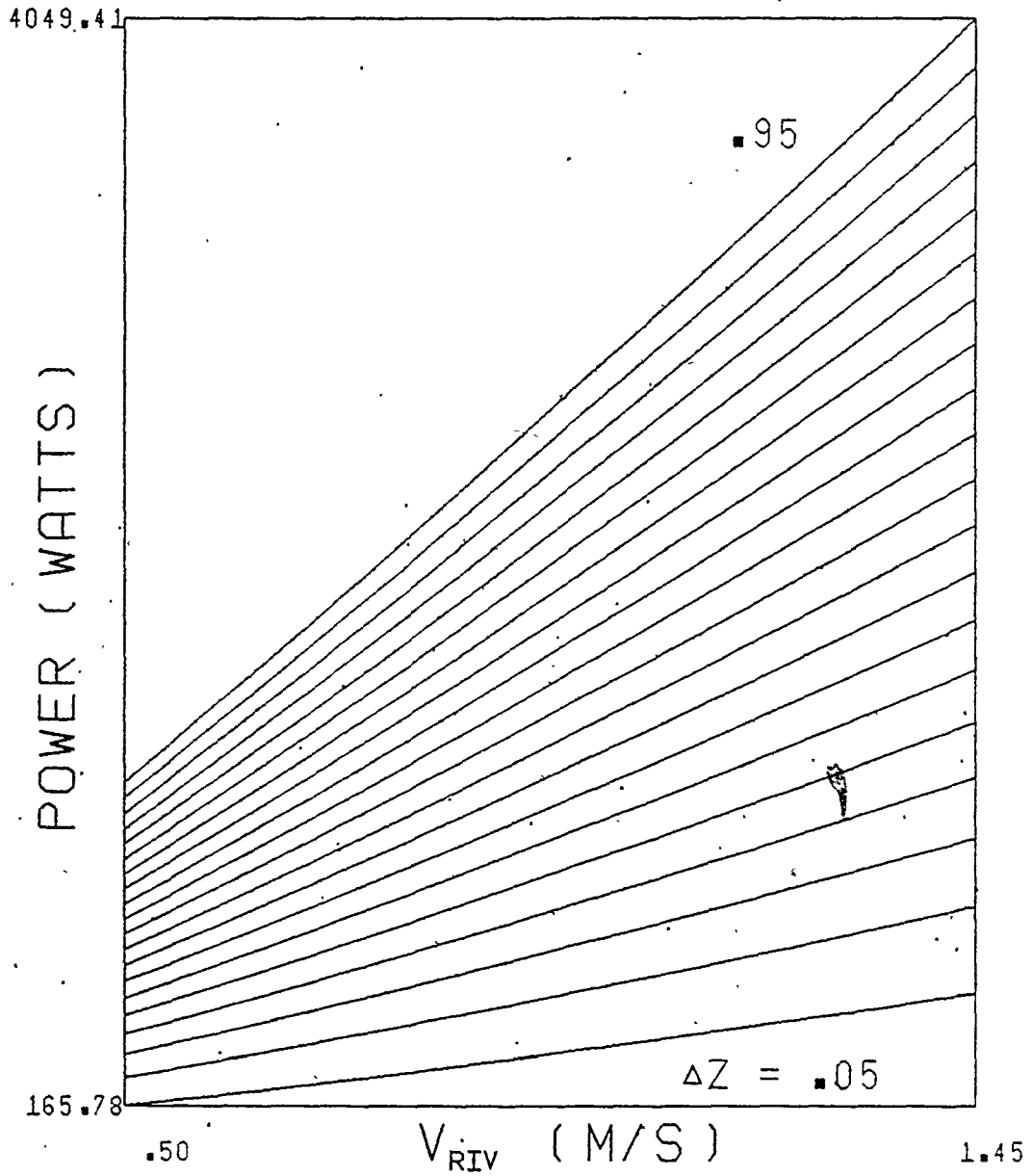
Figure 3-21   The Power Output versus the Upstream River Velocity.

PROGRAM DRIV   U = .5 M/S
                  COLOS = .02
                  ALPHA1 = .2 R
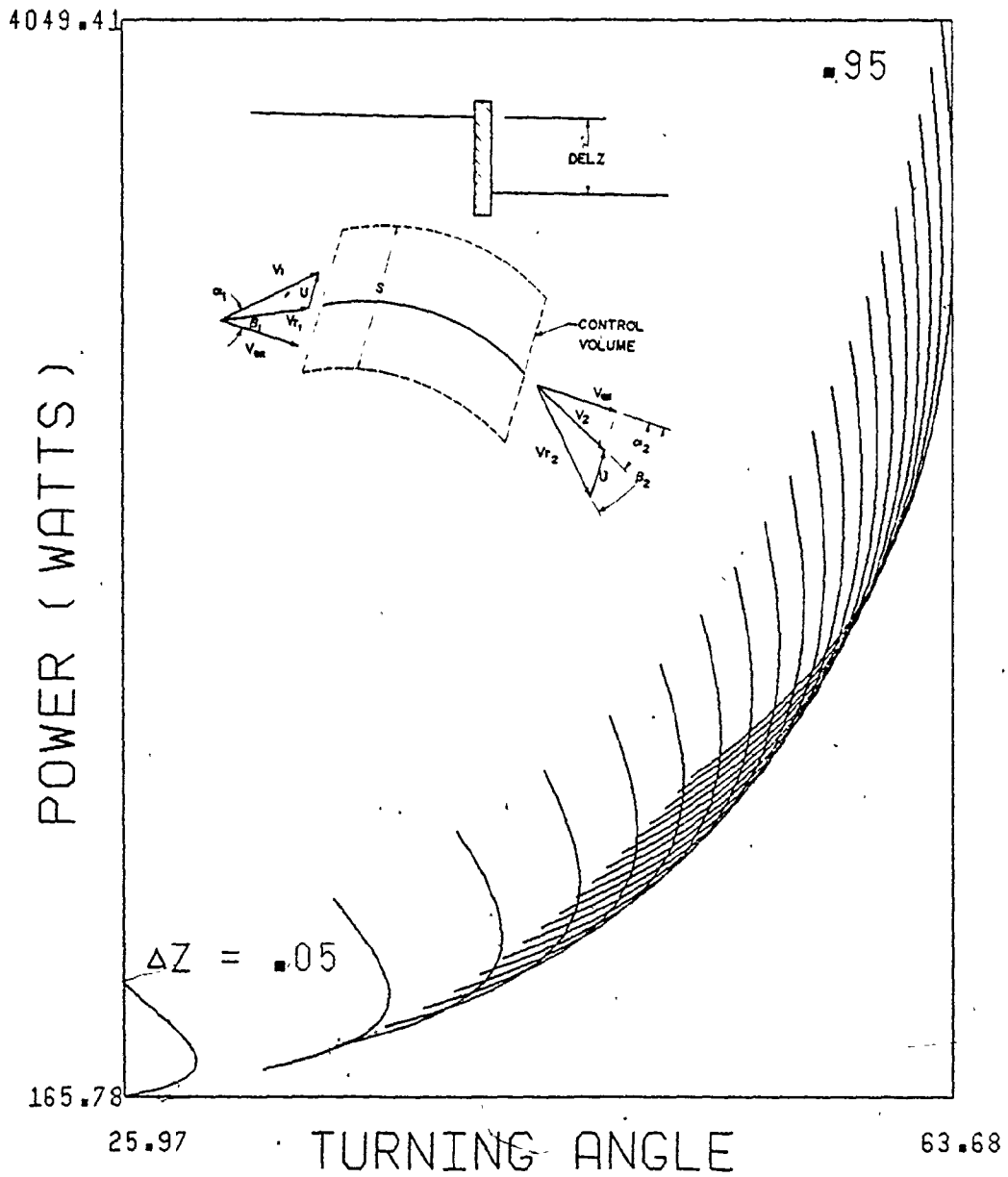
Figure 3-22 The Power Output versus the Fluid Turning Angle.

see Figure (3-20). Furthermore there appeared to be a relation between V_{RIV} and Δz. It is suspected that a minimum ratio exists between V_{RIV} and Δz such that for a value lower than this ratio a power input into the system would be required in order to cause the cascade to translate.

Finally Figure (3-22) presents a plot of the output power versus the turning angle.

The critical point with regard to V_{RIV} is that of blade geometry. The system must be somewhat responsive to changes in the incoming velocity. Two aspects may be considered. (1) The blade angles may be altered to compensate for changes in V_{RIV} in order to maintain a specific level of efficiency. (2) Alternatively blade angles may remain as specified and the resulting inefficiencies accepted. In either case the power into the generator must be governed to avoid generator overload. It was felt that this point could be clarified through further detailed analysis or by tests on an actual model.

3.6 Summary

The preceding sensitivity analysis illustrated several general trends to be considered in the design of a prototype. A large head differential and a high blade velocity are desirable for high power outputs. Also, the loss coefficient C_m is not critical in determining the system's performance. The stagger angle also appears to have little effect on the system. Finally the river velocity does introduce a certain measure of randomness that must be incorporated into a design.

The resulting trends were used on the design of a full size prototype. An outline of the design is given in Chapter (4).

CHAPTER 4

DESIGN THEORY

4.1 Design of a Typical Prototype

This chapter deals with the design of a typical prototype of the water ladder system. Decisions that were made regarding configuration, design variables, material selection, etc. are outlined to illustrate the various criteria which were considered in the design.

4.2 System Design Criteria

Before proceeding to the actual analysis, an overview of the design requirements is made. The following discussion outlines several points which were considered as necessary criteria for the design.

1) The system must first of all be technically feasible. It must be shown through the application of engineering principles that the water ladder system is capable of producing electric power as described.

2) The project must be economically feasible. The cost of construction must be compensated for by monetary returns from the electricity which is produced. Consideration should be given to such aspects as factory assembly, maintenance, etc.

3) Public safety must be assured.

4) The environment must not be seriously degraded.

5)   The implications to navigation, if present, must be considered.

6)   The system may be required to be aesthetically acceptable, depending on the site location.

In addition to the above criteria, consideration was given to the level of technology involved. The system may be constructed using 'state-of-the-art' technology or it may employ available technology for Third World applications. It was decided to pursue the former, for application in the First World Countries.

4.3   Alternate Configuration

The overall configuration of the system was a major point of consideration. The water ladder could conceivably resemble one of the arrangements which are illustrated in Figure (4-1 (a through g)).

A decision to specify horizontal or vertical blades was required. Horizontal blades translate through the depth of the river. Each blade experiences the same static pressure over its span, hence uniform loading on the blade was assumed. (This assumption ignores the river velocity profile due to the fact that the water ladder acts as a restriction. The boundary layer thickness and thus the boundary effects are reduced because of the increased velocity present through the cascade. Hence the water velocity would tend to be uniform along the span as a result of the forced flow of the water.)

a) WATER LADDER WITH NO IMPOSED HEAD CHANGE

b) WATER LADDER WITH RETAINING STRUCTURE

c) WATER LADDER WITH ANGLED CASCADE
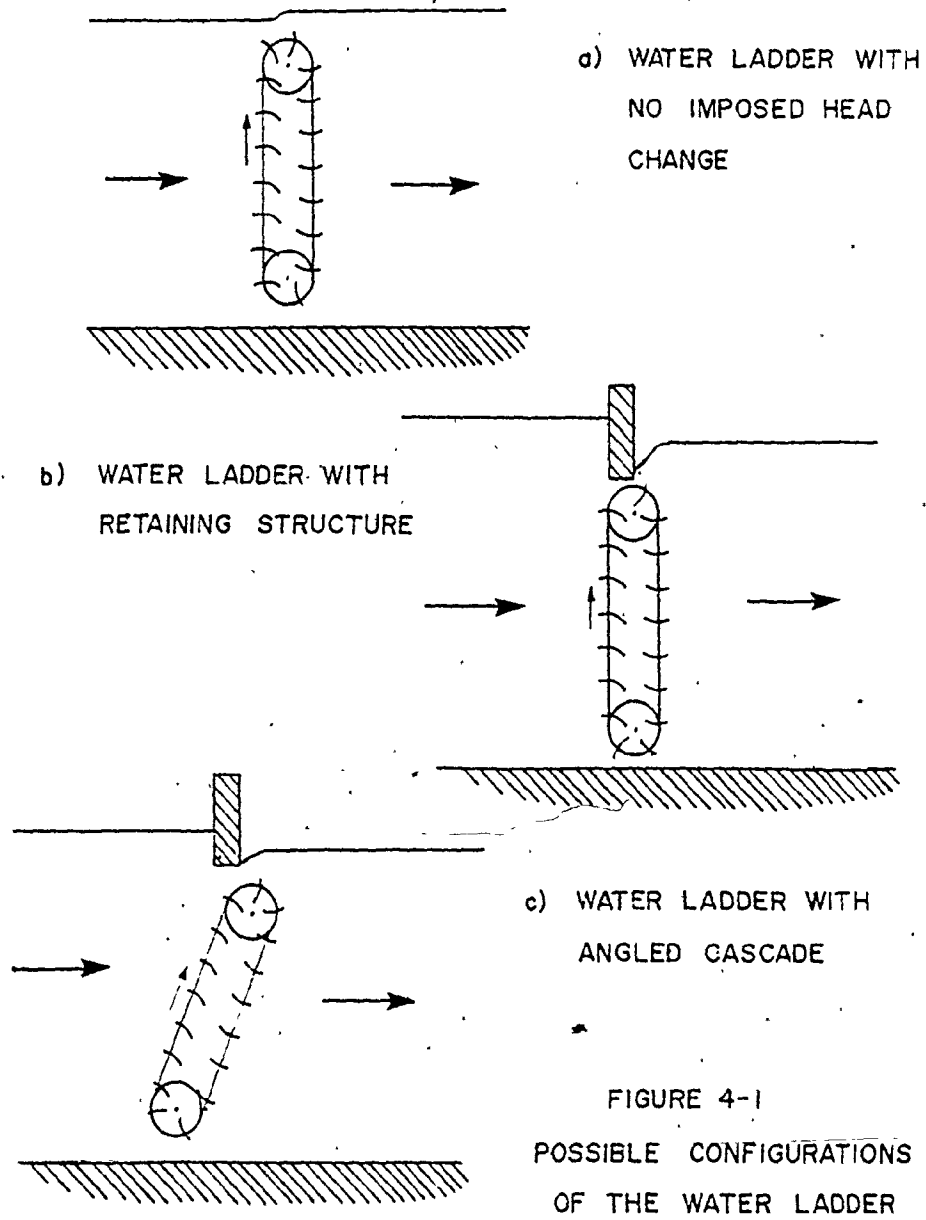
FIGURE 4-1

POSSIBLE CONFIGURATIONS OF THE WATER LADDER SYSTEM

FIGURE 4-1 (CON'T)
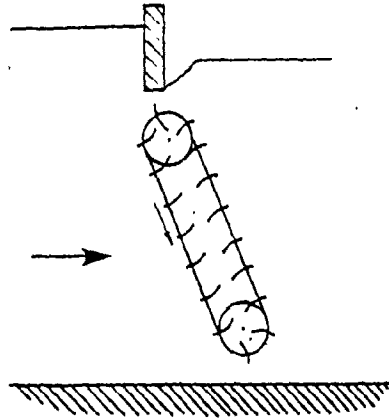
d) WATER LADDER WITH.
ANGLED CASCADE

e) THREE POINT
WATER LADDER
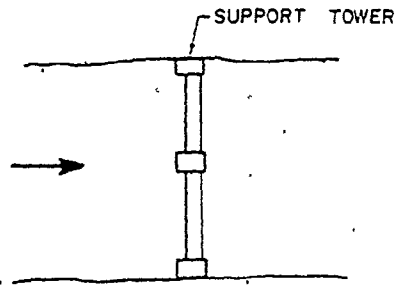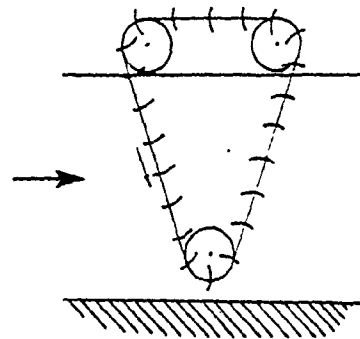
f) PLAN VIEW OF A
HORIZONTALLY BLADED
SYSTEM
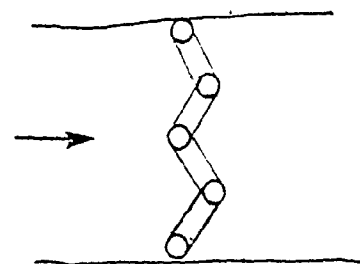
g) PLAN VIEW OF A
VERTICALLY BLADED
SYSTEM

The forces on the blades are likely to be symmetrical about the centre of the span, which is desirable.

Several variations of configurations are shown in Figure (4-1 (a-e)). Figure (4-1a) depicts the simplest arrangement. No head differential is specified although the fluid does reach an equilibrium level difference. The sensitivity analysis showed that the power generated in this case is small. In Figure (4-1b) a retaining structure has been added to the system, thus creating a head differential. This results in a higher power output than for (4-1a). The configurations shown in Figures (4-1c) and (d) incorporate an angled cascade. This allows a greater fluid turning angle and hence a higher power output. In (c) the front cascade of blades rise. The water descends whilst exiting the front cascade and entering the second. This drop in the elevation of the water offers additional potential energy for the system. The blades at the base of the cascade are rotating against the flow direction, thus an energy absorbing action is created. A means of reducing the energy loss is to incorporate a barrier arrangement at the base of the unit to produce an area out of the mainstream flow in which the blades could rotate. Figure (4-1d) illustrates a situation where the front cascade is descending. Water exiting these blades is directed upwards. This action increases the fluid head, thus lowers the output energy available to the blades. However, the blades rotate in the direction of fluid at the lower end of the cascade. Energy would not be wasted in this area as with configuration (c).

It was anticipated that guide vanes would be required bet-
ween the two cascades in both (c) and (d). This aspect is
discussed in further detail later in this section.

Figure (4-1e) illustrates an alternative design which
employs a three-shaft system. An advantage inherent in this
configuration is that guide vanes between the two cascades
are unnecessary, thus eliminating the cost of the vanes.
However, the fabrication cost of the system is expected to
be greater than that for a two-shaft system (4-1c) because
of the increase in the number of blades and the added complex-
ity of the mechanism.

Figure (4-1f) is a plan view of a horizontally bladed
system.

The other major alternative is to employ vertical
blades which would translate across the river. Figure (4-1g)
illustrates a possible configuration. The depth of the river
is not required to be as great as for the horizontal blade
system since the space required to rotate the blades would
be located to the sides, rather than at the bottom and top
of the river. There is more flexibility in system configura-
tion since the cascade may be angled to the direction of
water flow. Several disadvantages exist in a system incorporat-
ing vertical blades. Firstly, static pressures along the span
of the blades vary with depth. This may cause added stress
or an unevenly distributed stress on the blades. Secondly,
although the span of the blades would be smaller than in a
system with horizontal blades, the number of blades involved

is larger. Thus the number of blade supports, linkages,
etc. increase adding friction to the system, as well as
increasing the fabrication costs.

Considering the assets of horizontal and vertical
blades, horizontal blades were selected for the design. A
configuration similar to that shown in Figure (4-1c) was
adopted. The arrangement shown would seem to offer the highest
power output per unit cost, for reasons discussed above.

The necessity of guide vanes between the two cascades
was considered. Figure (4-2) shows a simplified velocity
diagram of fluid flow in the region between the cascades.
The fluid exiting the first cascade is likely turbulent,
producing vortices and wakes. Considering ideal flow, the
absolute velocity V_2 exits the front cascade at an angle α_2,
see Figure (4-2). The inlet angle β_3, is the angle between
the incoming velocity relative to the downstream blade and the
axial velocity. A negative incident angle results as Vr_3
encounters the rear cascade (since β_2 is great than β_3) which
would also be the case even if α_2 was zero. Hence guide vanes
are most likely necessary for maximum efficiency, however
the fluid flow characteristics in this region between the two
cascades require further study.

4.4   Preliminary Design Considerations

A hypothetical site was considered for the design of
the prototype as shown in Figure (4-3). The values of the
width and the depth are 6.0 and 4.2 metres respectively.
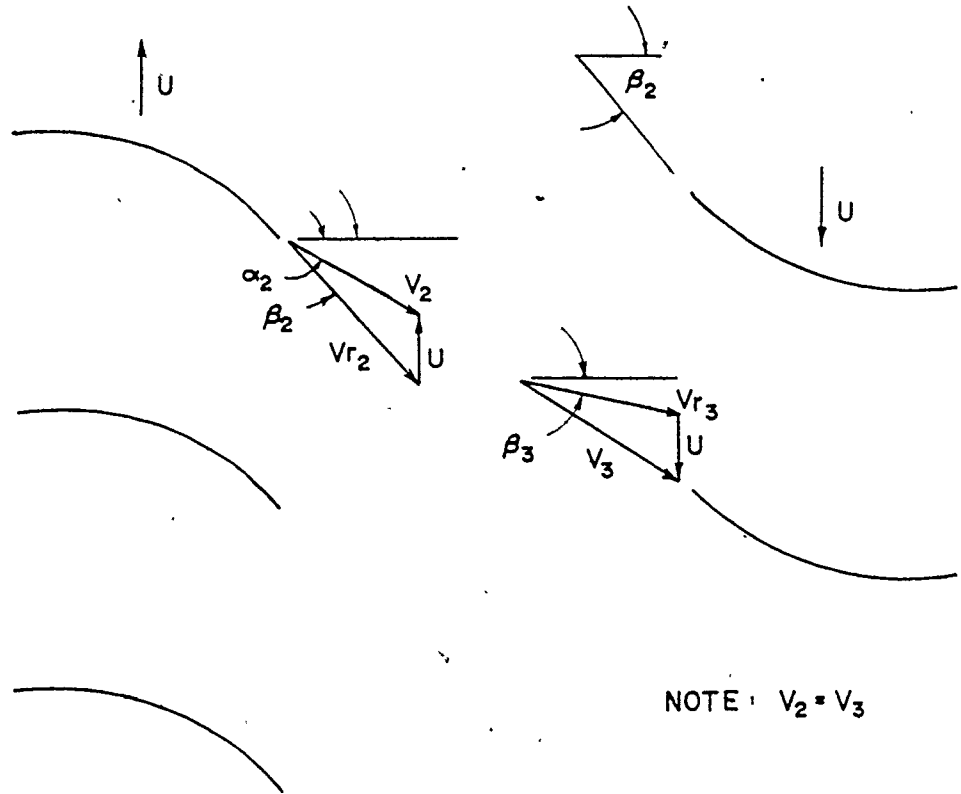
FIGURE 4-2

FLUID FLOW BETWEEN CASCADES

VRIV

DEPTH

WIDTH
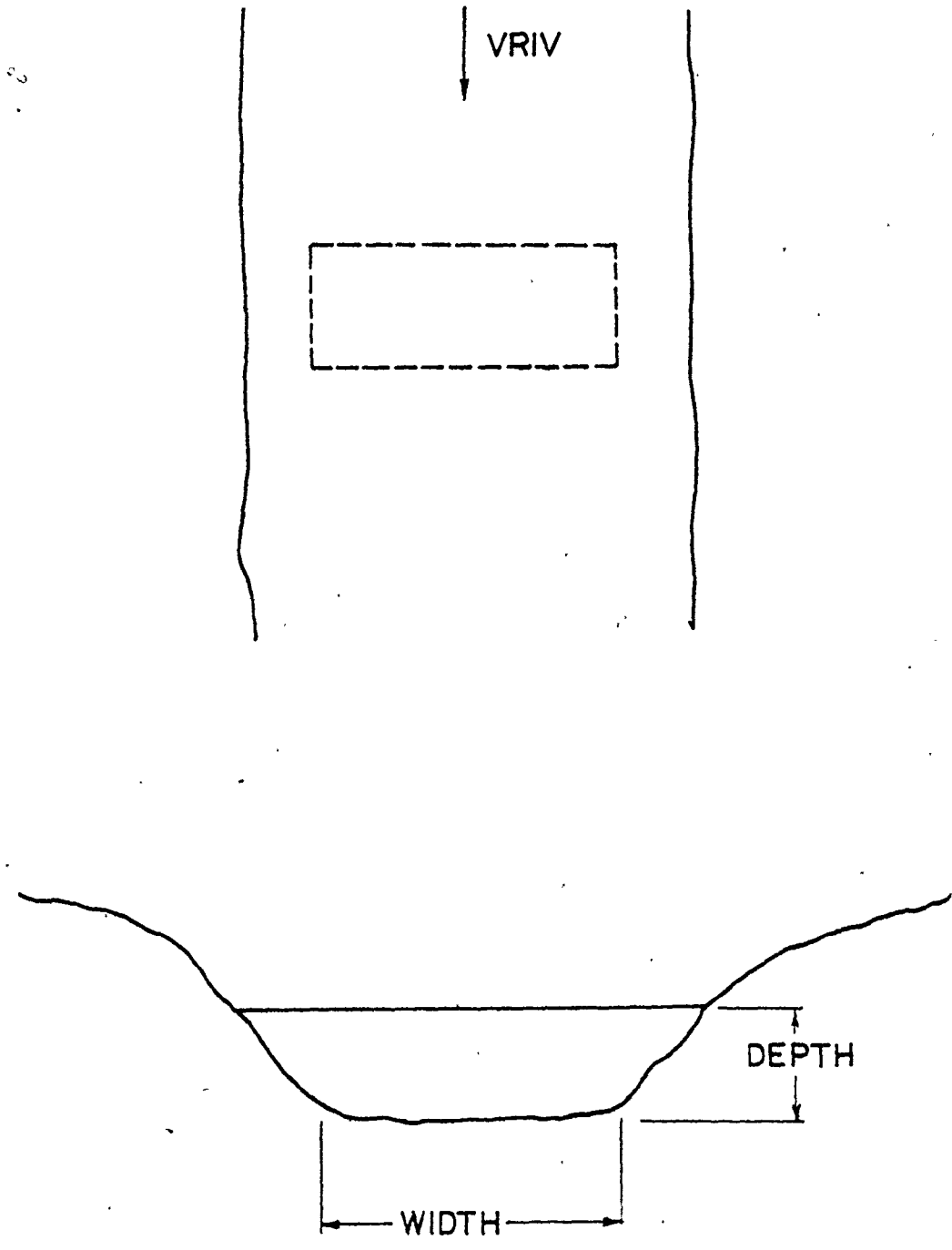
FIGURE 4-3

SITE CONDITIONS

The design variables of the blading were selected on
the basis of the sensitivity analysis and model similation.
The selection considered several major points as outlined
below.

It was found that the power output increased with the
fluid turning angle. There exists a maximum limit on the
magnitude of the turning angle, this being the point at
which separation occurs. By referring to existing turbine
data, this limit was established to be about 70°. It was
also determined in the sensitivity analysis that it was
advantageous to specify as large a value as possible for Δz.
However the actual value for Δz selected is dependent upon
site conditions as well as the limiting fluid characteristics.
In raising the water level upstream of the water ladder the
area of land required and the associated costs must be considered.
In this particular design, upstream conditions were assumed
to be favourable to permit a water level rise. Δz was arbitrarily
chosen to be .4 m. A corresponding value of 54° for the turn-
ing angle resulted.

There is a maximum amount of energy which can be
removed from the river. The amount is dependent upon the
entry and exit river velocities and the head differential.
The velocity at which the blade translates, u, is also
dependent upon the quantity of energy removed from the river.
A minimum force on the blade is required in order to overcome
the friction present in the system from the mechanical equip-
ment. Hence a peak blade velocity exists since the force on

the blade decreases with increasing blade velocity, see Chapter (3). Conservation of energy across the system determined the maximum blade velocity possible, see Equation (2.7).

The blade velocity u was chosen to be .5 m/s which is one half of the river velocity. Simulation tests showed that this blade motion utilized approximately 25% of the energy that was available upstream, as defined by Equation (2.21). A system with a blade speed as specified approaches the maximum possible velocity as limited by conservation of energy.

The energy lost over the blades, which was defined by C_m, was assigned a value of 2%. A survey of loss coefficient data established that this value was reasonable, although somewhat optimistic rather than conservative. The simulation had shown that the power output was not very dependent upon C_m, hence it was decided to evaluate the system at this optimistic value for C_m of 2%. The fact that C_m was chosen to be small, compensated for neglecting the effect of the incident angle on the blades. (It is anticipated that the fluid encountering the blade at an incident angle will contribute to the power output of the system.)

Finally, the river velocity V_{RIV}, was set at 1 m/s. It was thought that this was a reasonable magnitude for the system to be practical plus sufficiently small to be representative of certain typical rivers.

The computer simulation was programmed with the following values for the design variables.

$\alpha_1 = .2$ radians

$$\Delta z = .4 \text{ metres}$$

$$C_m = .02$$

$$u = .5 \text{ m/s}$$

$$V_{RIV} = 1 \text{ m/s}$$

This resulted in the following blade characteristics.

$$\theta = .946 \text{ radians } (54^\circ)$$

$$\alpha_2 = -1.128 \text{ radians } (-64.6^\circ)$$

$$\beta_1 = -.253 \text{ radians } (-14.5^\circ)$$

$$\beta_2 = -1.200 \text{ radians } (-68.8^\circ)$$

$$Vr_1 = 1.119 \text{ m/s}$$

$$Vr_2 = 2.99 \text{ m/s}$$

$$\text{Solidity} = .942$$

$$F_y = 2709 \text{ N/m}^2$$

$$P_T = 1382 \text{ Watts/m}^2 \text{ -span -depth}$$

$$\eta = .27$$

These values were used in the design of the prototype and are shown in Figure (4-5).

The form of the blade was chosen as being a cambered plate. A deviation angle, δ, was added to θ in order to determine the blade turning angle. See Figure (4-4). By Constant's Rule

$$\delta = .26 \cdot \theta \sqrt{\text{Solidity}} \qquad\qquad [45, \text{ pg. } 150]$$

Hence $\delta = .239$ or 13.7°. The blade exit angle is $\gamma_2 = -\beta_2 - \delta = -1.44$ or 82.4°.
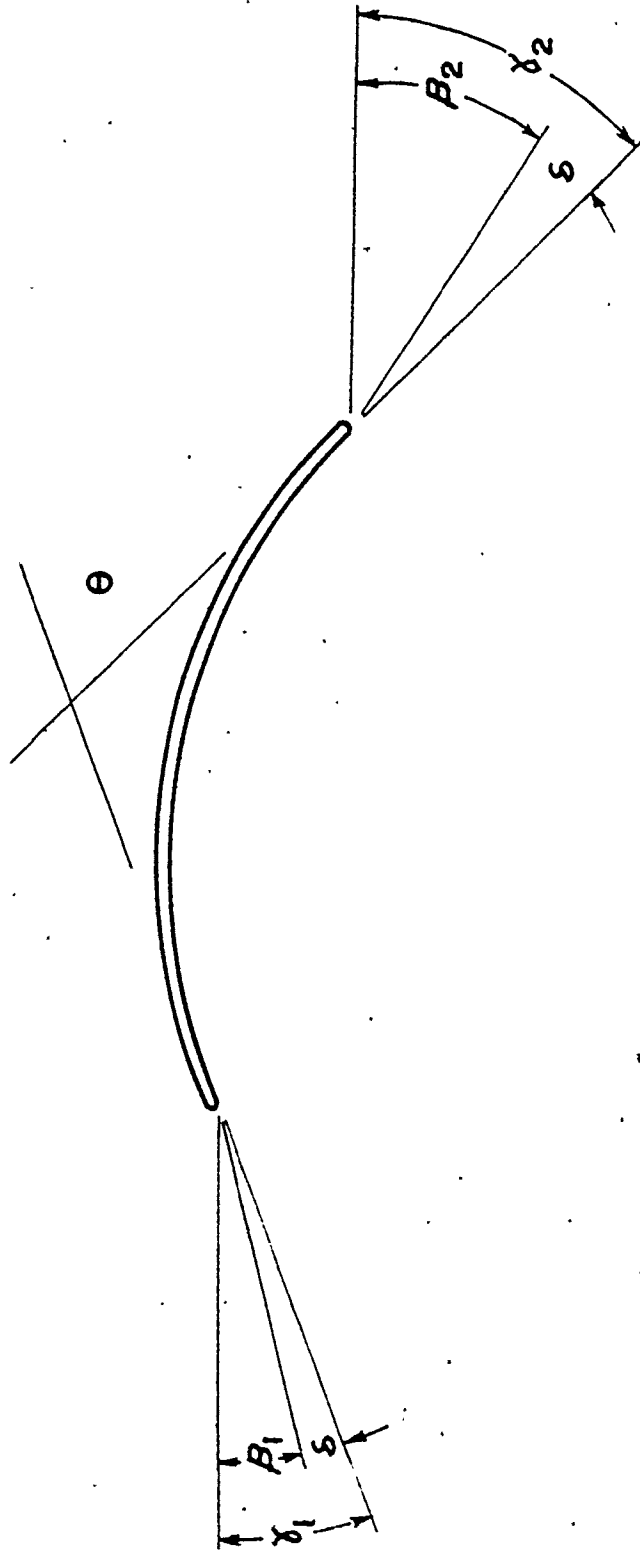
FIGURE 4-4

BLADE AND FLUID FLOW ANGLES

$\alpha_1 = 12°$ $V_1 = 1.1$ $U = .5$

$\beta_1 = 14.5°$ $Vr_1 = 1.1$

$\theta = 54°$

$V_{ax} = 1.08$

$\alpha_2 = 65°$

$\beta_2 = 69°$

NOTE: ALL VECTOR QUANTITIES ARE IN METRES / SEC

α_1

$V_2 = 2.5$

$Vr_2 = 3.0$ $U = .5$
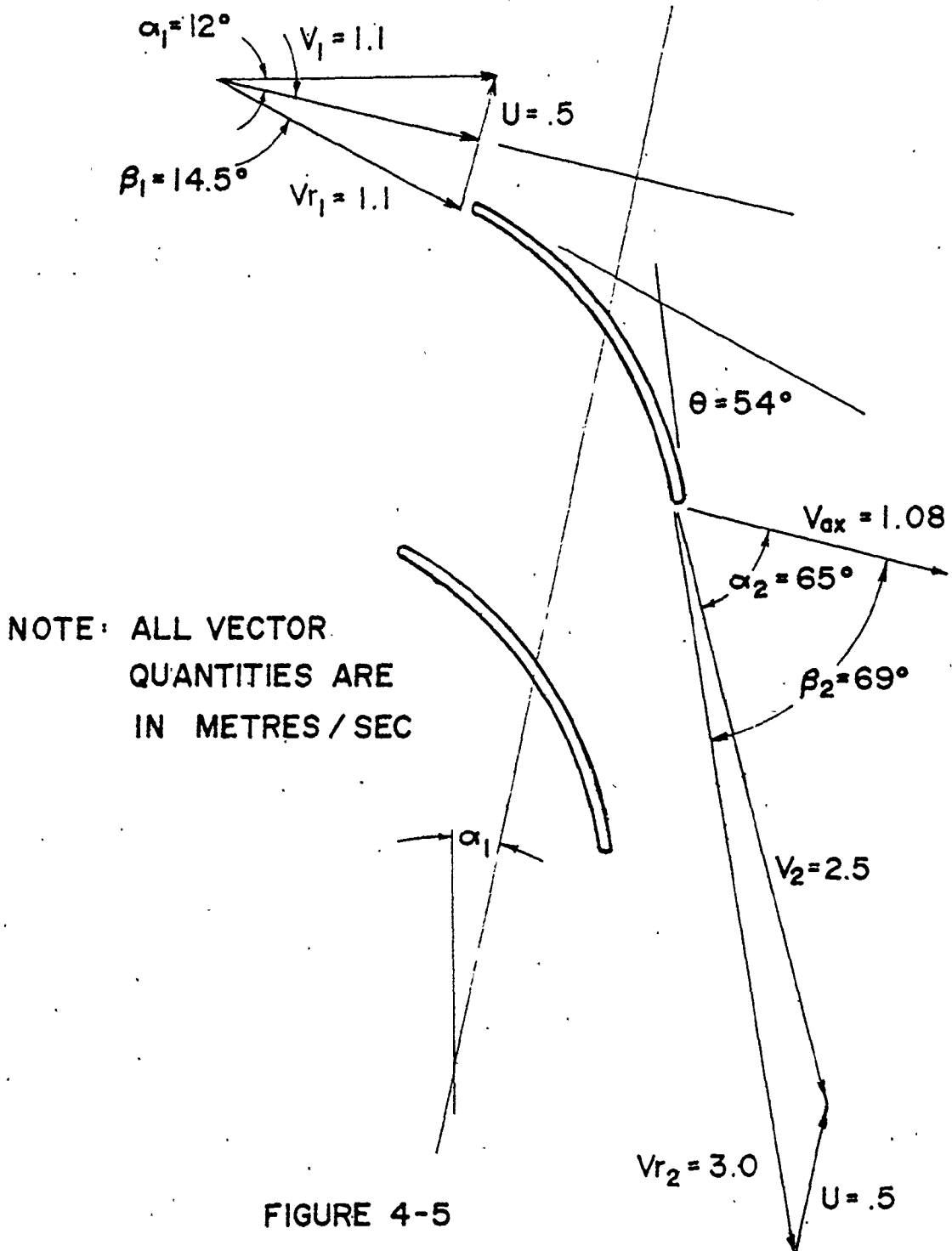
FIGURE 4-5

FINAL BLADE DESIGN

The value for the solidity was determined from Zwieffel's equation, Equation (2.22). The spacing s was found from

$$s = (\text{solidity})(\text{axial chord})$$

and axial chord = chord $(\cos \beta_m)$

where $\beta_m = \arctan((\tan(\beta_1) + \tan(\beta_2))/2)$

Therefore,

$$\beta_m = -.956 \text{ radians } (55^{\circ})$$

and   chord = $\cos(-.956)$ (.6)

$$= .35 \text{ m.}$$

spacing   s = (.942)(.35)

$$= .33 \text{ m.}$$

The spacing was assigned a value of .4 m. The slight increase in the selected value of s was made in order to reduce the number of blades since they are the most expensive component of the system. It was felt that the optimum spacing was not very critical at the low fluid velocities involved.

The values for the spacing and the chord length appeared acceptable in that the aspect ratio of the blades (span/chord) was of a reasonable magnitude.

The radius of curvature and the chord-depth ratio of the blade were determined from,

$$r = \frac{\text{chord}}{2 \sin \frac{\theta}{2}}$$

and

$$\frac{.6}{2 \sin (\frac{.946}{2})} = .66 \text{ m} \tag{45}$$

Depth to chord ratio $\frac{b}{c} = \frac{1}{2} \tan (\frac{\theta}{4}) = 12\%$ [45]

These parameters were used in stress calculations of the blade.

A calculation was done to determine whether cavitation would occur.

At a depth of .5 m below the upper water surface,

Vapour pressure of the water, p_v = 882 N/m^2 (5°C)

$\qquad\qquad\qquad\qquad\qquad\qquad$ = 2450 N/m^2 (20°C)

Cavitation No., $k = \dfrac{p - p_v}{\frac{1}{2} \rho V_m^2}$ where V_m is the average velocity

and p is the static pressure.

At a depth of .5 m, p = .5 (1000) (9.8) = 4900 N/m^2.

From the computer output Vr_1 = 1.119 m/s

$\qquad\qquad\qquad\qquad\qquad\qquad$ Vr_2 = 2.99 m/s

$\therefore \quad V_m = Vr_1 = \dfrac{\cos (\beta_1)}{\cos (\beta_m)} = 1.9$ m/s

The cavitation number, k, is

$$k = \frac{4900 - 822}{\frac{1}{2}(1000)(1.9)^2} = 2.22 \quad @ \ 5^\circ C$$

$$\frac{V_k}{V_1} = \sqrt{1+k}$$

Hence $\dfrac{V_k}{V_1} = 1.79$

$\qquad\qquad V_k$ = 2.0 m/s

Since the velocity at the onset of cavitation V_k is

less than the velocity of the fluid, cavitation will occur with a blade at a depth of /.5 m. Empirical tests to confirm the onset of cavitation may be required.

The force on the blade was calculated to be 2709 N/m^2 for blades having a spacing of 1 metre. In the case of the prototype design, spacing is .4 metres, hence the force on the blade is 1084 N/m span.

The power output was determined to be 1382 Watts/ m span - vertical depth. Eight blades were specified to be in the mainstream. Therefore the depth of the mainstream was (.4)(8) cos (.2) = 3.14 m. The span of the blades were assigned a preliminary value of 5 metres. Hence, the power output of the system would be

$$(5)(3.14)(1382) = 21.7 \text{ kW}$$

Note that this value was arrived at by only considering the power output of the front cascade. The power contribution by the rear cascade is uncertain because of the turbulent nature of the flow exiting the front cascade. Ignoring the contribution represents the minimum transfer of energy out of the river, thus producing a very conservative estimate of the power output. Guide vanes were omitted in the design.

It is appropriate to consider the energy mechanics of the system that has been specified, see Figure (4-6). The upstream and downstream static and dynamic heads are expressed in terms of an energy level in spite of the fact that the dynamic heads are unavailable to electric power generation as a result of continuity considerations.

a) ENERGY LEVELS

PRESSURE HEAD

ENERGY WITHDRAWN

VELOCITY HEAD

DATUM
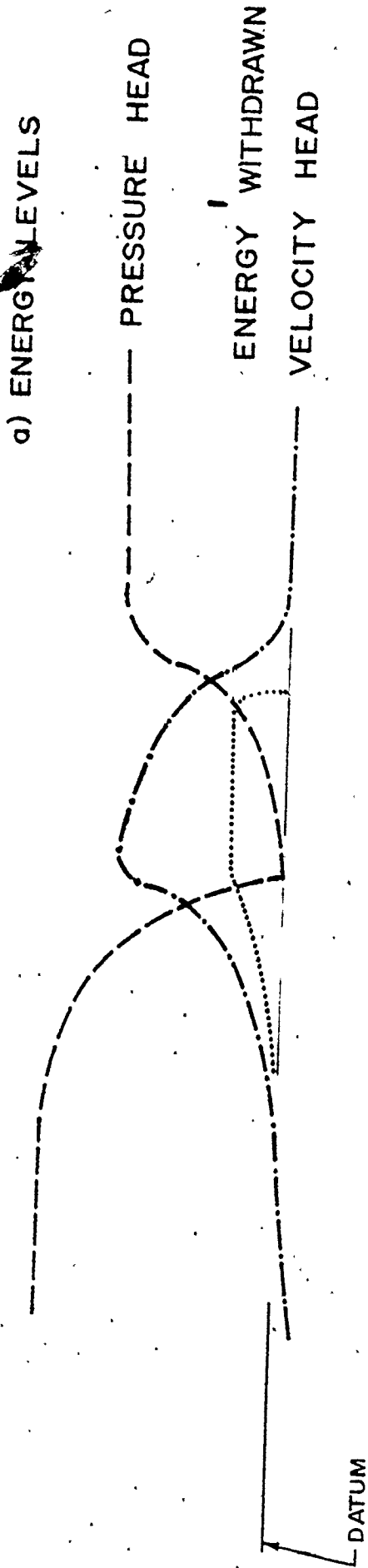
b) PROFILE VIEW
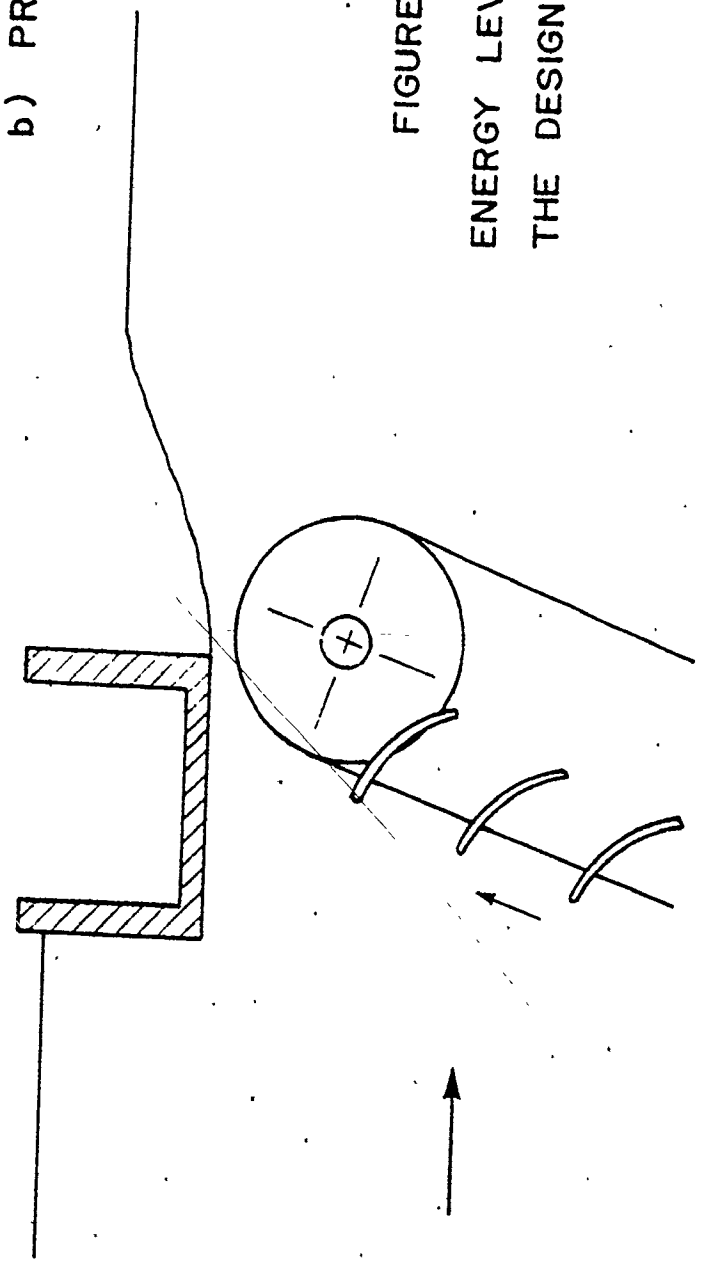
FIGURE 4-6

ENERGY LEVELS OVER
THE DESIGN CASCADE

At the upstream inlet of the cascade, the energy level of the static head is

$$E_z = z_1$$
$$= .4 \text{ m}$$

The upstream velocity head has an energy level of

$$E_{V_1} = \frac{V_1^2}{2g}$$

$$= \frac{(1.105)^2}{2(9.8)}$$

$$= .062 \text{ m}$$

Hence the energy level at the entrance of the water ladder system is .462 m.

As determined from the model, approximately 27% of the inlet energy may be converted to usable power. Hence,

$$E_{OUT} = .127 \text{ m}$$

and

$$P_{OUT} = E_{OUT} \cdot \rho \cdot g \cdot V_1$$

$$= (.1274)(1000)(9.8)(1.105)$$

$$= 1382 \text{ watts/unit area}$$

The value of P_{OUT} was also determined using the computer model.

Two percent of the inlet energy is wasted as friction and is defined by C_m.

$$E_f = .02 (.462) = .009$$

The exit velocity, V_2 was determined from Equation (2.14) to be 2.53 m/s. The energy level was

$$E_{V_2} = \frac{V_2^2}{2g}$$

$$= \frac{(2.53)^2}{(2)(9.8)}$$

$$= .326 \text{ m}$$

To ensure an energy balance a summation of the exit energy levels was performed.

$$E_{TOTAL} = E_{OUT} + E_f + E_{V_2}$$

$$= .127 + .009 + .326$$

$$= .462 \text{ m}$$

Thus the inlet and outlet energy levels are equal.

The downstream river velocity may be determined from continuity and energy considerations. The presence of the downstream cascade is ignored for the present. The energy level at the exit of the system was .326 m. However, the ultimate axial velocity must be 1.105 m/s in order for continuity to be upheld and assuming that the upstream and downstream cross-sectional areas of the river are equal. The upstream and downstream dynamic heads are then equal to .062 m. Hence the downstream water level must rise to an equilibrium level. In this particular case,

$$E_{z_2} = .326 - .062$$

$$= .26 \text{ m}$$

The depth downstream is approximately .26 m relative to the datum shown in Figure (4-6). As a result of the use in the water level, there will be an increase in the cross-

sectional area of the river. For mass continuity across the system, the river velocity is decreased, therefore z_2 has a slightly higher value than the .26 m calculated above. The exact value of z_2 may be determined through several iterations of the above energy and continuity calculations.

If the excess energy is sufficiently large at the exit of the system, a hydraulic jump may be found. Otherwise a gradual rise in the water level is observed.

In the preceding analysis it was assumed that only the upstream cascade withdrew energy from the river. If both upstream and downstream cascades are considered a greater amount of energy is removed. The result is that less energy remains in the river flow downstream of the cascades than in the previous case, hence the downstream water level will be lower. The ultimate result is that the system possesses a greater efficiency. i.e., As much as 50% of the available energy is being transformed into usable power, assuming ideal fluid flow. The actual amount of available power however would be somewhat lower.

The fact that only 50% of the available power is being removed suggests that a greater efficiency may be possible. From the previous calculations regarding the available power upstream, Δz produces the largest portion of the incoming energy. The velocity head is of secondary importance, since the exiting velocity head is approximately equal to the incoming velocity head at points taken far downstream and upstream respectively. Thus the energy represented by Δz is

converted into available power, losses or downstream static head, z_2. The design variables were selected to maximize power output and minimize losses and downstream static head. Note that z_2 equal to zero was considered to be optimum since this condition implies that all available energy was withdrawn for power production.

Explicit data is required to determine what portions of Δz are converted to losses and to downstream static head. Detailed information on the fluid flow characteristics in the region between the cascades is necessary to estimate these portions, since the majority of losses occur in this region. Ultimately it was decided to reduce the power contribution from the downstream cascade to one half of the upstream cascade as an approximation to compensate for losses incurred.

It should be noted that optimum operating conditions (i.e., $z_2 = 0$) may be achieved by altering the blade velocity as required. The design parameters (i.e., turning angle, blade shape, etc.) should be changed accordingly.

4.5   Detailed Prototype Design

At this point there was sufficient information to design the prototype. The design synthesis is given in Appendix (B).

The basic design consists of a completely factory assembled unit fabricated according to site requirements and river flow characteristics. The unit would be transported to the proposed system location and installed intact with minimum site work.

Major components of the unit are the blades, the blade mounts, sprockets, mainshafts, generator and support structure. The layout of these components is illustrated in Figures (E-1 through E-6) and in drawings presented in Appendix (B).

The proposed design exhibits a number of innovations. The blade mounts are the most intricate components of the system. They locate and maintain the blade in an appropriate position in space and provide a means by which the blades may translate and rotate.

The package concept for the water ladder system lowers the overall cost by reducing the site work required for installation. It also provides the water ladder with a certain degree of mobility, in that the unit may be relocated intact to a new site after the initial installation.

There is however a limit to the size of the factory completed unit for transportation reasons.

4.6   Winter Operation

Operation of the water ladder during the winter months requires that the system withstand cold temperatures, ice and snow. Of these three conditions, ice is potentially the most destructive. Ice can become lodged in the cascade blades or in the linkage thus jamming the mechanism. The restriction to the river flow which is created may result in upstream flooding.

The extent to which ice can be tolerated is a function

of the site characteristics. In small rivers, a sufficient
water supply may not be available to maintain the required
water level at the site. Thus the system components may be
exposed to ice, including the blades, sprockets, and linkage.

A means of protection is provided by the trash racks
upstream of the system since they prevent the bulk of the ice
from reaching the water ladder. However they must be cleared
and maintained throughout the winter months. In the immediate
vicinity of the water ladder a floating barrier may be
installed to restrict contact between the ice and the blades.

Snow and cold temperatures were not considered to be
serious problems. Adequate protection is required for the
electrical components however.

4.7   Environmental Impacts

One of the design criteria stated previously was to
ensure a minimum environmental impact. The negative effects
which are associated with most dam construction are significantly
reduced in the water ladder system. The reservoir which is
created is small, and as a result the river velocity is not
greatly altered. Hence the majority of silts, nutrients, etc.
remain suspended in the river flow.

The effect of the water ladder on fish is anticipated
to be lower than that for a hydraulic turbine facility. For
example, gas bubble disease and mortality in the blades is
reduced because of the lower fluid velocities involved. Fish
migration is interrupted however. A pass may be created if

deemed to be necessary.

Overall, river ecology is disturbed very little aside from the actual site during construction.

4.8 Navigation

The proposed design is incompatible with the requirements for navigation. If the water ladder is to be incorporated into a navigable river provisions must be made to accommodate this. Providing an alternate channel for vessels is a possible solution, however high costs are involved. On very large channels, a narrow section of the river may remain open. If the normal mass flow is sufficiently large, the open section will not allow equal water levels to be met on the upstream and downstream sides. The required differential head can then be provided.

For smaller watercraft, portaging is a possible solution.

Overall the general conclusion is that navigation and the water ladder system are incompatible as is the case for hydroelectric dams.

4.9 Public Safety

The risk to the public is basically to swimmers who may venture into the boundaries of the system. Trash racks which cover the entire cross-sectional area of the river both upstream and downstream of the system site would eliminate any danger to swimmers as described in Appendix (B).

CHAPTER 5

ECONOMIC ANALYSIS AND
PROJECT EVALUATION

The economic analysis for the project consisted
of an estimate of the construction cost and consideration
of the maintenance required. By studying these aspects of
the water ladder system an indication of the economic via-
bility was obtained.

5.1   Cost Estimate

The cost estimate attempted to entail all facets of
the system. Due to the complexity of the project, estimates
of detailed components were not made in general. Rather, .
material requirements were tabulated and a cost estimate was
made on the basis of this estimate. Obtaining the costs for
some particular components such as the main shafts, sprockets,
etc. involved contacting several suppliers. An overall bulk ·
estimate was made for small items such as bolts, bearings,
etc.

As stated in Chapter (4), it is proposed that the
unit be factory assembled and transported intact. To a cer-
tain·extent fabrication may involve mass production. No
provision was made for this fact in the cost calculations..

Table (5-1) summarizes the cost estimate for the system
and Appendix (D) gives detailed calculations of these figures. .

Table (5-2) introduces some added on site installation

Table 5-1

Cost Estimate

Item	Quantity	Amount kg	Price*	Total
Blades	24	160	$10/kg	$38,400
Blade Mounts	48	18.6	$10	$ 8,930
Sprockets (SS)	4		$1,200	$ 4,800
Main Bearings	4		$100	$ 400
Main Shaft	2		$1,000	$ 2,000
Structural Steel	1	2,650	$4/kg	$10,600
Misc. Parts				$ 5,000
20 kW Generator	1		$3,000	$ 3,000
			Total	$73,100
(Federal taxes, etc.)			+ 10%	$80,400

If 17 kW are produced, the cost is $4,700/kW

If 26 kW are produced, the cost is $3,100/kW

* Price includes fabrication where possible.

Table 5-2

Site Installation

This cost estimate was based on a site installation as described in Appendix B.

Site Work	$10,000
Gravel	$ 1,000
Rip-rap	$ 2,000
Unit	$80,400
Total	$93,400

@ 17 kW = $5,500/kW

@ 26 kW = $3,600/kW

costs. These costs are very rough estimates and the actual figures are highly dependent upon individual geographic site locations, available transportation routes, etc.

The cost estimate was based on a water ladder system with a blade span of five metres. An economy of scales exists with regard to the blade span. Increasing the span increases the power output; however construction costs do not increase proportionally. Much of the cost results from the blade mounts, hence a minimum number of mount linkages is desirable for a given river span.

The economy of scales of the system was not investigated any further.

5.2 Maintenance

The water ladder system can consist of many moving components, linkages, etc. and consequently it is anticipated that maintenance costs for the unit could be quite large. The fact that the majority of the components are exposed to the environment may create the need for system monitoring and/or regular maintenance. For example, the main shafts, sprocket, blade mounts, main bearings, linkage bearings and transmission belt would be immersed in moving water. If the river is silty, severe problems may be encountered with these components, hence maintenance and repair costs could be high. The majority of repairs would most likely involve bearing replacement.

Occasionally the trash racks upstream of the system

may require cleaning, however the costs involved are periodic. For example, for a crew of two men at $10/hr. working eight hours per month cost approximately $2000 per year.

Repair costs for the system cannot be accurately estimated, hence they were not attempted. Also, maintenance costs were not considered in the cost analysis for any of the facilities listed in Table (5-3).

5.3   Lifespan of the System

Literature [15] dealing with small-scale hydroelectric systems estimates that the hydraulic equipment has in general a long lifespan. Many units may be replaced by advances in technology rather than mechanical failure.

Reservoirs which are created by dams have a lifespan of about fifty years [26]. This limit is imposed by the deposition of river silt due to the decrease in the velocity of flow entering the reservoir.

The water ladder system requires only a small reservoir and water velocities are not expected to vary greatly from the original river velocities. Hence silting problems are not anticipated. A water ladder is expected to have a shorter lifespan than that for hydraulic turbomachinery due to wear on the components of the unit. An estimate of about 30 to 40 years appeared reasonable.

5.4 Economic Viability

A brief examination of the investment return period of the project was attempted. The pertinent data for which is given below:

Initial investment P = $93,400

Annual income from say 25 kW @ 4¢/kW hr.

= 25 x .04 x 24 x 365 = $8,760

Yearly maintenance costs = $2,000

Net yearly income, A = $6,760

Interest rate, i = 15%

Using $\frac{P}{A} = \frac{(1+i)^n - 1}{c(1+c)^n}$ (5.1)

Therefore $n = \frac{\ln(\frac{1}{1 - \frac{Pi}{A}})}{\ln(1+i)}$ (5.2)

Substituting the data into Equation (5.2) shows that the investment return of the project is impossible at the given sales and interest rates. To improve the economics the net return per year would have to exceed approximately $13,000. Thus electricity sales rates would have to increase to at least 7¢/kW hr. Other means of electricity generation would also become more economically attractive as a result of such a rise in sales rates.

The economics of a diesel generator were compared to that of the water ladder. The purchase price for a 25 kW unit is about $16,000 and the fuel consumption is of the order of 9.1 litres per hour.

Fuel costs for 1 year = $(9.1)(24)(365)($.28/\ell^{*})$

     = \$22,300

Amount of electricity generated = $(24)(365)(25)$

     = 219,000 kW hr.

Price = \$.10/kW hr.

To break even on the fuel costs involved, the electricity produced would require a sale price of \$.10/kW hr. This figure does not include maintenance costs nor the initial investment. Hence the water ladder is economically better than is a diesel generator.

5.5   Evaluation

In Appendix B, the power output of the system was estimated to be 17 kW, considering power is produced only by the front cascade. The power output is estimated to increase by fifty percent when power from the rear cascade was also considered. Hence a factor of 1.5 was assigned as a result of considering the losses which occur in the region between the two cascades. By applying the factor of 1.5 the power output is increased to 26 kW. As presented in Tables (5-1) and (5-2), the unit costs which result are \$4,300/kW and \$2,800/kW. Total costs, which include installation, are \$5,100 kW and \$3,300/kW for power outputs of 17 and 26 kW respectively.

The factor of 1.5 was considered a reasonable esti-

---

* 1980 Canadian dollars.

Table 5-3

Construction Costs of Electrical Generating Facilities

Type	Cost of Construction (in 1980 Canadian Dollars)
Nuclear	$1,200/kW
Large Hydroelectric (+ 10,000 kW)	$1,150/kW
Small Hydroelectric	$2,000-$3,000/kW*
Wind Power (small)	$4,500/kW
Water Ladder	$3,500-$5,000/kW
Diesel Generator (small)	$1,000/kW

The costs given correspond to installed, operating facilities. Fuel costs are not included.

* Depending on site location.

mate for the power produced by both upstream and downstream cascades since improved efficiencies require the use of guide vanes between the cascades as discussed in Section (4.1). The power output increases with improved efficiencies, hence the capital return from sales also increases. However, this added return is offset to a certain extent by the cost of the guide vanes.

To determine the economic attractiveness of the water ladder system, it was compared to existing generating facilities. Table (5-3) summarizes these costs. The larger centralized methods of producing electricity, namely nuclear and hydro-electric are the most economical at the present time. However most of the potential large scale hydroelectric sites have been developed, and the nuclear industry is under severe public scrutiny. Table (5-3) shows that small scale hydro and wind power and the water ladder are not competitive in the economic environment in which the cost figures were derived which, in the present case, is Ontario.

The price of the water ladder unit, neglecting site costs was calculated to be about $3,100/kW to $4,700/kW for a 21 kW unit, compared with hydraulic turbine generators which cost approximately $1,100/kW [13, 22] for a unit of about the same output. The difference in their costs lie in the complexity of the mechanism. Whereas the turbine has only one moving part, the water ladder has many. Note that the difference between costs becomes smaller when site expenditures are added. (Table (5-3)).

A survey of other hydraulic generating equipment confirms the price range given above. The search also showed that there are very few turbines on the market which can produce power with a head much less than 2 metres [13, 22]. The water ladder opens up a new, previously untapped source of energy - micro head small scale hydroelectricity generation. It is in this area of specialization that the water ladder is considered to have applications.

There has been an upsurge in the number of small scale hydro stations being constructed worldwide. This trend is especially prominent in Europe, and to a certain extent in the United States. In the Third World, the number of small scale stations is also on the rise owing to the fact that the level of technology involved is more congruent with existing industry, than say nuclear plants are. Hence local or national rather than international levels of industry would be able to meet the maintenance requirements of these hydraulic units. This aspect is appealing to the governments involved as it promotes local, decentralized industry. In addition, the capital investment for small hydro projects is relatively minute, thus adding to their attractiveness as development projects.

Certain areas of Canada on the other hand exhibit the cheapest sales prices for electricity in the world. As a result, small scale hydro is not competitive, as shown in Table (5-3) which gives the construction costs. Other costs are involved however. The installation cost of transmission

lines, plus the losses incurred in transmission must be considered. These added costs have promoted the construction of decentralized small-scale units in remote areas. The small scale hydroelectric facilities service pulp and paper industries, mining industries and small remote communities. It has been shown that small hydro installations are now less expensive to construct and operate than portable diesel generator sets [12]. Increased fuel costs have brought about this change.

The potential for small scale hydro is quite large. In Canada it has been estimated that there exists 67,000 to 250,000 megawatts [15, 34] of untapped hydroelectric power.

There are many simularities between the small scale hydraulic units, and the water ladder system. Hence the above discussion gives a general overview of the political and economic aspects with which the water ladder system is to operate. On the basis of the economics involved, the system can be expected to be exclusively applied to remote areas or in Third World countries.

The above evaluation emphasizes the fact that the proposed water ladder system is not presently a viable economic proposition. This does not signify that the system possesses no technological merits, only that the realm of application is limited to specific areas and conditions as outlined by the economics involved above.

CHAPTER 6

DISCUSSION ·AND
CONCLUSIONS

The credibility of this study has been evaluated .
and the results are summarized in this chapter.

6.1   Justification of Assumptions

In the computer simulation, several assumptions were
made as listed in Chapter (2). The validity of these
approximations is discussed here.

The exit velocity is not uniform over the exit plane
nor over the blade as assumed. The·use of average velocities
does not seriously affect the accuracy of the force calcula-
tions. Also, continuity is upheld regardless of the velocity
distribution.

The incident angle of Vr_1 on a blade was neglected
in this model. This produces a conservative result since the
consideration of the incident angles would add to the lift
created by the hydrofoil section. This was partially com-
pensated for by specifying a low value for C_m, the loss co-
efficient.

Separation in the flow passage induces a narrower
flow passage causing the fluid velocities and losses to increase.
The turning angle of the fluid was limited to a value which was
below the point at which separation was estimated to occur.

Hence losses due to separation do not enter into the analysis.

Cavitation was shown to occur on the blades near the water surface. At this point it is suggested that a thorough study of separation be done on models to confirm the onset of cavitation and to measure the severity of the phenomenon. Alternatively, the blade sections may be modified by reducing the turning angle or by lowering the blade speed. In either case the relative exit velocity is decreased, thus tending to eliminate cavitation, but reducing the specific power output and efficiency.

The assumption that the cascade blades are thin with respect to blade spacing was made as a result of considering a control volume with thin horizontal boundaries representing the blades. In reality the velocity of the flow in the passage is somewhat higher because the cross-sectional area of the passage is decreased by the thickness of the blade. In this case the error amounts to less than five percent, and is assumed to be acceptable.

In summary the assumptions made should introduce minimal errors, aside from the fact that cavitation onset is disregarded.

The fluid mechanics of the problem are sufficiently complex to warrant the above assumptions. To establish figures of greater certainty involves further computation and other approximations. Much research has been done on blade losses [25, 32].

Important details regarding the flow characteristics
in the vicinity of hydrofoil sections have been documented.
A series of papers which were produced by Waldin [42, 43, 44]
discuss the results of tests that were performed on hydrofoils
of various shapes, aspect ratios and depths beneath a free
surface. A significant point was that the lift created by
the hydrofoils decreased as the blades approached the free
surface. This effect was most pronounced at depths equal to
or less than the chord of the blade and may be exhibited in
the water ladder system. Specifically, blades at the upper
end of the cascade may create a smaller lifting force than
those at greater depths. The net effect is to lower the force
on these upper blades and ultimately decrease the power output.
The interaction between the free surface and the translating
blades was not considered in the present model analysis.
Future refinements in the system analysis may consider this
relationship between the blade depth and chord.

6.2   Related Current Studies

The only reference encountered was that by Kocivar
[23]. In the paper Schneider, the originator of the water
ladder concept, estimates that construction costs of $700/kW*
were possible. The present preliminary study showed that
these costs are unrealistic. The paper also suggested that
hydraulic heads of up to twenty feet could be applied to the

---

* 1978 U.S. dollars are assumed. This is equivalent to approxi-
mately $1,000/kW in 1980 Canadian dollars.

water ladder, operating at low blade speeds. Again the results of this present study are in disagreement. Firstly, the fluid mechanics of the system prohibit the specification of high head differentials (Δz) together with a low blade speed (u) because of the limitations on the turning angle, as discussed. Secondly if the water ladder could operate under the proposed conditions it would be in competition economically with small-scale hydraulic turbomachinery since both systems could be used in the suggested application. Hydraulic systems are more cost efficient than the water ladder and hence would be favored in the prescribed application. In order to use the water ladder with hydraulic heads of twenty feet, the support structure required would be similar in construction and in cost to that of a turbomachine. Chapter (5) compared the unit cost alone and showed that the water ladder is viable due to minimum amount of site work which is required. Considering that the cost of a turbomachine is much less than that for a water ladder system with a similar power output the proposal by Schneider is in error.

6.3 Discussion

The water ladder system has been shown to be technically feasible, and economically feasible under certain conditions. Apart from meeting these traditional criteria for measuring the viability of a proposal, the water ladder exhibits additional benefits. The system withdraws energy from a 'renewable source' and in so doing does not contribute to environmental

degradation. The system can be labelled as being at a level of technology which is termed 'appropriate', and would be somewhat consistent with technological levels in Third World nations. It is a decentralized source of electricity and as such may be suitable for households or small communities.

In summary, the water ladder is a part of the search for clean, renewable energy sources. Unlike solar and wind power, the water ladder is not extremely sensitive to short term fluctuations in the weather. The water ladder does not have the inherent dangers which are exhibited by wind generators. In extreme weather conditions, damage has resulted from the failure of support towers used to mount the wind power units, for example.

Of the so-called renewable energy resources mentioned above, small-scale hydroelectricity is the most inexpensive energy producer. The water ladder system is a specialized member of the hydraulic group. As previously discussed, the water ladder is able to produce electricity under low head conditions which is not possible with most turbomachinery. The water ladder system as described is a clean, safe means of producing electricity which at this point is worthy of further consideration for future applications.

6.4   Conclusion

This study provides an evaluation of a proposed facility for hydroelectric power generation. The facility

is to operate under low head, high volume flows. The system consists of a cascade of hydrofoils mounted in an arrangement similar to that of a conveyor belt. The equipment required is factory assembled in the form of a complete unit, thus minimizing site work.

The author has found the proposed system to be technically feasible. Analysis of the fluid mechanics by means of computer simulation provided sufficient insight into the problem to arrive at this conclusion. In addition to illustrating the feasibility, a number of innovations were made in the system's design. The most prominent of these was the blade mounts which support the blade and form part of the transmission linkage. The rotation and translation of the blades were made possible by incorporating these mounts into the system's design. Another innovation was one of concept rather than analysis. The water ladder system as proposed is a factory assembled unit. The unit is transported to the site as a complete package where it is then installed. The actual site work involved is minimal, hence costs are reduced.

The foreseeable problems involved in the design of the system have been covered. Flooding, trash problems, public safety, and environmental problems have been discussed and proposals made to optimize the system's design.

6.5 Future Work

This thesis has presented a basic analytical and technical framework for the design of a water ladder system. At

this point it is felt that further research is required in various aspects of the design.

The construction and testing of an actual model has been suggested in the thesis. It is argued that the test results would verify or refine the analysis which was performed in this thesis. Aspects of interest include the determination of the loss coefficient C_m given a specific set of design variables, and the measurement of the maximum blade speed possible. Forces on both stationary and translating blades would also be determined. Furthermore, the efficiency of the system may be improved by a refinement of the blade shape and its construction. Specifically, the weight of the blade should be reduced which in turn would decrease the mechanical friction throughout the system.

Investigation of the above aspects of the system may ultimately improve the economics of the water ladder system, thus broadening the range of application.

REFERENCES

1. Adams, P. F., Krantz, H. A., and Kulak, G. L., Limit States Design in Structural Steel, CISC, 1977.

2. Beer, F. P. and Johnson, E. R., Vector Mechanics for Engineers - Dynamics, McGraw Hill Book Co., U.S.A., 1972.

3. Boston Gear, Mechanic Components, Boston Gear and Incom International Inc., 1979.

4. Betz, A., The Theory of Flow Machines, Pergamon Press, London, England, 1966.

5. Brown, R. S. and Goodman, A. S., "Small Hydropower - Promise and Reality for New York State and the Northeast", Alternative Energy Sources, Geothermal and Hydro Power, 1977, V6, pg. 2856-2875.

6. Budinski, K., Engineering Materials: Properties and Selection, Reston Publishing Co., Virginia, U.S.A., 1979.

7. Canadian Institute of Steel Construction, Limit States Design Manual, CISC, Toronto, 1977.

8. CISC, SI Properties of Structural Steel Sections and Selected Data, CISC, Toronto, Canada, 1979.

9. Dixon, S. L., Fluid Mechanics, Thermodynamics of Turbo-machinery, Pergamon Press, England, 1975.

10. El-Shamy, F. M., "Environmental Impacts of Hydroelectric Power Plants", Journal of the Hydraulics Division, ASCE, Sept. 1977, pg. 1007-1020.

11. Everdell, R. A., "Installation of Mini Hydel Unit at Wasdell Falls", Presentation to Hydraulic Power Section, Canadian Electrical Association, March, 1979.

12. Flagher, G., Common Sense on the Rocks, Harrowsmith Magazine, No. 29, pg. 40-47, 1980.

13. Galt Energy Systems, "The GS Packaged Generating Station", Company Brochure, Galt Energy Systems, Cambridge, Ont., 1980.

14. Gasiorek, J. M., Mechanics of Fluids for Mechanical Engineers, Hart Publishing Co., U.S.A., 1968.

15. Gibbins, R., "Use of Small Hydro is Urged to Power Developments in Future, Globe & Mail, Sept. 2/80, pg. B6.

16. Horlock, J. H., Axial Flow Compressers, Butterworths
     Scientific Publications, London, 1958.

17. Horlock, J. H., Axial Flow Turbines, Robert E.
     Krieger Publishing Co., U.S.A., 1973.

18. Houghton, E. L., Brock, A. E., Aerodynamics for
     Engineering Students, St. Martin's Press, N.Y.,
     1970.

19. Hsieh, Y., Elementary Theory of Structures, Prentice
     Hall, New Jersey, U.S.A., 1970.

20. Imlay, F. H., "Theoretical Motions of Hydrofoil Sections",
     Tech. Rep. R-918 NACA, 1948.

21. John, J. E. and Haberman, W., Introduction to Fluid
     Mechanics, Prentice Hall, New Jersey, U.S.A., 1971.

22. Jyoti Ltd., "Small Sets With Big Benefits - Jyoti
     Hydel Sets", Company Brochure, Jyoti Ltd., Baroda,
     India, 1980.

23. Kocivar, Ben, "Lifting Foils Tap Energy of Flowing Air
     or Water", Popular Science, February 1978, pg. 71-74.

24. Langhaar, H. L., Dimensional Analysis and Theory of
     Models, John Wiley and Sons, N.Y., 1951.

25. Lieblein, S., and Roudebush, W., "Theoretical Loss
     Relations for Low Speed Two Dimensional Cascade
     Flow", NACA TN 3662, Washington, D.C., U.S.A.,
     1956.

26. Linsley, R. K. and Franzini, J. B., Water Resource
     Engineering, McGraw Hill Book Co., U.S.A., 1972.

27. Mayo, H. A., "The Cost of Inefficiency in Fluid Machinery",
     The Cost of Inefficiency in Fluid Machinery, ASME
     Conference, November, 1974, pg. 19-45.

28. Megson, T. H. G., Aircraft Structures for Engineering
     Students, Edward Arnold Publishers Ltd., London,
     England, 1972.

29. Meriam, J. L., Engineering Mechanics, Vol. 1, John Wiley
     and Sons, U.S.A., 1978.

30. Mills, J. I. and Smith, G. L., "Low Head Hydroelectric
     Power: A Realizable Alternative" Alternative
     Energy Sources, Geothermal and Hydro Power, 1977,
     V6, pg. 2843-2855.

31. Newman, J. N., _Marine Hydrodynamics_, MIT Press, U.S.A.,
     1978.

32. Parkin, Blaine R., "Experiments on Circular-Arc and
     Flat Plate Hydrofoils in Noncavitating and Full
     Cavitating Flows", Journal of Ship Research,
     March, 1958, pg. 34-56.

33. Popov, E. P., _Introduction to Mechanics of Solids_,
     Prentice Hall Inc., New Jersey, U.S.A., 1968.

34. Radz, M., Turbulence, Inc., _Harrowsmith Magazine_,
     No. 29, pg. 33-39, 1980.

35. Reynolds, A. J., _Thermofluid Dynamics_, J. Wiley and
     Sons, Toronto, 1971.

36. Sabersky, R. H., and Acosta, A. J., _Fluid Flow_, MacMillan
     Company, U.S.A., 1964.

37. Shanley, F., _Weight-Strength Analysis of Aircraft
     Structures_, McGraw-Hill, Toronto, 1952.

38. Shigley, J. E., _Mechanical Engineering Design_, McGraw
     Hill, U.S.A., 1977.

39. Streeter, V. L. and Wylie, E. B., _Fluid Mechanics_,
     McGraw Hill Book Company, U.S.A., 1975.

40. Thuesen, H. G. and Fabrycky, W. J., _Engineering
     Economy_, Prentice Hall, New Jersey, U.S.A., 1964.

41. Thwaites, B., _Incompressible Aerodynamics_, Oxford
     University Press, 1960,

42. Waldin, K. and Christopher, K., "A Method for Calculation
     of Hydrodynamic Lift for Submerged and Planing
     Rectangular Lifting Surfaces", Tech. Rep. R-14,
     NASA, 1959.

43. Waldin, K. L., Ramson, J. A. and McGehee, J. R., "Tank
     Tests at Subcavitation Speeds of an Aspect Raio
     10 Hydrofoil with a Single Strut", NACA RML9K14a,
     July, 1950.

44. Waldin, K. L., Shuford, Jr., C. L., and McGehee,
     "A Theoretical and Experimental Investigation
     of Lift and Drag Characteristics of Hydrofoils at
     Subcritical and Supercritical Speeds", NACA
     Report 1232, 1955.

45. Wallis, R. A., _Axial Flow Fans_, George Newnes Ltd.,
     U.K., 1961.

46.   Wisclicensus, G. F., Fluid Mechanics of Turbo-
             machinery - V-1, Dover Publications, U.S.A.,
             1965.

47.   Zweifel, O., "The Spacing of Turbo-Machine Blading,
             Especially with Large Angular Deflection", The
             Brown Boveri Review, December 1945, pg. 436-444.

APPENDIX A

COMPUTER SIMULATION

Appendix A contains a listing of the computer program which was used to model the cascade of hydrofoils. The following is a brief description of the program to illustrate its use.

A.1   Program Description

The computer program entitled DEAL has been selected as an example. The remaining three versions DEOC DEUU DRIV, are identical except that the variables which are studied in the sensitivity analysis differ. For example, DEAL varies DELZ and ALPHAI, DEOC varies DELZ and COLOS, etc.

The program is explained according to line numbers. Refer to the program listing for specific fortran statements. Table (A-1) lists the variable names as they appear in the computer program.

00100   Program TST

00110   Variables are dimensioned for plotting. The variable names are preceeded by a letter 'D' to indicate a dimensioned variable.

00240   Variables list.

00520   Variables which are not changed in the program are defined.

94

00650	Design variables are defined. Two of ALPHAI, DELZ, COLOS, VRIV and u are varied in do loops.
00800	Calculation of AREA1, VEL1, VAX, PETA1, and RVEL1 according to equations presented in Chapter (2).
00930	Subroutine LOSS is called to calculate exit parameters.
00970	A check is made to ensure continuity was not defied.
01000	Subroutine WOREFF is called to calculate power and efficiency.
01030	Print statement to create a table of flow charac- teristics for a given set of input design variables.
01070	Plotting arrays are assigned data.
01300	Plots are made by calling FOPLO.
01920	End of MAIN program.
01920	SUBROUTINE LOSS - RVEL2, BETA2, TURN, ALPHA2, VEL2, BETM, SOLID, FORCE, and RVELM, are calculated according to equations in Chapter (2).
02350	Variables are given a value of zero if continuity is defied.
02470	End of subroutine LOSS.
02480	SUBROUTINE WOREFF - calculates the power and efficiency of the cascade.
02650	SUBROUTINE FOPLO (XAX, YAX, N, NOS)
	XAX and YAX are two dimensional arrays to be plotted along the X and Y axes respectively. N - the number of points per curve (20). NOS - the number of curves (20).

03230   SUBROUTINE GRID plots the outline of the graph.

03350   SUBROUTINE NAME prints data regarding the plot
on the graph.

03450   SUBROUTINE AX labels the X-axis of the plot.

Table A-1

Variable Names As Used in the Computer Program

Program Variable Name	Variable Name	Description
VEL1	V_1	absolute fluid inlet velocity
VEL2	V_2	absolute fluid exit velocity
RVEL1	V_{r_1}	relative fluid inlet velocity
RVEL2	V_{r_2}	relative fluid exit velocity
u	u	blade velocity
VRIV	V_{RIV}	upstream river velocity
VAX	V_{ax}	axial velocity in the cascade
ARIV	A_{RIV}	cross-sectional area of the river upstream
AREA1	A_1	cross-sectional area of the river at the cascade
DEPTH	D	depth of the river
WIDTH	W	width of the river
ALPHA1	α_1	direction of V_1
ALPHA2	α_2	direction of V_2
BETA1	β_1	direction of V_{r_1}
BETA2	β_2	direction of V_{r_2}
TURNING ANGLE	θ	turning angle
SPACE	S	the space between the blades

Program Variable Name	Variable Name	Description
CHORD	c	the blade chord.
SOLIDITY	s/c	the solidity
FY	F_y	the upward force on the blade
FX	F_x	the axial force on the blade
EFF	η	the efficiency of the blade system
POWER	P	the power output of the system
TPOWER	P_T	the power output per unit vertical depth
COLOS	C_m	the energy loss coefficient
DELZ	ΔZ	the head differential

A.2 Computer Program Listing

```
00100 PROGRAM TST(INPUT,OUTPUT,TAPE5=INPUT,TAPE6=OUTPUT)
00110  DIMENSION DSOLID(20,20),DALPHA1(20,20),
00120+ DALPHA2(20,20),DBETA1(20,20),DBETA2(20,20),
00130+ DVEL2(20,20),DRVEL1(20,20),DRVEL2(20,20),
00140+ DEFF(20,20),DVAX(20,20),DUVAX(20,20),DFORCE(20,20),
00150+ DU(20,20),DDELZ(20,20),DCLIFT(20,20),
00160+ DTPOW(20,20),DTURN(20,20)
00170C
00180C DEAL2 IS A PROGRAM WHICH MODELS A WATER LADDER GENERATOR SYSTEM
00190C WITH THE INTENTION OF PREDICTING THE SYSTEM'S FEASIBLITY.
00200C
00210C ALL VARIABLES ARE METRIC.
00220C
00230C
00240C VARIABLES LIST
00250C  ALPHA1 - ABSOLUTE VELOCITY INLET ANGLE.
00260C  ALPHA2 - ABSOLUTE VELOCITY EXIT ANGLE.
00270C  BETA1  - RELATIVE VELOCITY INLET ANGLE.
00280C  BETA2  - RELATIVE VELOCITY EXIT ANGLE.
00290C  DELZ   - CHANGE IN WATER DEPTH OVER THE CASCADE.
00300C  SOLID  - THE SOLIDITY OF THE BLADES.
00310C  CHORD  - THE BLADE CHORD.
00320C  NOB    - THE NUMBER OF BLADES.
00330C  POWER  - THE AVAILABLE POWER.
00340C  EFF    - EFFICIENCY OF THE CASCADE.
00350C  VEL1   - ABSOLUTE ENTRY VELOCITY.
00360C  VEL2   - ABSOLUTE EXIT VELOCITY.
00370C  RVEL1  - RELATIVE ENTRY VELOCITY
00380C  RVEL2  - RELATIVE EXIT VELOCITY.
00390C  COLOS  - LOSS COEFFICIENT.
00400C  U      - BLADE VELOCITY.
00410C  VRIV   - VELOCITY OF THE RIVER UPSTREAM.
00420C  DEPTH  - DEPTH OF THE RIVER AT THE CASCADE.
00430C  ARIV   - AREA OF THE RIVER.
00440C  VAX    - AXIAL VELOCITY THROUGH THE THE CASCADE.
00450C  UVAX   - BLADE VELOCITY / FLUID VELOCITY
00460C  TURN   - THE FLUID TURNING ANGLE.
00470C  FY     - FORCE ON ONE BLADE PER METRE**2 CHORD-SPAN.
00480C  POWER  - POWER PRODUCED PER METRE**2 CHORD-SPAN.
00490C  TPOW   - TOTAL POWER FOR GIVEN DEPTH AND CHORD.
00500C  RHO    - DENSITY OF WATER.
00510C
00520C SPECIFY THE INITIAL VARIABLES.
00530  G = 9.8
00540  RHO = 1000.
00550  CHORD = .6
00560  IFLAG = 0
00570  DEPTH = 4.2
00580  WIDTH = 5.5
00590  ARIV = DEPTH
00600  VRIV = 1.0
00610  DEG = 57.2958
00620C
00630  WRITE(6,10) VRIV
00640C
00650C INITIATE VARIABLES ALPHA1,U,DELZ, AND COLOS.
00660  DO 27 K=1,20
00670  ALPHA1 = FLOAT(K-1)*.02
00680C  DO 26 K=1,20
00690C  U = .05*FLOAT(K-1)
00700  U = .25
00710C  ALPHA1 = .2
00720  DO 22 L=1,20
00730  DELZ = .05*FLOAT(L)
00740C  DELZ = .02
00750  DO 28 I=1,2
00760  COLOS = FLOAT(I-1)*.020
```

```
00780    IFLAG = 0
00790C
00800C CALCULATE THE INLET VELOCITY TO THE CASCADE.
00810    AREA1 = ARIV - DELZ
00820    VEL1 = ARIV * VRIV/AREA1
00830C
00840C CALCULATE THE AXIAL VELOCITY THROUGH THROUGH THE CASCADE.
00850    VAX = VEL1*COS(ALPHA1)
00860C
00870C CALCULATE THE VALUE OF BETA1.
00880    BETA1 = ATAN(TAN(ALPHA1)-U/VAX)
00890C
00900C CALCULATE THE RELATIVE VELOCITY AT THE INLET.
00910    RVEL1 = VAX/COS(BETA1)
00920C
00930C CALCULATE THE LOSSES BY CALLING LOSS
00940    CALL LOSS(RVEL2,VEL2,DELZ,G,ALPHA2,U,BETA2,RVEL1,FY,VAX,
00950+   EFF,BETA1,CLIFT,TURN,SOLID,CHORD,RHO,ALPHA1,COLOS,IFLAG)
00960C
00970C CHECK IF VAX .GT. RVEL2.
00980    IF(IFLAG.EQ.1) GOTO 30
00990C
01000C CALL WOREFF TO CALCULATE THE WORK AND EFFICIENCY.
01010    CALL WOREF(U,VEL1,VEL2,RHO,SOLID,CHORD,DELZ,TPOWER,ALPHA1,
01020+   EFF,G,FY,COLOS,RVEL1)
01030C
01040    WRITE(6,12) U,ALPHA1,RVEL1,BETA1,BETA2,ALPHA2,RVEL2,
01050C+  TURN,FY,TPOWER,EFF,DELZ,SOLID
01060  30 CONTINUE
01070C
01080C DIMENSION THE VARIABLES FOR PLOTTING.
01090    DALPHA1(K,L) = ALPHA1 * DEG
01100    DALPHA2(K,L) = ALPHA2 * DEG
01110    DBETA1(K,L) = BETA1 * DEG
01120    DBETA2(K,L) = BETA2 * DEG
01130    DVEL2(K,L) = VEL2
01140    DRVEL1(K,L) = RVEL1
01150    DRVEL2(K,L) = RVEL2
01160    DFORCE(K,L) = FY
01170    DEFF(K,L) = EFF
01180    DDELZ(K,L) = DELZ
01190    DVAX(K,L) = VAX
01200    DUVAX(K,L) = U/VAX
01210    DTURN(K,L) = TURN * DEG
01220    DU(K,L) = U
01230    DTPOW(K,L) = TPOWER
01240C
01250  28 CONTINUE
01260  22 CONTINUE
01270  26 CONTINUE
01280  27 CONTINUE
01290C
01300C CALL THE PLOTTING ROUTINE.
01310    CALL FOPLO(DTURN,DTPOW,20,20)
01320C
01330C PUT ON A TITLE.
01340    CALL NEWPEN(2)
01350    CALL LETTER(13,.2,90.,.7,3.5,1CHPOWER (WATTS) )
01360    CALL LETTER(13,.2,0.0,2.1,1.6,1CHTURNING ANGLE )
01370    CALL NAME
01380    CALL PLOT(10.,0.01,-3)
01390C
01400C PLOTS ARE MADE AS REQUIRED.
01410    CALL FOPLO(DALPHA1,DRVEL2,20,20)
01420    CALL NEWPEN(2)
01430    CALL LETTER(1,.2,90.,.7,3.5,1HV )
```

```
01440    CALL LETTER(2.,1.90.,.75,3.7,2HR2 )
01450    CALL LETTER(5.,2.90.,.7,4.0.5H(I/S) )
01460    CALL AX
01470    CALL NAME
01480    CALL PLOT(10.,.01,-3)
01490    CALL FOPLO(DALPHA1,DEFF,20,20)
01500    CALL NEWPEN(2)
01510    CALL GREEK(.7,4.0,.2,90.,7)
01520    CALL AX
01530    CALL NAME
01540    CALL PLOT(10.,.01,-3)
01550    CALL FOPLO(DALPHA1,DFORCE,20,20)
01560    CALL NEWPEN(2)
01570    CALL LETTER(15,.2,90.,.7,3.5,15HFORCE (NEWTONS) )
01580    CALL AX
01590    CALL NAME
01600    CALL PLOT(10.,.01,-3)
01610    CALL FOPLO(DALPHA1,DBETA2,20,20)
01620    CALL NEWPEN(2)
01630    CALL GREEK(.7,3.5,.2,90.,2)
01640    CALL LETTER(1.,1.90.,.75,3.7,1H2 )
01650    CALL LETTER(10,.2,90.,.7,3.9,10H (DEGREES) )
01660    CALL AX
01670    CALL NAME
01680    CALL PLOT(10.,.01,-3)
01690    CALL FOPLO(DALPHA1,DBETA1,20,20)
01700    CALL LETTER(16,.2,0.,1.5,1.,16H BETA1 VS ALPHA1 )
01710    CALL NAME
01720    CALL PLOT(10.,.01,-3)
01730    CALL FOPLO(DALPHA1,DTPOW,20,20)
01740    CALL NEWPEN(2)
01750    CALL LETTER(13,.2,90.,.7,3.5,13HPOWER (WATTS) )
01760    CALL AX
01770    CALL NAME
01780    CALL PLOT(10.,.01,-3)
01790    CALL FOPLO(DALPHA1,DVAX   ,20,20)
01800    CALL LETTER(15,.2,0.,1.5,1.,15HVAX VS ALPHA1     )
01810C
01820    CALL PLOT(0.01,0.01,999)
01830C
01840 10 FORMAT(1H1,10X,*FOIL OUTPUT WITH :*,/,
01850+   10X,*VRIV = *,F10.4,10X,/,/,
01860+   8X,*U*,6X,*ALPHA1*,5X,*RVEL1*,5X,*BETA1*,5X,
01870+   *BETA2*,5X,*ALPHA2*,5X,*RVEL2*,5X,*TURN *,4X,*FORCE*,5X,
01880+   *POWER*,6X,*EFF*,6X,*DELZ*,5X,*SOLID*,/,/)
01890 12 FORMAT(3X,8(F8.3,2X),2(F10.3,1X),F5.3,2X,2(F8.3,2X))
01900C
01910    STOP
01920    END


01930 SUBROUTINE LOSS(RVEL2,VEL2,DELZ,G,ALPHA2,U,BETA2,RVEL1,FY,VAX
01940+   ,EFF,BETA1,CLIFT,TURN,SOLID,CHORD,RHO,ALPHA1,COLOS,IFLAG)
01950C
01960C THIS ROUTINE CALCULATES THE EXIT VELOCITY AND FORCE ON
01970C THE BLADES FOR DIFFERENT LOSS COEFFICIENTS.
01980C
01990C CALCULATE THE RELATIVE EXIT VELOCITY.
02000    RVEL2 = SQRT((2*G*DELZ + RVEL1**2)/(1+COLOS))
02010C
02020C CHECK IF VAX .GT. RVEL2. (THIS CONDITION DEFIES CONTINUITY.)
02030    IF(VAX.GT.RVEL2) GOTO 40
02040    BETA2 = -1*ACOS(VAX/RVEL2)
02050C
02060C CALCULATE THE TURNING ANGLE.
02070    TURN = BETA1 - BETA2
```

```
02080C
02090C CALCULATE ALPHA2, VEL2, BETM.
02100  ALPHA2 = ATAN(U/VAX + TAN(BETA2))
02110  VEL2 = VAX/COS(ALPHA2)
02120  BETM = ATAN((TAN(BETA1) + TAN(BETA2))/2)
02130C
02140C CALCULATE THE OPTIMUM SOLIDITY OF THE BLADES.
02150  DEN = (TAN(ALPHA1)-TAN(ALPHA2))
02160  IF(DEN.EQ.0.) DEN = .0001
02170  SOLID = .4/(DEN*(COS(ALPHA2))**2)
02180C
02190C CALCULATE THE VERTICAL FORCE ON THE BLADE.
02200C (FORCE PER BLADE PER METRE CHORD)
02210  11  FY = RHO*VAX**2 *(TAN(ALPHA1)-TAN(ALPHA2))
02220  RVELM = VAX/COS(BETM)
02230C
02240C CALCULATE THE CHANGE IN LEVEL AS A RESULT OF LOSSES.
02250  PDIFF = DELZ*RHO*G
02260  FX = -PDIFF
02270C
02280C  CALCULATE THE LIFT AND DRAG COEFFICIENTS.
02290  LIFT = FX*SIN(BETM) + FY*COS(BETM)
02300  DRAG = FY*SIN(BETM) - FX*COS(BETM)
02310  CLIFT = LIFT/(.5*RHO*RVELM**2)
02320  CDRAG = DRAG/(.5*RHO*RVELM**2)
02330C
02340  GOTO 41
02350  40  IFLAG = 1
02360  BETA2 = 0
02370  ALPHA2 =0.
02380  VEL2 = 0.
02390  SOLID = 0.
02400  FY = 0.
02410  CLIFT = 0.
02420  CDRAG = 0.
02430  EFF = 0.
02440  WRITE(6,33)
02450  33  FORMAT(10X,*VAX.GT.RVEL2*)
02460  41  RETURN
02470  END




02480 SUBROUTINE WOREF(U,VEL1,VEL2,RHO,SOLID,CHORD,DELZ,
02490+ TPOWER,ALPHA1,EFF,G,FY,COLOS,RVEL1)
02500C
02510C WOREF CALCULATES THE WORK AND EFFICIENCY OF THE CASCADE.
02520C
02530  POWER = FY * U
02540   TPOWER = POWER/COS(ALPHA1)
02550C
02560  IF(COLOS.GT.0) GOTO 21
02570  POWID = RHO*VEL1*((VEL1**2)/2 + DELZ*G)
02580C
02590C CALCULATE THE EFFICIENCY.
02600  21  EFF = POWER/POWID
02610C
02620C
02630  RETURN
02640  END
```

```
02650 SUBROUTINE FOPLO(XAX,YAX,N,NOS)
02660 DIMENSION XAX(N,1), YAX(N,1)
02670C
02680C THIS ROUTINE PLOTS THE VARIABLES XAX VS YAX.
02690C XAX AND YAX ARE ARRAYS CONTAINING TWO ARGUMENTS.
02700C N IS THE NUMBER OF POINTS PER CURVE.
02710C NOS IS THE NUMBER OF CURVES TO BE PLOTTED.
02720C
02730 CALL GRID
02740C
02750C INITIATE LABELLING VARIABLES.
02760 XMAX = XAX(1,1)
02770 XMIN = XAX(1,1)
02780 YMAX = YAX(1,1)
02790 YMIN = YAX(1,1)
02800C
02810C FIND THE MAX AND MIN VALUES IN THE ARRAYS.
02820 DO 50 L=1,NOS
02830 DO 51 J=1,N
02840C
02850 IF(XAX(J,L).LT.XMIN) XMIN=XAX(J,L)
02860 IF(XAX(J,L).GT.XMAX) XMAX=XAX(J,L)
02870 IF(YAX(J,L).LT.YMIN) YMIN =YAX(J,L)
02880 IF(YAX(J,L).GT.YMAX) YMAX=YAX(J,L)
02890C
02900 51 CONTINUE
02910 50 CONTINUE
02920C
02930C SCALE THE DATA.
02940 DATX = (XMAX - XMIN)/5.0
02950 DATY = (YMAX - YMIN)/6.
02960 XO = XMIN - DATX
02970 YO = YMIN - DATY 2
02980 CALL PLTIN(DATX,DATY,XO,YO,XMIN,XMAX,YMIN,YMAX)
02990C
03000C PLOT THE CURVES.
03010 DO 60 L=1,NOS
03020 NS = N-1
03030 DO 61 J=1,NS
03040 CALL PLTLN(XAX(J,L),YAX(J,L),XAX(J+1,L),YAX(J+1,L))
03050C
03060 61 CONTINUE
03070 60 CONTINUE
03080C
03090C LABEL THE AXES.
03100 ENCODE(10,52,MAX) XMAX
03110 ENCODE(10,52,MIX) XMIN
03120 ENCODE(10,52,MAY) YMAX
03130 ENCODE(10,52,MIY) YMIN
03140 CALL LETTER(10,.1,0.0,.4,1.7,MIX)
03150 CALL LETTER(10,.1,0.0,5 3,1.7,MAX)
03160 CALL LETTER(10,.1,0.0,.01,1.95,MIY)
03170 CALL LETTER(10,.1,0.0,.01,7.95,MAY)
03180C
03190 52 FORMAT(F10.2).
03200C
03210 RETURN
03220 END
```

```
03230 SUBROUTINE GRID
03240C
03250C THIS ROUTINE DRAWS THE GRID FOR PLOTTING.
03260C
03270    CALL PLOT(1.0,2.0,3)
03280    CALL PLOT(1.0,8.0,2)
03290    CALL PLOT(6.0,8.0,2)
03300    CALL PLOT(6.0,2.0,2)
03310    CALL PLOT(1.0,2.0,2)
03320C
03330 RETURN
03340 END




03350  SUBROUTINE NAME
03360C
03370C THIS ROUTINE PRINTS DATA ON THE PLOTS.
03380C
03390    CALL LETTER(28,.1,0.,1.2,8.9,28HPROGRAM DEAL     U = .25 M/S)
03400    CALL LETTER(12,.1,0.,2.9,8.7,12HCOLOS = .02 )
03410    CALL LETTER(12,.1,0.,2.9,8.5,12HVRIV = 1 M/S)
03420C
03430    RETURN
03440    END




03450  SUBROUTINE AX
03460C
03470C  THIS ROUTINE LABELS THE X AXIS.
03480    CALL GREEK(2.7,1.6,.2,0.0,1)
03490    CALL LETTER(1,.1,0.0,2.9,1.55,1H1 )
03500    CALL LETTER(9,.2,0.0,3.2,1.6,9H(DEGREES) )
03510C
03520    RETURN
03530    END
```

A.3 Plotting

The plotting routine is arranged so that two variables can be plotted against one another, while also varying a third variable.

For example, in program DEAL, DELZ and ALPHA1 are varied by means of do loops as follows:

```
ALPHA1  =  FLOAT(K - 1) * .02          Line 600
DELZ    =  .05 * FLOAT(L - 1)          Line 660
```

Note the loop varying 'L' is within the 'K' loop.

The plotting variables are assigned as follows:

```
DALPHA1 (K, L)  =  ALPHA1
DTPOW  (K, L)   =  POWER
```

The do loops are concluded.

The plotting routine FOPLO is called as follows:

```
CALL FOPLO (DALPHA1, DPOWER, N, NOS)
```

A plot as shown in Figure (3-14) will result.

APPENDIX B

DETAILS OF THE
PROTOTYPE DESIGN

B.1 Blades

The blades of the cascade were expected to be the most expensive component of the water ladder system. In determining the specific design, one objective was to use materials which are easily obtainable and common manufacturing methods where possible in order to reduce costs and improve scheduling of the fabrication process.

The material selected for the blades must possess adequate strength to withstand the imposed loads, stiffness to limit deflection, be corrosion resistant, be of light weight and be relatively inexpensive. Galvanized steel was considered, however it was felt that the weight would be prohibitive, and possibly have corrosion problems. Alternatively an aluminum alloy was chosen due to its low weight, good strength qualities, and corrosion resistance. The class of aluminum selected was 6061 which has a Young's Modulus of 6.87×10^{10} Pa and a yield strength of 1.72×10^6 Pa.

The shape of the blade was taken to be a cambered plate. A cross-section of the blade resembles an arc, as shown in Figure (B-2).

The power output of the mechanism obviously increases linearly with the blade span. It is thus desirable to specify as large a span as possible, however the span is limited by

deflection considerations along the length of the blade. A shorter span requires a greater number of support structures and transmission mechanisms for a given river width which greatly increases the cost.

A span of 5 metres was chosen for the design based on the above considerations.

The force on the blade was 2709 N for a spacing of 1 m, as given in Chapter (4). For a spacing of .4 m, the force was 1800 N/m, assuming it is distributed evenly over the blade chord. A safety factor of 2 was applied to compensate for stresses induced by unsteady turbulent flows and the actual force profile distribution.

$$F_{dist} = 2(1800) = 3600 \text{ N/m.}$$

For a span of 5 m, F_{dist} = 18,000 N/m along the chord.

Both ends of the blade span are assumed to be securely fastened at the centre point of the chord, hence the centre line along the span which joins the two ends is considered to be rigid. Thus the leading and trailing edges of the blade act as cantilever beams which project from the centre line. The maximum moment is assumed to occur at the centre point of the chord, labelled B in Figure (B-1a). The blade is also assumed to be a flat plate for this analysis.

$$M_{max} = \frac{(18000)(.3)^2}{2} = 810 \text{ N-m}$$

Moment of inertia of the plate, $I = \frac{bh^3}{12}$

where b = span of the blade

t = thickness of the plate

F_{dist} = 18000 N/m

.6 m

B
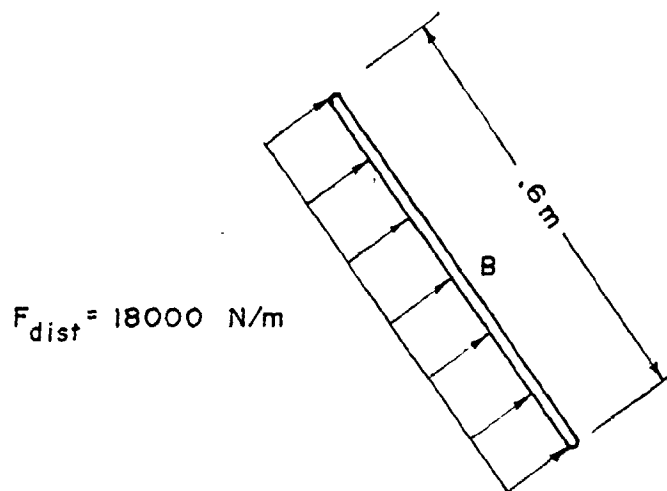
a) FORCE DISTRIBUTION ALONG THE CHORD

5.0 m
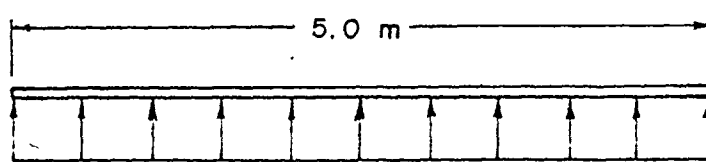
F_{dist} = 2160 N/m

b) FORCE DISTRIBUTION ALONG THE SPAN

FIGURE B-1

Hence $\sigma = \dfrac{M(\frac{h}{2})}{I} = \dfrac{(810)(\frac{h}{2})}{\dfrac{(5)(h^3)}{12}} = \dfrac{972}{h^2}$

For aluminum, $S_y = 172$ MPa

172 MPa $= \dfrac{972}{h^2}$

and $\quad h = .24$ cm.

Considering bending along the span of the blade, as shown in Figure (B-1b)

$F_{dist} = 3600(.6) = 2160$ N/m

The maximum moment is at the centre of the span

$M_{max} = \dfrac{2160(5)^2}{8} = 6750$ N-m

From Appendix (C), the moment of inertia of a curved plate is

$$I_c = r^3 t \left(\phi + \frac{1}{2}\sin 2\phi - \frac{2\sin^2\phi}{\phi}\right)$$

where r, t and ϕ are defined in Figure (B-2).

For the blade selected in Chapter (4), the following values apply

radius $r = .66$ m

$\phi = .473$ r

thickness $t =$ to be determined

Substituting, $I_c = .0002930$ t.

The distance to the centroid is

$\bar{y} = \dfrac{r \sin \phi}{\phi} = .635$

as shown in Figure (B-2).
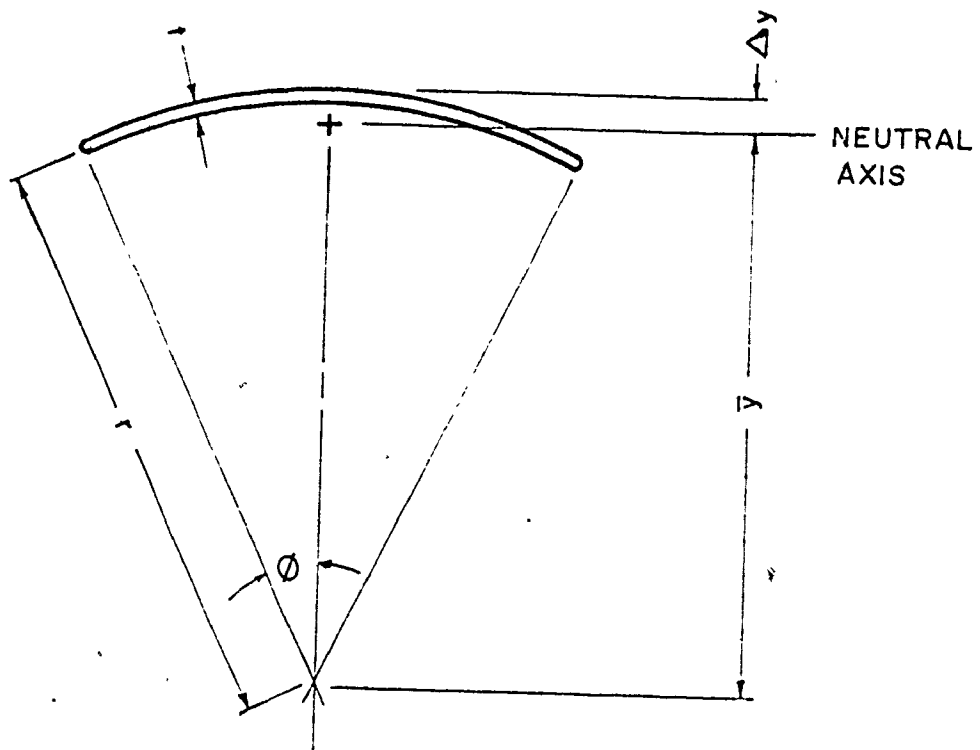
FIGURE B-2

BLADE GEOMETRY

The distance from the centroid to the extreme fibre of the blade is

$$\Delta y = r + \frac{t}{2} - \bar{y}$$

$$= .024 + \left(\frac{t}{2}\right)$$

Therefore $\quad S_y = \frac{M \, y}{I_c}$

$$172,000,000 = \frac{6750\left(.024 + \frac{t}{2}\right)}{.000293 \, t}$$

$$t = .3 \, cm.$$

The maximum deflection of a uniformly loaded simply supported beam is defined as

$$\Delta = \frac{5 \, p_o \, L^4}{384 EI}$$

The maximum deflection was limited to one percent of the span. Hence for a 5 metre span, the allowable deflection is 5 cm.

$$.05 = \frac{5(2150)(5)^4}{384(68.7 \times 10^9)(.000293t)}$$

$$t = 1.75 \, cm$$

Buckling of the blade was also considered. The anticipated failure results from the force which is applied to the leading edge of the blade. This force is due to the drag on the blade. For a 12% cambered plate, which is approximately the curvature of the blade being considered, $C_p = .025$ [21].

$$\therefore \quad D = C_p \frac{1}{2} \rho V^2 A, \quad \text{where } V = \text{average velocity}$$

$$= (.025) \frac{1}{2} (1000)(2m/s^2)(.6x5m^2)$$

$$= 150 \text{ N} \quad (2 \text{ m/s}^2)$$

A low drag force resulted because of the low velocities involved. Since the axial load on the blade is small, buckling was not considered a possible failure mode.

The weight of the blade was calculated on the basis of the thickness calculated for deflection requirements.

Cross sectional area $A = 2 \; t \; r \; \phi$

Length = 5 m

Specific gravity of Aluminum = 2.7

$$\text{Weight} = (2tr\phi)(L)(S_g)(\rho)$$

$$= 2(.019)(.66)(.473)(5)(2.7)(1000)$$

$$= 160 \text{ kg}$$

A further analysis of the blade deflection using steel instead of aluminum as a blade material resulted in $t = .006$ m. The weight was 440 kg. A steel blade was considered too heavy for use in the water ladder system. The weight of the aluminum cambered plate was not excessive however, the use of aluminum may be expensive.

An investigation of composite foil sections such as those used in aircraft was done. The section was identical to that pictured in Figure (B-2) except that two parallel plates were present with a separation distance of 3 cm

$$A_1 = 2 \; t \; r_1 \; \phi$$

$$A_2 = 2 \; t \; r_2 \; \phi$$

$$A_{TOTAL} = 2(.473)(.645 + .675) = 1.249t$$

The moments of inertia about c are

$$I_1 = r_1^3 t \left(\phi + \frac{1}{2} \sin 2\phi\right)$$

$$I_2 = r_2^3 t \left(\phi + \frac{1}{2} \sin 2\phi\right)$$

$$I_{TOTAL} = (.473 + \frac{1}{2} \sin .946)(t)(.645^3 + .675^3)$$

$$= .5059t$$

The neutral axis is at

$$\bar{y} = \frac{.794t}{1.249t} = .636$$

The moment of inertia about the neutral axis is

$$I_6 = .5059t - 1.249t\,(.636)^2$$

$$= .0006844t$$

The distance from the neutral axis to the extreme edge of the blade is

$$\Delta y = .66 + .05 + t - .363 = .039t$$

Therefore, using $S_y = \frac{M\,y}{I}$

$$172,000,000 = \frac{6750(.039+t)}{.0006844t}$$

$$t = .002 \text{ m for aluminum}$$

Checking deflection,

$$.05 = \frac{5(2160)(5)^4}{384(68.7 \times 10^9)(.0006844t)}$$

$$t = .0075 \text{ m for aluminum}$$

Weight is $A_T \cdot L \cdot S_g \cdot \rho$

$$= 1.249 \ (.0075).5.(2.7)(1000)$$

$$= 127 \ kg$$

Additional weight and strength would be added by the tips of the blades and an interior structure. Therefore it was decided weight savings may be moderately significant, however a decision was made to use a solid cambered plate in the prototype design.

B.2 Power Transmission Mechanism

A mechanism was required which would both position the blades appropriately and allow the blades to translate. Several configurations were proposed and are depicted in Figure (B-3). In Figure (B-3a), the blades are mounted at the centre and leading edge by pins which are connected to the transmission chain. The chain is used to turn a sprocket. A problem with this arrangement is that the pins which are required to support the blades cannot be made sufficiently large to withstand the imposed shear stress given the space limitations. Figure (B-3b) illustrates a system of two chains used to support the blades. There is a problem of synchronization since the outer chain translates faster than the inner. In Figure (B-3c) the blades are supported by plates which also form part of the linkage. Each linkage length is equal to the spacing of the blades. This configuration reduces the number of pinned joints, thus decreasing

115
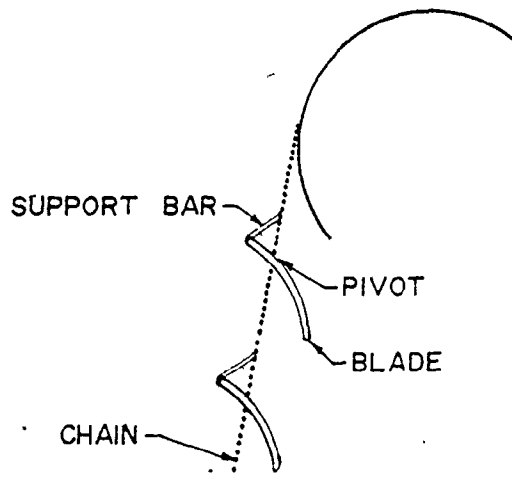
a) SINGLE CHAIN BLADE
MOUNT

SUPPORT BAR

PIVOT

BLADE

CHAIN

b) TWO CHAIN BLADE
MOUNT

CHAINS
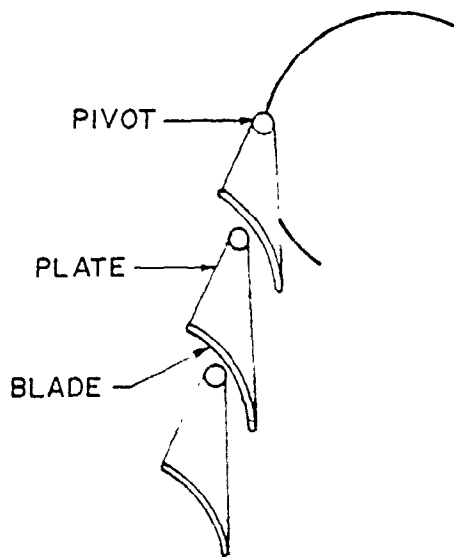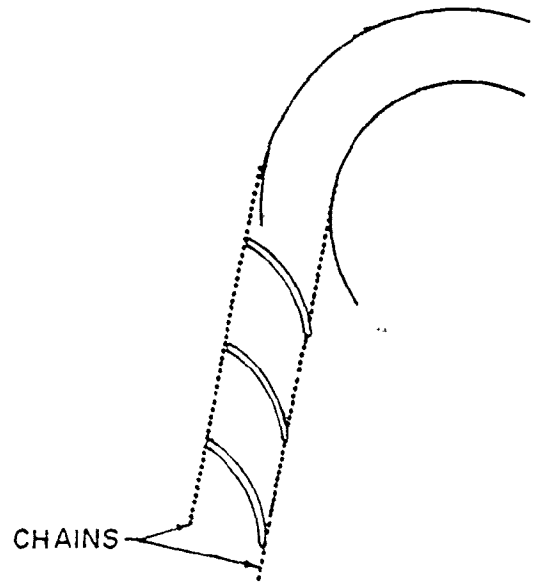
c) PLATE BLADE MOUNT

PIVOT

PLATE

BLADE

FIGURE B-3

BLADE MOUNT ALTERNATIVES

friction and wear. The ease of lubrication of the transmission linkage is improved by these fewer and larger pinned joints. The blade mount is illustrated in Figure (B-4).

B.3   Sprockets

The sprockets used in the system serve two purposes. Firstly they are used to transmit power from the blades to the mainshaft, hence they must withstand the imposed loads. Secondly the sprockets are used to locate the blades in the required position within the system. The blades mounted on the front and rear cascades must not interfere with each other while translating. Space may be required between the cascades for guide vanes and for mainshaft clearance. For the blades specified, the axial chord is .35 m. The minimum diameter of the sprocket is the sum of the axial chord plus the shaft diameter. Min. diameter = .35 + .1 = .45 m.

A larger diameter was specified, to allow for guide vanes and a slower rotation of the mainshaft.

From a manufacturer's specifications [3, pg. 230],

Pitch = 2"

Pitch Diameter = 38.215"

Catalogue number = 160A60 17182

Thickness = 1.156"

Horsepower rating = 171 HP [3, pg. 165]

Since u = .5 m/s, the radius r = .5 m, the angular velocity is then w = 1 r/s. which is 9.5 rpm. Power transmitted
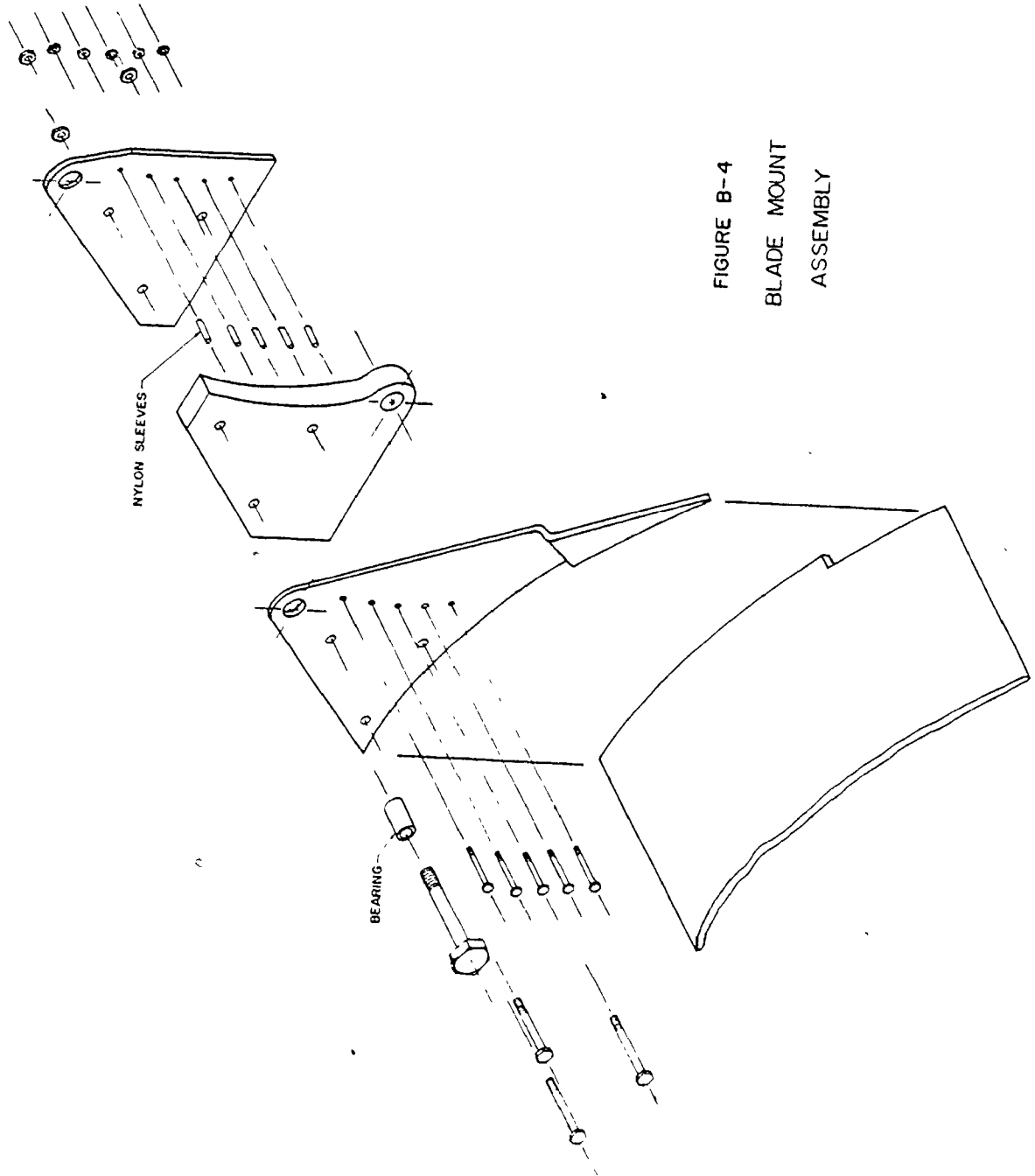
FIGURE B-4
BLADE MOUNT
ASSEMBLY

NYLON SLEEVES

BEARING

through the sprockets is 22 kW, as computed from the simulation.

B.4   Blade Mounts :

The blade mounts are the single most complex component of the water ladder system. Their purpose is to maintain the blades in a horizontal position and link the blades together to form a cascade, yet provide a means of rotating the blades at the top and bottom of the cascade system. Finally the blade mounts must transfer power from the blades to the sprockets.

The blade mounts were designed as shown in Figure (B-4). The mount consists of three plates. The inner plate is welded to the blade. It is formed as shown in order to avoid inter-ference between the mounts as the blades are being rotated on the sprockets. The centre plate acts as a spacer for the sprocket and provides a collar for connection to the mount below. The outer plate is bolted to the others to form a complete unit. Bolts are spaced at 2 inch intervals, since the pitch of the sprocket is 2 inches. These bolts provide rods with which the sprocket can mesh. Nylon sleeves on the bolts prevent wear between the sprocket and the bolts.

The blade mounts are linked together to form a complete chain. The connections between the plates are as shown in Figure (B-4). Nylon-lined sleeve bearings lubricated with water join the links together.

The axial fluid force on the blade causes them to be deflected in the axial direction. The severity of this action was considered significant. Guide rollers are provided on every second linkage to maintain the blades and linkage in the proper position.

The weight of the plates was calculated to be approximately the following:

Outer Plate   3.8 kg

Centre Plate   12.6 kg

Inner Plate   2.2 kg

These weights were used to approximate the cost of fabrication.

B.5   Main Shafts

The forces on the blades were given as

FORCE = (1084 N/m) (5m) $\approx$ 5400 N

A safety factor of 1.5 was applied to compensate for flow variation. The safety factor was reduced from the previously selected value of 2 because in this case the entire mechanism is being dealt with. It was felt that the effects of variations in the flow would not be as severe on the system as for individual blades.

Therefore FORCE = 1.5(5420) = 8100 N

Approximately one metre of the total water depth of 4.2 m was required to provide space for the blades to rotate, leaving a distance of 3.2 m between the two mainshafts. Hence with a spacing of .4 m between the cascade blades, 8 blades were in

the mainstream flow, per side.

The total lifting force is

8(8100) = 64800 N

which is 32400 N per linkage chain.

It was assumed that the forces cancel where the blades rotate at the top and bottom ends of the cascade. Blades on the rear cascade were considered not to contribute a force in this initial analysis, as discussed in Chapter (4).

The torsion was calculated as follows.

Weight of each blade = 160 kg = 1570 N

Per side = 785 N

The tension in the linkage as a result of blade weight

= 785 cos (.2) = 770 N

The tension at point A due to weight of blades, See Figure (B-7a)

= 770(16) = 12300 N

The tension at point B due to fluid flow

= 8(4050) = 32400 N

Maximum tension in the linkage is a C

= 32400 + 12300 N = 44700 N

∿ 45000 N

The torsion in the upper shaft from two sprockets

$= 32,400 \ (\frac{.97}{2}) 2$

= 31430 N-m

given the sprocket is .97 m in diameter.

Shaft size is determined by calculations of the strength requirements resulting from the applied torsion and moments. Figure (B-5) summarizes the proposed arrangement and
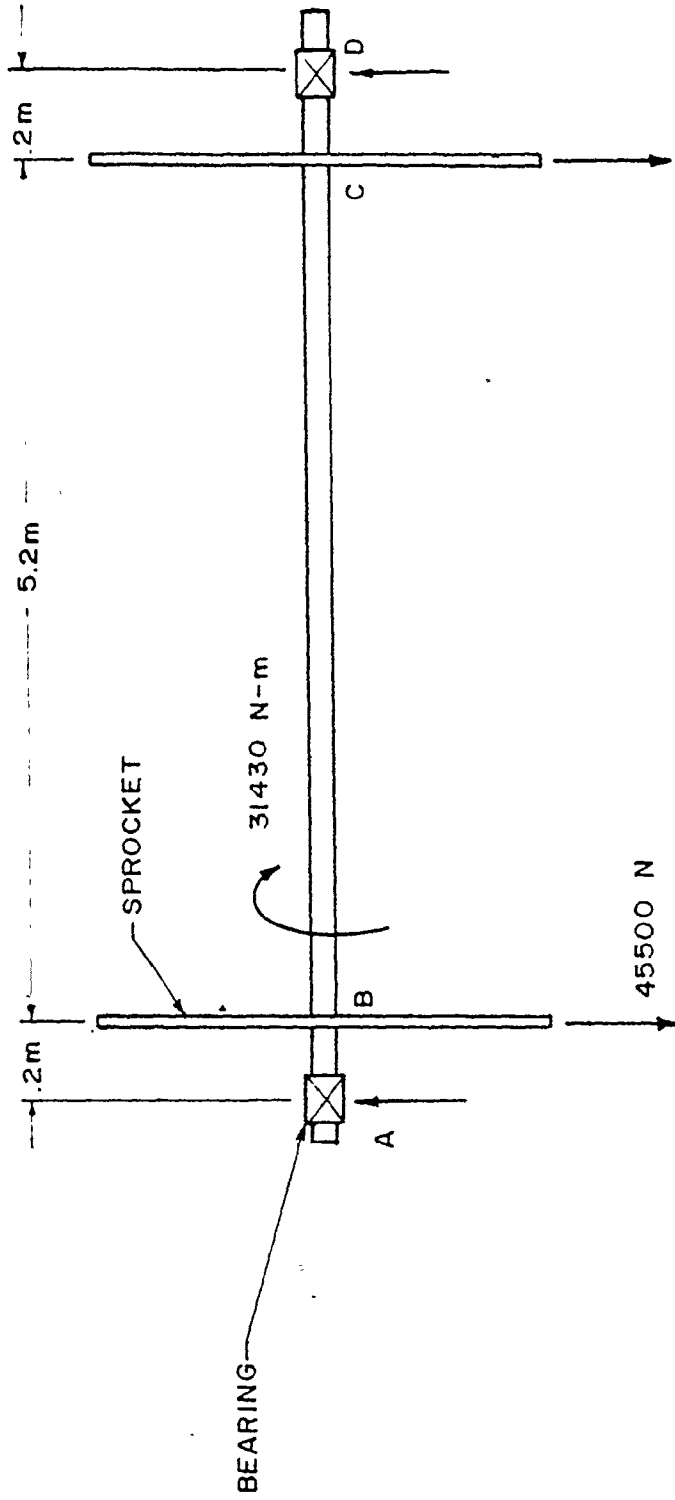
FIGURE B-5

FORCES ACTING ON THE UPPER SHAFT

the applied loads. The load at the sprockets includes the weight of the sprocket which is 300 N * S.F.

A maximum bending moment occurs between the sprockets. Assuming points A and D are simple supports

$$M_{max} = .2(45500) = 9100 \text{ N-m}$$

The shaft was specified to be made of stainless steel, 530100, 1/4 hard.

$$S_y = 515000 \text{ kPa}, \quad S_{ut} = 859000 \text{ kPa}$$

Endurance limits concerning fatigue, reliability, temperature effects, etc. were applied to the shaft [38, pg. 188].

$$S_e = k_a \, k_b \, k_c \, k_d \, k_e \, k_f \, S_e'$$

$k_a = .62$ (Fig. 5-17, 38)

$k_b = .85$ (Section 5-15, 38)

$k_c = .897$ for 90% Reliability (Table 5-2, 38)

$k_d = 1, T < 160^\circ F$ (38)

$k_e = .8$ for stress concentration about points B and C.

$k_f = .9$ for corrosion protection.

Therefore

$$S_e = .340 \, S_e'$$
$$= .340 \, (.5 \, S_{ut})$$
$$= 146000 \text{ kPa}$$

The diameter of the upper shaft was determined using

$$d = \left[\frac{32n}{\pi} \left[\left(\frac{T}{S_y}\right)^2 + \left(\frac{M}{S_e}\right)^2 \right]^{1/2} \right]^{1/3} \qquad \text{(Eqn. 13-6, 38)}$$
$$= .096 \text{ m.}$$

with n = 1, since a safety factor had already been applied.

The lower shaft size was determined using the following expression, since there is no applied torsion on the shaft.

$$d = \left(\frac{32 \ Mn}{\pi \ S_e}\right)^{1/3}$$ (Eqn. 13-3, 38)

$$d = .086 \ m$$

The deflection was checked, for the upper shaft

$$\Delta_{max} = \frac{Pa}{24EI} \ (3L^2 - 4a^2)$$

$$= \frac{45500(.2)(3(5.4)^2-4(.2)^2)}{24(2.061 \times 10^{11})(\frac{\pi}{64} \ (.093)^4)}$$

$$= .044 \ m$$

The deflection ratio is $\frac{.044}{5.4}$ .008 << .01.
Therefore the shaft is acceptable.

Similarly for the lower shaft,

$$\Delta_{max} = .080 \ m$$

The deflection ratio is $\frac{.080}{5.4}$ = .015 > .01, however the lower shaft was accepted as adequate on the basis of the safety factor involved.

The final sizes for the shafts were assigned according to stock sizes. The upper shaft, calculated to be .096 and was for convenience specified as 0.102 m (4") whereas the lower shaft was specified as 0.089 m (3.5"). The weights of the shafts are:

$$W_{upper} = (.102)^2 \frac{\pi}{4} (6.0) (7850) = 385 \text{ kg}$$

$$W_{lower} = (.089)^2 \frac{\pi}{4} (5.8)(7850) = 285 \text{ kg}$$

where 6.0 and 5.8 are the lengths of the upper and lower shafts respectively.

These weights are large, however, corresponding values for tubular shafts show very little improvement.

B.6   Bearings - Mainshaft

Bearings on the mainshafts must be able to withstand an aqueous environment and for this reason it was decided to select a nylon or polymeric material. This material is to be encased in a metallic sleeve with water lubrication. Depending upon the particular river involved, problems may arise as a result of excessive silt in the water. The design would be modified to employ a sealed bearing of some type. The nylon bearing is acceptable based on the fact that the shafts rotate at low speeds.

B.7   Belt Transmission

A belt system is used to transmit power from the main-shaft to the generator. The belt is required to have teeth to eliminate slipping, this being especially important in an aqueous environment. The speed of rotation of the mainshaft is 9.5 rpm while that of a standard generator is 1800 rpm. Hence a speed reduction of about 190 is required and is to be achieved using a series of pulleys.

B.8   Generator

The mechanical power of the mainshaft is transmitted through a set of belts to increase the speed of rotation of the generator shaft. An appropriate generator was selected to have the following details,

3 Phase, 60 Hz

.8 Power Factor

Speeed - 1800 rpm

Capacity - 21 kW

Efficiency at full load 85%

The power output to the blades is estimated to be 21.7 kW, see Chapter (4). The electrical power which is generated is determined by applying efficiency factors.

Hence

Efficiency of generator = .85

Efficiency of gearbox   = .9

Power out = 21.7 (.85)(.9)

       = 17 kW

B.9   Support Structure

The philosophy behind the support structure was to construct a packaging case for the system. In essence it was desired to fabricate a rigid structure which would contain the essential components of the system, thus enabling factory assembly, simple transportation and minimum site work. The objective in using this approach was to reduce the overall unit cost.

Contact points between the structure and the mech-
anism are at the upper and lower mainshaft bearings and at
the generator mounts. This is schematically shown in Figure
(B-6). The structure is required to support the configuration
shown. Loads on the structure are given in Table (B-1).

In addition to the static loads given in Table (B-1)
dynamic loads exist in the form of tension in the blade
linkage. As previously calculated the maximum tension is
45000 N, including a design safety factor. The loads on the
structure are shown in Figure (B-7a,b). The forces have been
resolved into perpendicular directions.

The design of the structural members was done on the
basis of limit states design [7]. Only two member sizes were
specified in order to simplify material requirements. The
size of the members were sufficiently small to render the
optimization of the structural design unnecessary. The
resulting structure is depicted in Figure (B-8) and represents
a first approximation in the design.

The following is the structural steel design synthesis
based on [7].

Column 1:

$V = 2020 \text{ lb}_f$

$L = 13.9 \text{ ft}$

$C_f = 17.8 \text{ kip}$

$M_{f_1} = 11.850 \text{ ft - kip}$
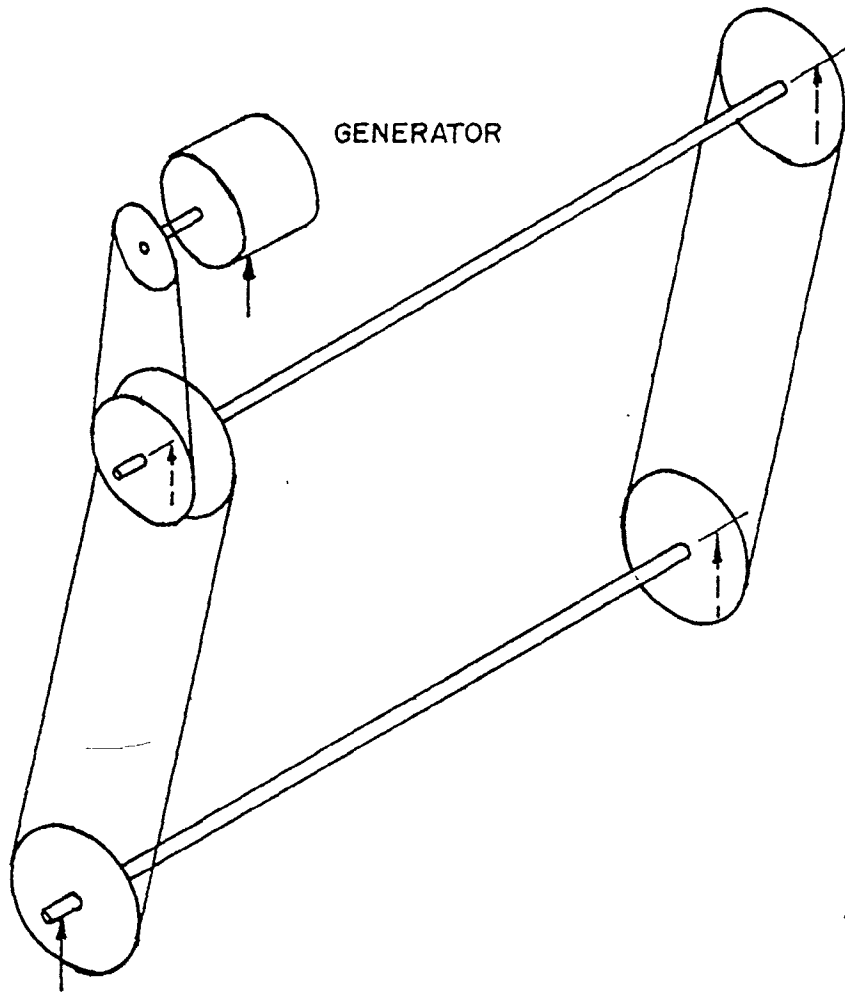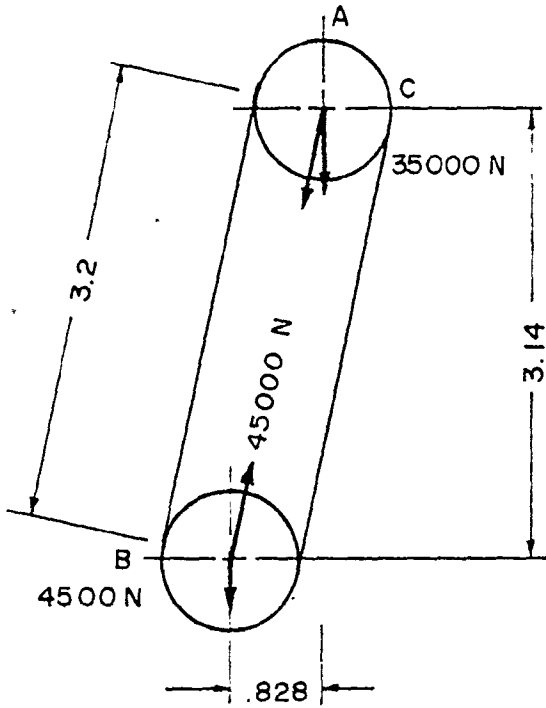
$M_{f_2} = 0$

GENERATOR
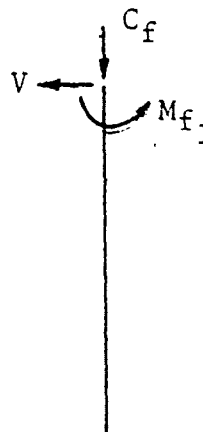
FIGURE B-6

MECHANISM AND SUPPORT LOCATIONS

a) RESULTING FORCES
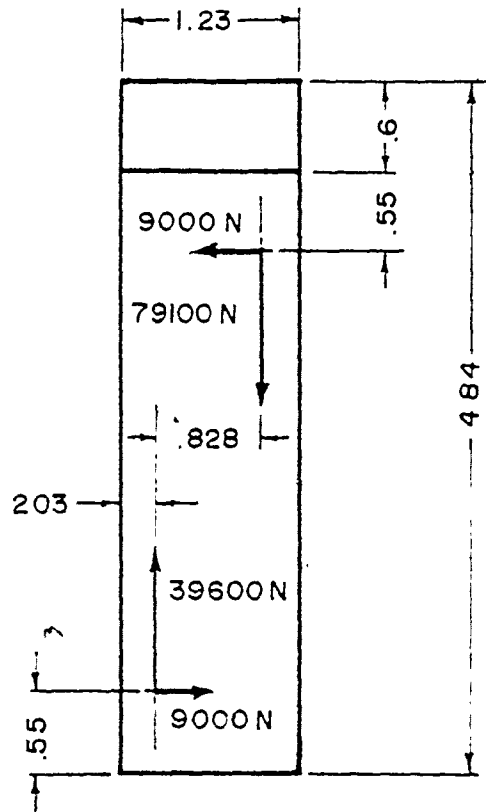   FROM THE MECHANISM

b) STRUCTURE SIZE
   AND APPLIED FORCES

FIGURE B-7

ALL MEMBERS ARE M4 x13
UNLESS OTHERWISE SPECIFIED.
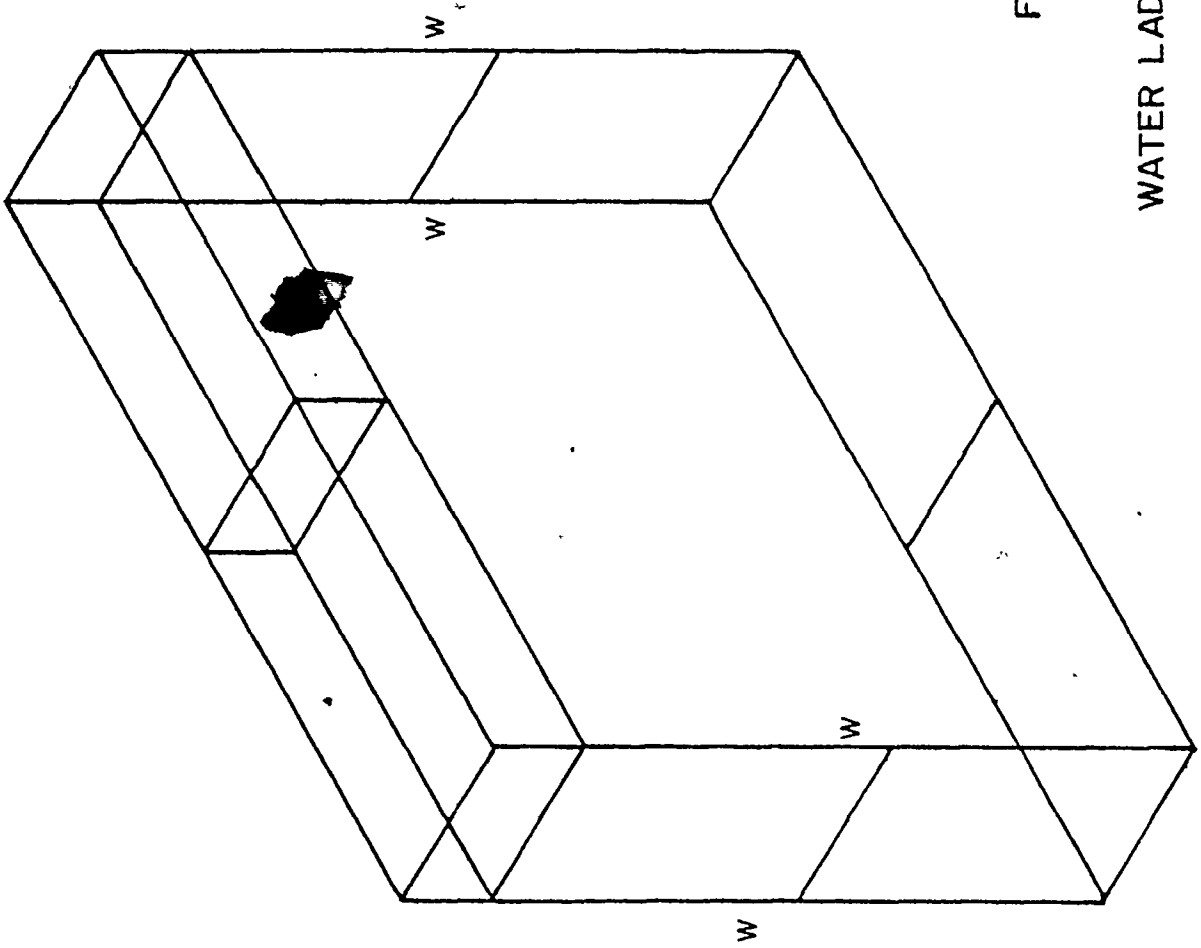
COLUMNS DENOTED "W" ARE
W6 x 15.5

APPROXIMATE SCALE= 1:50

FIGURE B-8

WATER LADDER SUPPORT STRUCTURE

Both top and bottom of column are flexible.

From Table 4-4 $K_x = K_y = 1.00$ [7]

$K_x L_x = 13.9$ ft

$K_y L_y = 13.9$ ft

Try 1.W6

$r_x/r_y = 1.77$

$K_x L_x / r_x / r_y = 13.9/1.77 = 7.85 < 13.9$ ft

For a 6 x 6, $B_x = 4.05$ for strength

$C_f' = C_f + B_x M_{f_2}$

$= 17.8 + (4.05)(11.85) = 65.8$ kips

Select a W6 x 15.5 Class 3 section in 620.21 44w

Area $= 4.56$ in^2

$r_x = 2.57$ in

$r_y = 1.46$ in

$C_{r_0} = 187$ lbf

$C_{r_L} = 68$ lbf $(KL = 139)$

$M_{r_x} = 33.0$ ft lbf

$r_x/r_y = 1.76$

$C_{r_L} = 68$ ft lbf $L > C_p' = 65.8$ k

From Table 4-5 (stability) [7]

$B = 4.77$

$C_f'' = C_f + w M_{f_2} B_{r_x} \dfrac{C_{r_L}}{C_{r_0}} u$

$w = 1.0$ since $M_{f_1} = 0$ and no sway effects are present.

Table B-1

Loads on the Structure

(1) Upper Shaft

Blade Weight = $(127)(24)(9.8)(1.5) = 44800$ N

Blade Mounts = $48(3.8+12.6+2.2)(1.5)(9.8) = 13120$ N

Upper Shaft Weight = $385(9.8)(1.5) = 5660$

Sprocket Weight = $(170x2)(9.8)(1.5) = 5000$ N

Total weight on upper shaft = 68600 N

including a safety factor of 1.5

Weight per side ≈ 35,000 N

(2) Lower Shaft

Sprocket = $(170)(2)(9.8)(1.5) = 5000$ N

Lower Shaft = $285(9.8)(1.5) = 4190$

Total = 9190 N

Weight per side = 4500 N

Note:

It was assumed that the upper shaft supported the weight of the mechanism since it is essentially hanging from the shaft.

$$\frac{K_x L_x}{r_x} = \frac{13.9}{2.57} = 5.4$$

$$\frac{C_e}{A} = 7944 \text{ ksi}$$

$$C_e = 7944(4.56) = 36225 \text{ kips}$$

$$\frac{C_f}{C_e} = \frac{17.8}{36225} = .000491$$

$$u = 1$$

$$B_x = 4.77$$

$$C''_f = 17.8 + 10(11.85)(4.77)(\frac{68}{187})(1.)$$

$$= 38.35 < 68 \text{ OK}$$

B. (i) Strength Check w6x15.5

$$\frac{C_f}{C_r} + .85 \frac{M_f}{M_r} < 1.0$$

$$\frac{17.8}{187} + .85(\frac{11.85}{33}) = .40 < 1.0$$

(ii) Stability Check

$$\frac{C_f}{C_r} + \frac{w_x M_{f_x} u}{M_{r_x}} \leq 1.0$$

$$\frac{17.8}{187} + \frac{1.0(11.85)(1.0)}{33} = .45 < 1.0$$

Check y direction

$$M_{max} \sim .2(45,500)$$

$$= 9100 \text{ N-m.}$$

$$= 6712 \text{ ft-lb}_f$$

$$= 6.7 \text{ ft kips} \sim \text{small}$$

The column is over-designed, however the size is required, the mounting purposes.

Column 2 is also a W6x15.5.

Cross Beams

Axial Load - 2 kips

Weight of generator is minimal.

$K = 1.237 \ m = 4.1 \ ft$

$K_x = K_y = 1.0$

Hence $K_x L_x = 4.1 \ ft$

An M4 (4x4) beam is adequate.

Span beams

$$w = 800 \ lb_f/ft$$

Top
View

Force on the plate is

$1/2 (.4)(1000)(.4)(9.8) = 784 \ N/m$

.4 m

For a span of 5 m, 3920 N
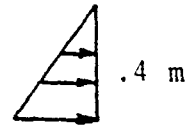
Max moment $= \dfrac{wl^2}{8} = \dfrac{800(5)^2}{8} = 2500 \ N\text{-}m$

$$= 3390 \ ft \ lb_f$$

$$= 3.4 \ ft \ kips$$

This load is small-use a 4x4 M section. 4 beams are used.

Steel plate is suggested to be used on the structure to form the barriers which would retain the water upstream and provide some means of protection for the system. A 1/4" (8 mm) thickness for the plate was specified. The

position of the plate is shown in Figure (B-9). End plates A and B protect the bearings and blades from objects entering from the sides of the structure. These plates are U-shaped to allow space for the ends of the upper and lower shafts to slightly protrude beyond the limits of the structure. This is necessary in order to provide a space for mounting the belt drive pulley for the generator. Plates D, E and F form a barrier which imposes the required ΔZ as shown in the Figure. Plates were specified both on the upstream and downstream sides to prevent water from entering in the space above plate F. Finally, plate G acts as a barrier to reduce flow velocities in the region where the blades rotate, see section (4.2).

The plates also contribute to the rigidity of the structure.

Calculation of the weight of the structure is given in Table (B-2).

A recalculation shows no change in the structure design as a result of considering its own weight.

Column design - Recalculation

Length $=$ 13.9 ft

V $=$ 2020 lb$_f$

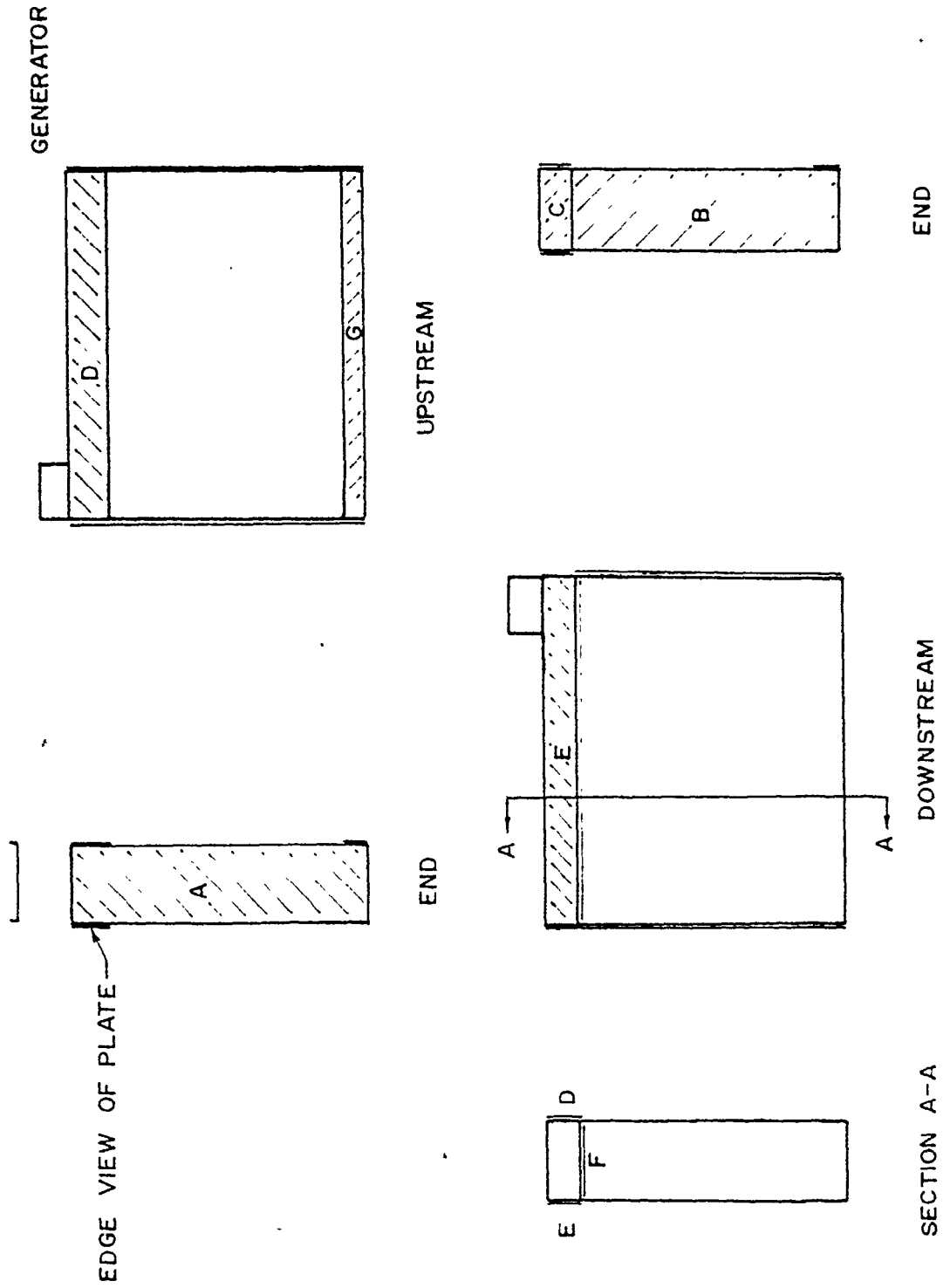C_f $=$ 17.8 kips

M_{f_1} $=$ 11.85 ft - kips

135

FIGURE B-9 - PLATE PLACEVENT

$$M_{f_2} = 0$$

Add the weight of the structure.

Total weight = 1408 kg (members)

+ 1241 kg (plate)

= 25960 N

Assume the weight is supported equally by the four columns

p = 6490 N

Applying a safety factor of 1.5

p = 9735 N = 2188 lb.

Therefore C_p = 17.8 + 2.2 = 20.0 kips

That is, no change is necessary in the structural design since consideration of the weight of the structure introduces only a small load.

B.10 Site Installation

The low power output of the water ladder system created the need for an alternate site construction concept instead of the typical concrete dam and penstock generally built with hydroelectric turbines. By designing the water ladder system as a factory completed unit, site installation costs could be minimized. This section deals with the site requirements for the unit.

The river bed at the site should be fairly flat across the river. If the bed is composed of soft silt or clay, the bearing strength of the bed should be checked.

Table B-2

Weight of Structural Steel

Member	Size (Imperial)	Length	Mass	Qty.	Total
Cross 1	M4x13	1.23	19.4 kg/m	11	262.5
Column	w6x15.5	4.84	23.1 kg/m	4	447.2
Span	M4x13	5.8	19.4 kg/m	6	675.1
Mid Upright	M4x13	.6	19.4 kg/m	2	23.3
					1408 kg

Steel Plate

Plate	Dimensions	Thk cm	Volume	Mass
A	(1.23+2(.2))x4.84	.635	.0500	393.2
B	(1.23+2(.2))x4.24	.635	.0438	344.5
C	1.23 x .6	.635	.0047	36.8
D	.6 x 5.8	.318	.0 10	86.7
E	.6 x 5.8	.318	.0110	86.7
F	1.23 x 5.8	.318	.0227	177.8
G	.4 x 5.8	.635	.0147	115.6

Note: Plates A and B are U-shaped.   1241 kg

Gravel or some other means of support may be required.

Once the adequacy of the foundation has been assured, the water ladder unit may be installed in the river. The unit is held in place by guide cables which are fastened to piles on the shore of the river, see Figure (B-10). This is easier to accomplish if the river cross-section is approximately rectangular. The space between the sides of the unit and the shoreline are then filled in with rip-rap. This stone fill prevents the water from flowing around the system, thus channelling a greater volume of water through the cascade. It is anticipated that the resistance to flow is greater through the rip-rap rather than the cascades. The rip-rap also adds to the stability of the unit. Rip-rap is also located upstream of the raised plate on the lower front side, to contribute in directing the flow around the plate, see Figure (B-10).

Remaining site work consists of electrical connections and upstream trash racks. Trash racks are required to prevent debris from becoming lodged in the cascades, and hence their installation is imperative in most situations. Trash racks may consist of a standard sized fence which extends above and below the anticipated range of water levels. The fence need not extend to the river

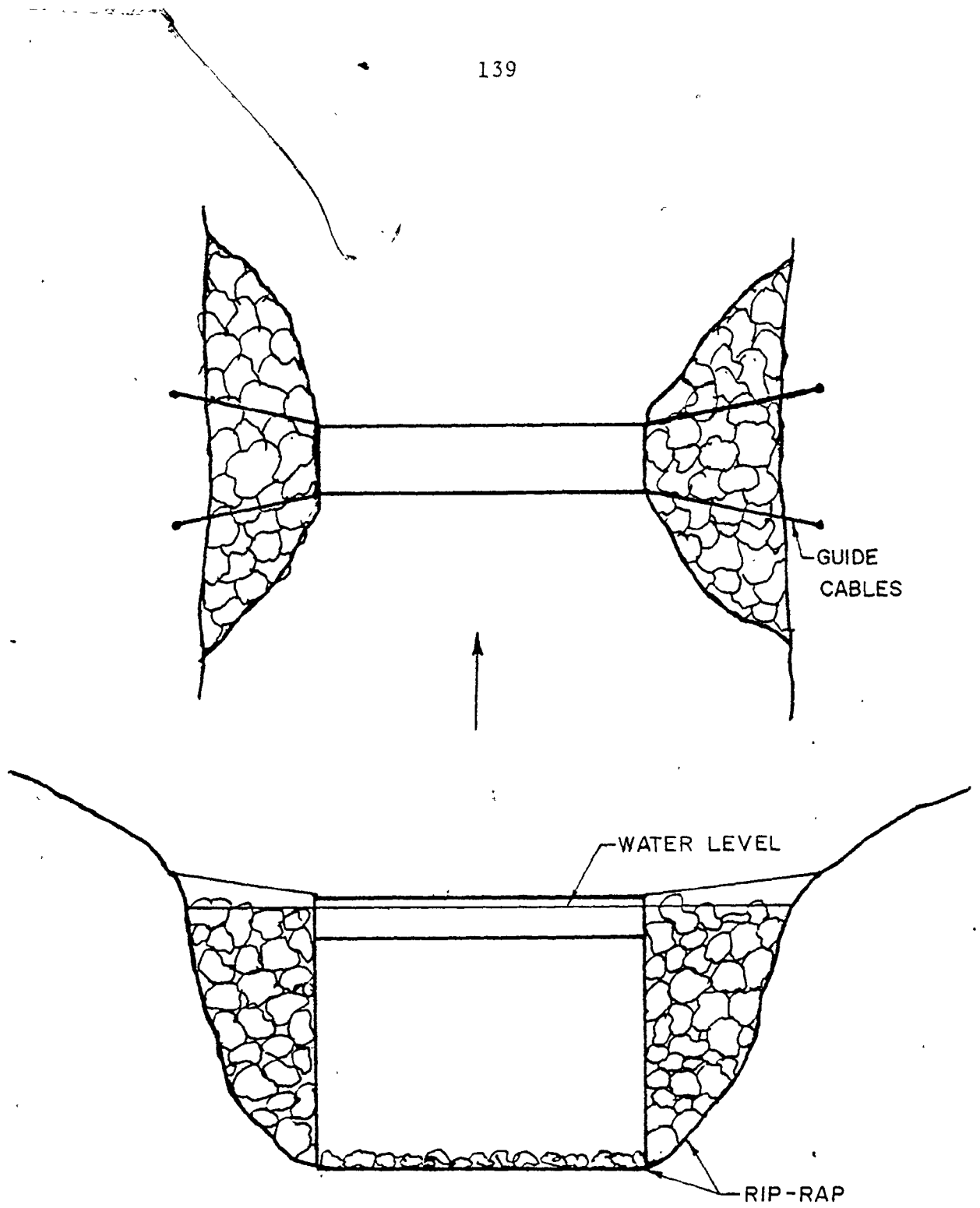GUIDE CABLES

WATER LEVEL

RIP-RAP

FIGURE B-10

SITE INSTALLATION

bottom. From a safety point of view however, swimmers, if present, would be protected from accidents by a fence of the full depth. A means of protection downstream may be required as well, depending on river conditions. In either case the fence is mounted on piles, or hung on a cable and anchored by weights, see Figure (B-11). It should be noted that there will be a maintenance cost involved with cleaning the racks.

A more elaborate installation may be required on larger rivers. The width of a river may be of such an extent as to prevent the use of guide wires to shore. In that event, an alternate means of support is required. The most obvious is the use of piles or a concrete foundation, however, this installation was considered economically prohibitive. A possibility is to mount the water ladder to bridge foundations. Since these underwater structures are in existance, installation costs would be minimal. The system could be mounted on the downstream side of the bridge, using the upstream structures as supports for a trash rack.

Either of these simple installation methods is consistent with the pre-packaged concept of the water ladder system.
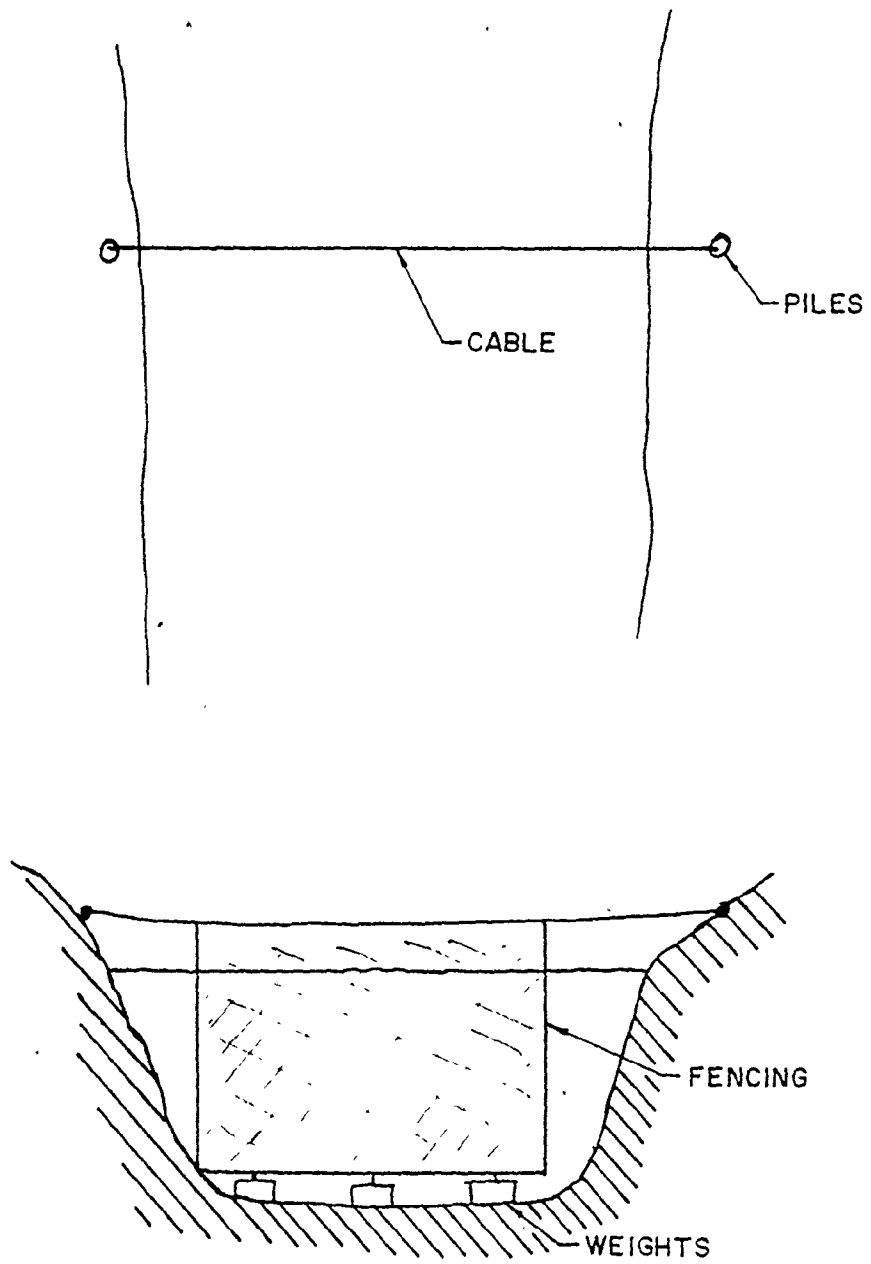
FIGURE B-11

SUSPENDED TRASH RACK

B.11 Conclusion

Appendix B has summarized the design of a prototype water ladder unit. The design is not optimum however enough detail and scope exists to assess the project. The water ladder system is deemed to be technically feasible as a result of the design proposal.

The proposal is summarized graphically by the various drawings contained in Appendix B and the drawings included at the end of this report, in Appendix E.

APPENDIX C

MOMENT OF INERTIA OF A BLADE SECTION

The derivation of the definition of the moment of inertia for a cambered plate about the neutral axis is presented. Refer to Figure (B-2) for variable definitions.

From Figure (B-2)

$$dA = rt\, d\phi$$

$$y = r\cos\phi$$

Area of the blade

$$A = \int_{-\phi}^{\phi} tr\, d\phi$$

$$= 2tr\phi$$

Position of the neutral axis:

$$\int_{-\phi}^{\phi} y\, dA = \int_{-\phi}^{\phi} rt\,(r\cos\phi)\, d\phi$$

$$= r^2 t\, \sin\phi \Big|_{-\phi}^{\phi}$$

$$= 2r^2 t\, \sin\phi$$

$$\bar{y} = \frac{\int y\, dA}{A} = \frac{2r^2 t\, \sin\phi}{2tr\phi}$$

$$= \frac{r\sin\phi}{\phi}$$

Moment of Inertia

$$I = \int_{-\phi}^{\phi} y^2\, dA \qquad \text{(about the radius centre)}$$

$$= \int r^2 \cos^2 \phi rt \, d\phi$$

$$= \int r^3 t \quad \cos^2 \phi \, d\phi$$

$$= r^3 t \int \frac{1 + \cos 2}{2}$$

$$= \frac{r^3 t}{2} [\quad d\phi \quad + \quad \cos 2\phi \, d\phi]$$

$$= \frac{r^3 t}{2} [\phi + 1/2 \sin 2\phi] \Big|_{-\phi}^{\phi}$$

$$= r^3 t (\phi + 1/2 \sin 2\phi)$$

Moment of inertia about the neutral axis is calculated by

$$I_o = I_r + A\bar{y}^2$$

$$= r^3 t (\phi + 1/2 \sin 2) - 2tr\phi \left(\frac{r \sin\phi}{\phi}\right)^2$$

$$= r^3 t (\phi + 1/2 \sin 2\phi) - 2r^3 t \frac{\sin^2 \phi}{\phi}$$

APPENDIX D

COSTS

Costs for the various components and materials specified in the system are listed in Table D-1.

Note that in the cost estimate the heading entitled 'Miscellaneous Parts' includes:

Nylon linkage bearings, bolts, nuts, nylon sleeves, pins, rollers and guides.

Table D-1

Prices Obtained For Estimations

Item		Cost	Source
Aluminum Plate ~ 1/2"	~	$3.00/lb.	Machine Shop, McMaster University
	in bulk	$2.50/lb.	
Steel Plate ~ 1/2"		.50¢ -.45¢/lb.	Machine Shop, McMaster University
Structural Steel - assembled		$2.00/lb.	IEC Consultant
Concrete - complete		$150.-600/lb. e.g. slab - $150/lb. manhole - $600/lb.	IEC Consultant
Excavation	large - small -	$10/yd. $100/yd.	IEC Consultant
Granular backfill		$50/yd.	IEC Consultant

Main Bearing - Lubricated Nylon	4" ID x 6" OD x 10" long	$100.	Plastic & Allied Building Products
Sprockets - PD = 38.2 in.	~	$1200 ea.	Canadian Bearing
Main Shaft 4" x 21' long	~	$1000 ea.	

APPENDIX E

DETAILED DRAWINGS

Appendix (E) contains several detailed drawings which depict various aspects of the water ladder system

Figure (E-1) is a perspective drawing which conveys the overall appearance of the assembled water ladder unit. Figure (E-2) shows the mechanism assembly. Figures (E-3 through E-6) illustrate details of the blade mounts.

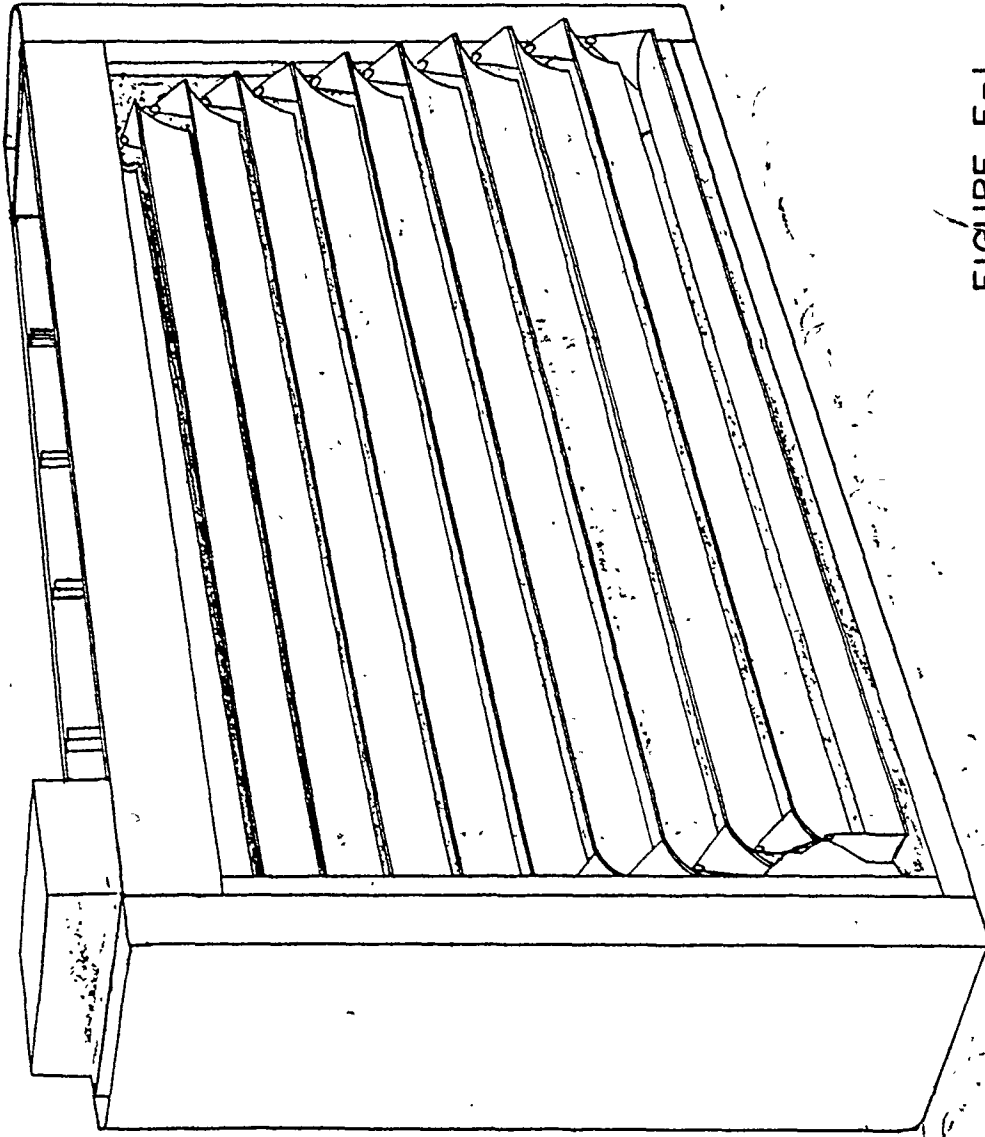Note that dimensions contained on the drawings are approximate and are given in millimeters.
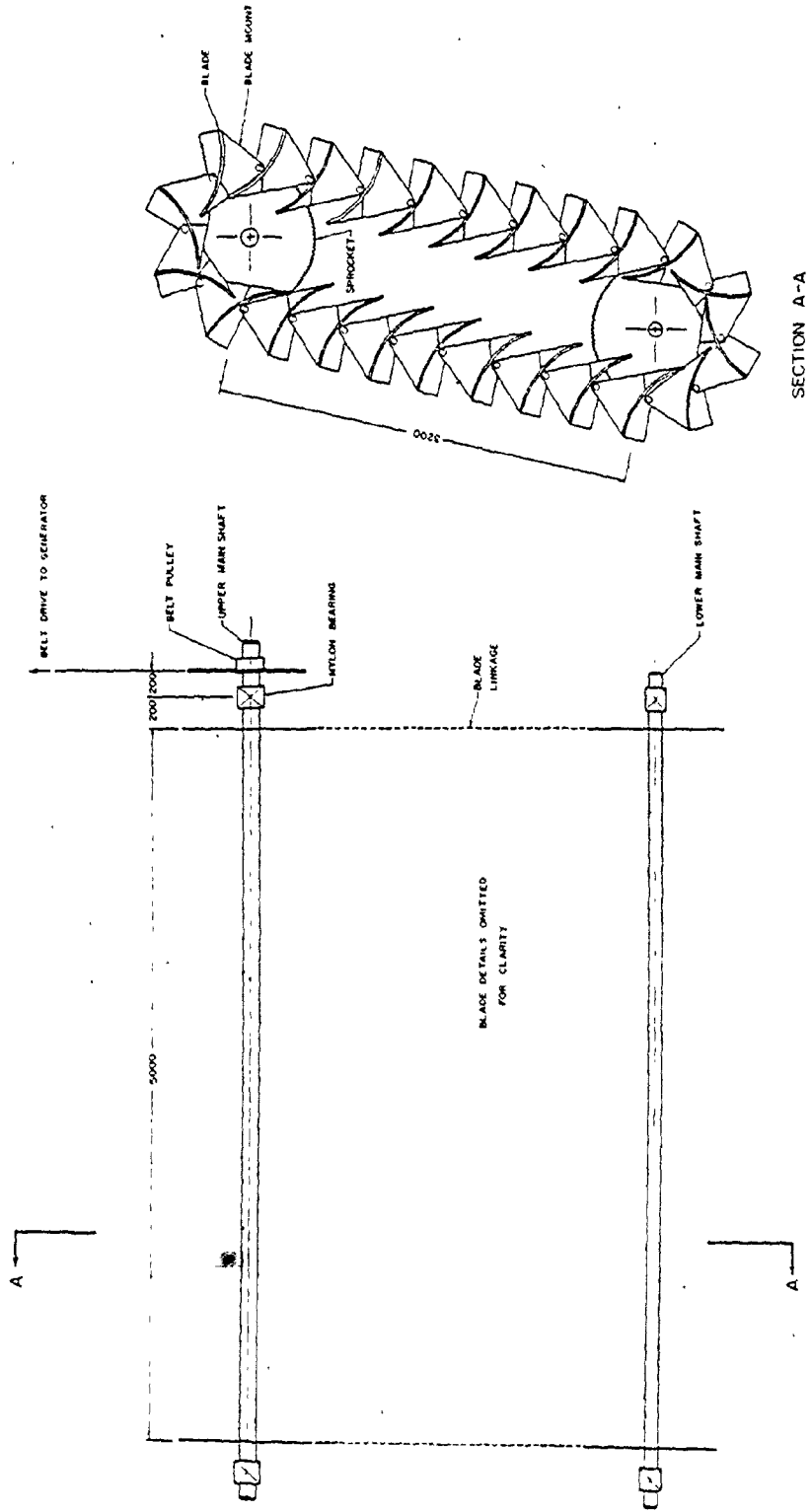
FIGURE E-1

THE WATER LADDER ASSEMBLED UNIT

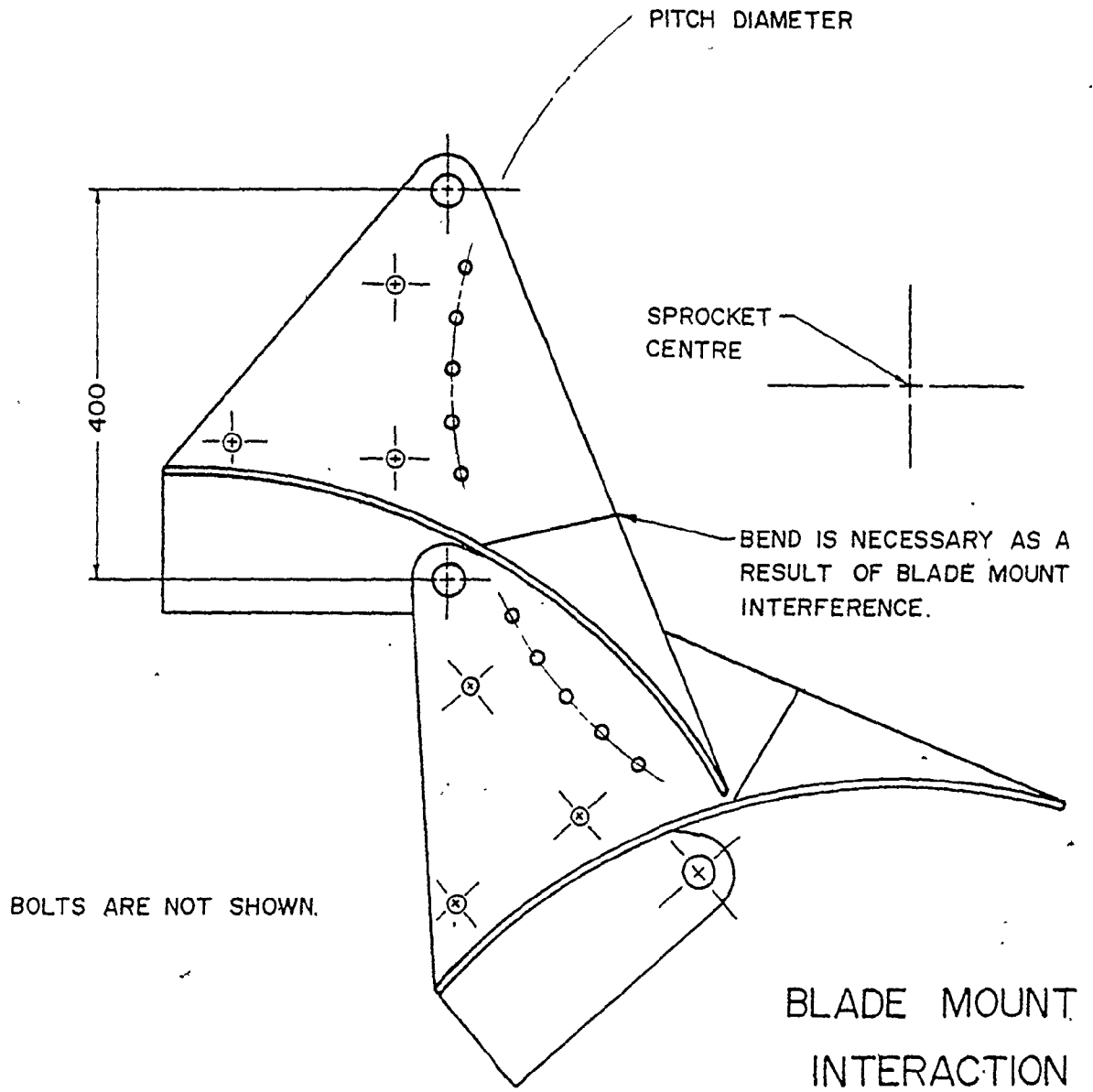SECTION A-A

FIGURE E-2

MECHANICAL ASSEMBLY

PITCH DIAMETER

SPROCKET
CENTRE

BEND IS NECESSARY AS A
RESULT OF BLADE MOUNT
INTERFERENCE.

400

BOLTS ARE NOT SHOWN.

BLADE MOUNT
INTERACTION

FIGURE E-3

13∅ -5 HOLES AT 51 mm CENTRES
ON A 485 mm RADIUS.

38r

38∅

19∅ TYP

100

160

400

85

20

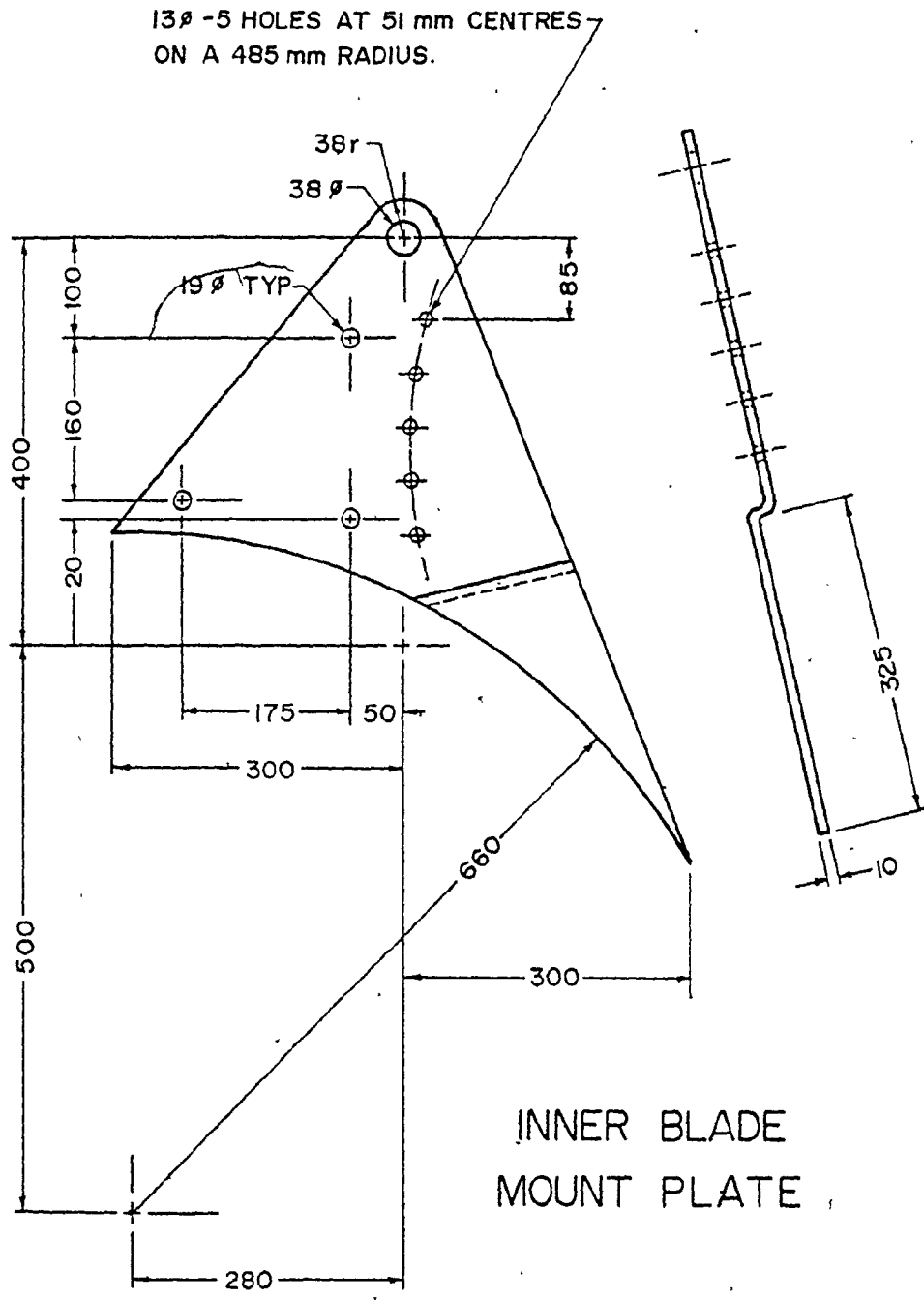175   50

300

660

300

500

280

325

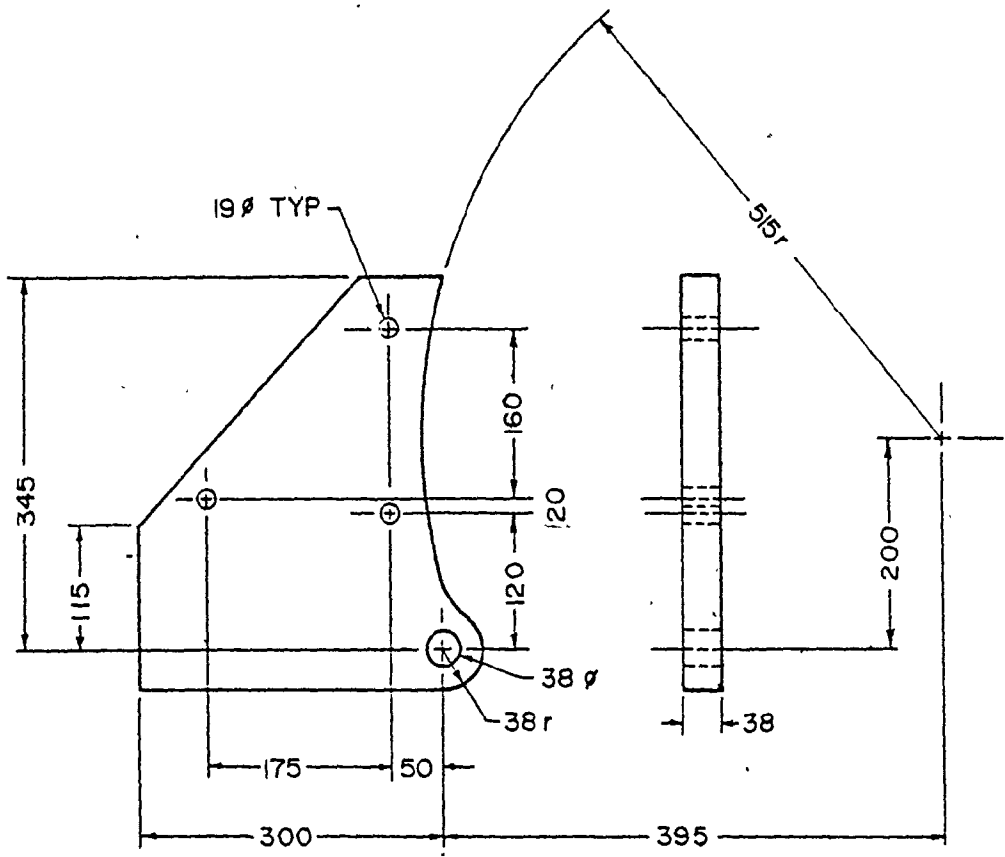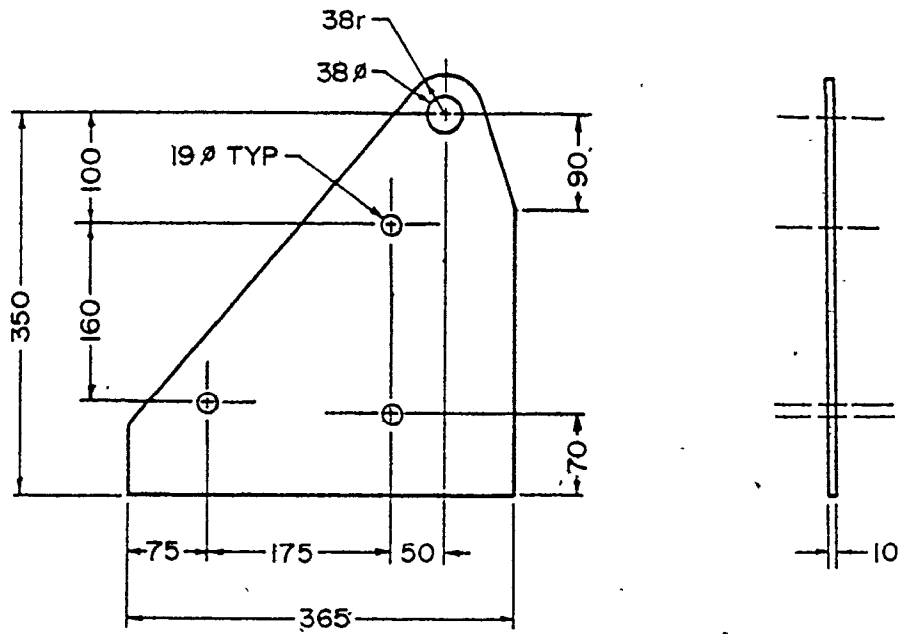10

INNER BLADE
MOUNT PLATE

FIGURE E-4

CENTRE BLADE
MOUNT PLATE

FIGURE E-5

OUTER BLADE
MOUNT PLATE

FIGURE E-6